Title
One Fish, Two Fish, Small Fish, Huge Fish: Utilizing Zebrafish as a Model for Studying Mitochondrial Function

Author
Johnson, Meghan Elizabeth

Publication Date
2012

UNIVERSITY OF CALIFORNIA

Los Angeles

One Fish, Two Fish, Small Fish, Huge Fish: Utilizing Zebrafish as a Model for Studying Mitochondrial Function

A dissertation submitted in partial satisfaction of the requirements for the degree Doctor of Philosophy in Biochemistry and Molecular Biology

by

Meghan Elizabeth Johnson

2012

ABSTRACT OF THE DISSERTATION

One Fish, Two Fish, Small Fish, Huge Fish:

Utilizing Zebrafish as a Model for Studying

Mitochondrial Function

by

Meghan Elizabeth Johnson

Doctor of Philosophy in Biochemistry and Molecular Biology

University of California, Los Angeles, 2012

Professor Carla M. Koehler, Chair

The mitochondrion is a complex organelle, conserved throughout evolutionary history. Although the mitochondrion contains its own genome, most of the proteins required for function are encoded within the nucleus and need to be imported into mitochondria. As a result, many of these import components are essential for viability, making their study via canonical knockdown methods extremely difficult. To this end, small molecules have been identified that block these proteins temporally. Here I describe the work done to characterize 2 inhibitors of mitochondrial function identified in the laboratory. Through the work done with zebrafish, we show that these drugs affect particular aspects of embryonic development, providing validation for the MitoBloCK compounds as tools for targeted *in vivo* study, as well as providing information as to

the importance and role of mitochondria during embryonic development. Over the past decade neurodegenerative diseases such as Parkinson's disease and Huntington's disease have been found to contain pathological links to mitochondrial dysfunction. Additionally, many known mitochondrial myopathies such as Leigh's syndrome and MERRF have neurodegenerative components.

Here we utilize the MitoBloCK compounds to study mitochondrial function and dynamics in motor neuron development. Through small molecule treatment with MitoBloCK-6, an identified inhibitor of mitochondrial import protein ALR, I show that inhibition of ALR results in a significant decrease in the growth and branching of developing zebrafish motor neurons. Additionally, treatment with MitoBloCK-6 drastically reduces the distance and velocity of mitochondrial trafficking within axonal projections. Together, this work illustrates a new method for studying mitochondrial biology *in vivo,* and highlights the important role mitochondria play in development as a whole, as well as specifically within neuronal environment.

The dissertation of Meghan Elizabeth Johnson is approved.

Catherine F. Clarke

Jay D. Gralla

Michael A. Teitell

Alexander M. van der Bliek

Carla M. Koehler, Committee Chair

University of California, Los Angeles

2012

DEDICATION PAGE

This dissertation is dedicated to my grandfathers for their encouragement and love. They taught me that if you work diligently and believe in your convictions, anything is possible.

TABLE OF CONTENTS

LIST OF FIGURES

ACKNOWLEDGMENTS

I would first like to thank my mentor, Carla M. Koehler, for her guidance and support during my graduate tenure. This project exemplifies a new avenue of research focus in our lab, and her patience and never-ending efforts helped me progress, and succeed. It has been a privilege to work under, and be trained by, her. I also extend my gratitude to the other members of my committee: Catherine F. Clarke, Jay D. Gralla, Michael A. Teitell, and Alexander M. van der Bliek, for their encouragement along the way.

I thank the Cell and Molecular Biology Training Grant (Ruth L. Kirschstein National Research Service Award GM007185) for funding and supporting this work. I also would like to extend my appreciation to Susan Walsh, for teaching me everything I know about working with zebrafish. Her knowledge and instruction was instrumental to the development and execution of this project.

I would like to acknowledge Samuel A. Hasson and Deepa V. Dabir for their role and contributions to the previous research done with Mito-BloCK-2 and MitoBloCK-6. Without their screens to identify, and then subsequently characterize, these modulators of mitochondrial function, none of the work here would have been possible. Chapter 2 contains information adapted from a manuscript currently in submission to *Developmental Cell*, titled "A Small Molecule Inhibitor of Redox-Regulated Protein Translocation Into Mitochondria" by Deepa V. Dabir, Samuel A. Hasson, Kiyoko Setoguchi, Meghan E. Johnson, Johannes Zimmerman, Robert Damoiseaux, Michael A. Teitell, and Carla M. Koehler.

I could not have gotten through the challenging times of graduate education without my colleagues, the current, and former, members of the Koehler Nation: Susan Walsh, Deepa Dabir, Non Miyata, Esther Nüebel, Janos Steffen, Geng Wang, Yavuz Oktay, Heather Tienson, Samuel

Hasson, Jenny Glavin, Sonya Neal, Colin Douglas, Juwina Wijaya, Matthew Maland, Eriko Shimada, Moses Liau, Tanya Hioe, Justin Hotter, Samuel Irving, Cennyanna Boon, and Sravya Keremane. I thank them for their assistance and technical knowledge during experiments, for their discussions of results, for providing materials, and (most importantly) for their friendship. I would also like to thank Alvaro Sagasti and the members of the Sagasti lab for allowing me access to their confocal microscope, for sharing plasmids with me, and for the discussions on neuronal biology. Their expertise was invaluable and much appreciated.

I would like to extend a special thank you to Colin Douglas for always being there for me, and for having faith in me whenever I temporarily lost it in myself. Lastly, I offer my most heartfelt gratitude and appreciation to my parents, Gerard and Judith Johnson, my sister Sarah, and the rest of my extended family, for the love and encouragement they have shown me over the years. My parents instilled their passion for research in me, and nurtured my dreams and aspirations with unwavering support and fervor. They taught me to wonder, to question, and to truly love science: all through a lesson about chickenpox and quizzes at the dinner table. Without my family, I would never succeed.

VITA

2003	Summer Intern Centocor, Inc. Radnor, Pennsylvania
2004	Summer Internship Sanofi-Aventis Malvern, Pennsylvania
2005-2007	Undergraduate Researcher Department of Biochemistry and Biophysics University of Pennsylvania Medical School Philadelphia, Pennsylvania
2007	B.A. in Biochemistry University of Pennsylvania Philadelphia, Pennsylvania
2008	Teaching Assistant Department of Chemistry and Biochemistry University of California Los Angeles Los Angeles, California
2011	Teaching Assistant Department of Chemistry and Biochemistry University of California Los Angeles Los Angeles, California

PUBLICATIONS AND PRESENTATIONS

Johnson, M.E., Liau W.S., and Koehler, C.M. (2009) Developing Zebrafish as a Model for Mitochondrial Myopathies. Presented at Annual Molecular Biology Institute Lake Arrowhead Retreat, Lake Arrowhead, California.

Dabir, D.V. Hasson, S.A., **Johnson, M.E.**, Zimmerman, J., Damoiseaux, R., and Koehler C.M. (2010) Chemical Inhibitors of the Erv1 Mitochondrial Oxidative Folding Pathway by a Small Molecule Inhibitor. Presented at Gordon Research Conference: Protein Transport Across Cell Membranes, Galveston, Texas.

Johnson, M.E., Dabir, D.V., Hasson, S.A., and Koehler C.M. (2010) Mitochondrial Protein Translocation Inhibitors Cause Defects in Cardiac and Somite Development. Presented at 9th International Conference in Zebrafish Development and Genetics, Madison, Wisconsin.

Johnson, M.E., Dabir, D.V. Hasson, S.A., and Koehler C.M. (2011) Small Molecule Modulators of Erv1 Alter Protein Import and Impair Development in Zebrafish. Presented at EMBO Conference Series: Protein Transport Systems: Structures, Mechanisms, and Medical Aspects, Santa Margherita di Pula, Italy.

Johnson, M.E., Dabir, D.V., Hasson, S.A., and Koehler, C.M. (2011) Mitochondrial Biogenesis in Studies in Zebrafish. Presented at 4th Strategic Conference of Zebrafish Investigators, Pacific Grove, California.

Johnson, M.E. (2011) Mitochondrial Studies: Fishing for Information. Presented during Cell and Molecular Biology Seminar Series, Los Angeles, California.

Johnson, M.E., Dabir, D.V., and Koehler C.M. (2012) Small Molecule Modulators of Erv1 Alter Protein Import and Impair Development in Zebrafish. Presented at Gordon Research Conference: Protein Transport Across Cell Membranes, Galveston, Texas.

Johnson, M.E. (2012) Small Molecule Modulators of Erv1 Alter Protein Import and Impair Development in Zebrafish. Presented at Gordon Research Conference: Protein Transport Across Cell Membranes, Galveston, Texas.

Johnson, M.E. (2012) Small Molecule Modulators of Erv1 Alter Protein Import and Impair Development in Zebrafish. Presented during Cell and Molecular Biology Seminar Series, Los Angeles, California.

Dabir, D.V., Hasson, S.A., Setoguchi, K., **Johnson, M.E.**, Zimmerman, J., Damoiseaux, R., Teitell, M.A., and Koehler C.M. (2012) A Small Molecule Inhibitor of Redox-Regulated Protein Translocation into Mitochondria. Developmental Cell (in submission).

AWARDS

2007–2012	University Fellowship University of California Los Angeles Los Angeles, California
2008	Excellence in Teaching Award Department of Chemistry and Biochemistry University of California Los Angeles Los Angeles, California
2009–2012	Cell and Molecular Biology Training Grant University of California Los Angeles Los Angeles, California

Chapter 1: Introduction – Zebrafish as a Model Organism: A Practical Way to Study Mitochondrial Function in a Vertebrate System

Abstract

Zebrafish (*Danio rerio*) have served as a model for developmental study for more than 70 years but they have recently begun to be used for genetic and proteomic study. With their ability to produce many progeny in a single crossing utilizing external fertilization, the optical clarity of the embryo, and rapid and well-documented developmental patterns, makes them ideal organisms to serve as vertebrate models for molecular study as well as human disease mimicry. Zebrafish also have a completely sequenced genome, the majority of which is mapped and characterized. On a cellular level, the mitochondria of zebrafish are very homologous to humans, including the respiratory chain mitochondrial DNA organization and structure, and protein import pathways. Here we discuss the benefits that make zebrafish an ideal vertebrate model organism, the intricate pathways and functions of the mitochondrion, and the aspects that show that zebrafish provide a useful platform for studying mitochondrial biology.

Introduction

Mouse as a Model

Much of biomedical research involving the study of human disease is conducted through the use of animal models. Beginning in the early 1980s, mouse *(Mus musculus)* models were designed to mimic human problems in a workable vertebrate system.(1) There is a remarkable gene homology between mice and humans. Approximately 90% homology exists between the 2.5 Gb mouse genome and the 2.9 Gb human genome.(2) Of the estimated 30,000 protein genes encoded by the genomes, there is an average of 70% homology on the amino acid level.(2,3) Mouse embryos can be genetically modified via direct injection of DNA or manipulation of embryonic stem cells.(4)

The average gestation period of a mouse is between 19 and 20 days, and each mating can yield an average litter size of 6 to 8 pups approximately every 3 weeks.(4) Generation time is approximately 12 weeks (3 weeks for gestation, 3 to 4 weeks for suckling, and 5 to 6 weeks to reach sexual maturity).(5) Once the mouse has reached maturity, it can be crossed for approximately 7 or 8 months before retirement, producing 4 or more litters, though some strains are capable of producing only 2 litters.(5) Through calculation, it can be deduced that a breeding pair of mice can produce approximately 50 offspring over the course of their breeding span.

Although mice are still used as the primary vertebrate model organism in laboratories worldwide, there are drawbacks to their usage. It takes a large number of mice to produce enough material for many embryonic studies. Additionally, embryo development occurs internally within the mother, requiring surgery if early developmental stages are to be studied and making it virtually impossible for real-time observation.(4) Maintaining mouse colonies and

performing diagnostic testing, such as pregnancy assays and genotyping of progeny, can be time consuming as well as expensive.

Zebrafish as a Model

Using zebrafish as an alternative vertebrate model to mouse eliminates many of these drawbacks. Other systems such as the fruit fly *(Drosophila melanogaster)* or nematode worm *(Caenorhabditis elegans)* may be effective models for studying certain cellular processes, but they fall short when trying to observe vertebrate-specific features, such as the kidney, complex-heart development, and multicell lineage hematopoiesis, to name a few.(6) Zebrafish *(Danio rerio)* have been studied as a classical developmental model for decades, beginning as early as the 1930s.(7) As an organism, zebrafish are inexpensive to procure from commercial sources, and are easily maintained using a contained water filtration setup.(8,9) Because its circadian clock governs many zebrafish behaviors, including mating, and because the clock is completely reliant on photosensitivity, ideal conditions are achieved when zebrafish are kept on a strict day/night schedule.(10) It is accepted practice to maintain zebrafish on a 14-hour-light/10-hour-dark cycle.

When treated and cared for properly, mating zebrafish can produce hundreds of embryos at a time.(11) Moreover, the unique characteristics of the zebrafish embryo make it ideally suited for developmental study. Zebrafish embryos are released and mature externally from parental fish, allowing for quick and simple collection of embryos upon fertilization.(7) The embryo is also surrounded by a proteinaceous shell, the chorion, that is optically clear, allowing for real-time observation of all developmental stages, beginning as early as the single-cell stage.(12)

Zebrafish Embryonic Development

Zebrafish follow a well-documented developmental pattern, allowing for specific points in development to be targeted for research purposes. During the zygote and cleavage stages, the embryo goes through several rapid rounds of synchronous division beginning approximately 45 minutes after fertilization (Figure 1.1: A–F).(13) Following the rounds of synchronous division, longer, asynchronous cleavage occurs (approximately 3 hours post fertilization); giving way to the blastula and gastrula periods (Figure 1.1: G–N). During these epibolic phases, involution, convergence, and extension of the epiblast, and formation of the embryonic axis can be noticed.(13)

Ten hours after fertilization, segmentation begins, giving rise to 30 to 34 somites (Figure 1: O–P).(14) In zebrafish, somites develop predominantly into skeletal muscle, with a minor portion developing into vertebrae.(15) Subsequently, after segmentation, the pharyngula period begins. The body axis straightens out, pigmentation appears, and circulation can be seen. This phase begins approximately 24 hours after fertilization and lasts for another 24 hours (Figure 1.1: Q–R).(13)

During this period, the emergence of the heart can be seen (Figure 1.1: R, arrow). The heart is one of the first organs to develop in zebrafish, with cardiac progenitor cells developing around 5 hours post fertilization; however, these cells do not form the premature heart, or cardiac disc, until approximately 22 hours post fertilization.(16) Following formation, the cardiac disc migrates laterally, with the ventricle moving right toward the anterior, and the atrium migrating left toward the posterior. The 2 chambers then begin to balloon and expand, ultimately leading

to the constriction of the atrioventricular canal, and looping of the chambers; beginning around 40 hours post fertilization.(16)

Beginning at 48 hours post fertilization, most embryos start hatching and are considered larvae. During this time, organ systems are in rapid formation as well, and cartilage has begun developing in the head and tail. Between 48 and 60 hours post fertilization, one can see the obtrusion and expansion of the pectoral fins, and the primary appearance of a small mouth forming between the eyes. By 72 hours the mouth has become protruding, and the beginnings of gill slits and gill filaments can be seen (Figure 1.1: S, arrow). Also at 72 hours, one can see the appearance of the first visible bone within the larvae.(13)

From 72 to 96 hours post fertilization, the swim bladder inflates and the gut tube drops more ventrally (Figure 1.1: T, arrow). During this period, the larvae begin to swim around more actively and are able to move their jaws, pectoral fins, and eyes rapidly and accurately.(13) They are also able to respond to external stimuli with hasty precision. Between 5 and 7 days post fertilization, the yolk sack is depleted and embryos must be fed exogenously.(17)

At 5 days post fertilization, the zebrafish larvae can be transferred to nursery tanks for further growth. Until the larvae reach 14 days post fertilization, they need to be fed baby food that is 50 μM or smaller because their mouths are too small to eat brine shrimp. Zebrafish are considered adolescents from 21 days post fertilization until 3 months post fertilization, at which point the fish have reached sexual maturity and are able to produce offspring.(18)

Zebrafish have been used for decades as models for developmental study, but it is only recently that they have been analyzed on a genomic and proteomic level.(7) Zebrafish also have a close gene homology to humans. The zebrafish genome is markedly smaller (1.5 billion bases split between 25 chromosomes) than the human genome (2.9 billion bases split between 23

chromosomes).(19,20) It is estimated that the human genome has approximately 20,000 to 25,000 protein-encoding genes.(21)

Although sequencing has been completed on the zebrafish genome, mapping is still ongoing, so it is currently unknown how many genes are encoded. It is expected that gene number will be on par with other known vertebrates because the base-pair numbers compare. At some time in evolutionary history, the zebrafish genome underwent a gene duplication event, resulting in a number of genes with multiple isoforms, many of which encode for proteins within the mitochondrion.(22,23) This duplication is another benefit of using zebrafish as a model because it allows for the study of proteins that are normally considered lethal when knocked down.

Perhaps the founding advantage that hurtled zebrafish as a model organism to the forefront of developmental biology is its susceptibility to genetic manipulation. Because zebrafish are external fertilizers, embryos can be collected immediately after formation and genes can be introduced or targeted for knockdown almost immediately upon conception.

Genetic Knockdown: Morpholinos

Much of zebrafish gene manipulation is done through the use of morpholinos.(24) Morpholinos are synthetic oligonucleotides that are approximately 20 to 25 nucleotides in length.(25,26) They comprise typical nucleic acid bases bound to a morpholine rings instead of the customary deoxyribose or ribose rings.(27) The main difference between morpholine rings and deoxyribose or ribose rings is that they have phosphorodiamidate base-pair linkages instead of phosphodiester bonds.(27)

Because of the nonionic nature of the phosphorodiamidate linkage, morpholinos cannot be elongated by normal transcriptional methods, so they cannot be altered.(26) They also are not degraded by typical cell nucleases, nor do they activate immune responses or modify the methylation of DNA.(28) The actual longevity of morpholino levels in an organism varies widely for each morpholino. Some are active for only a few hours, whereas others can still be detected days later, depending on protein concentration (dilution effects occur as the organism develops and grows over time) and the specificity of the morpholino.(29)

Morpholinos bind to the primary sequence of mRNA and block protein expression via 2 different mechanisms (Figure 1.2). Translation-blocking morpholinos bind to the ATG start codon of the mRNA sequence, inhibiting the ability of the tRNA carrying the initial methionine to start translation (Figure 1.2: B).(25) Splice-blocking morpholinos are designed to bind to the border of an exon and intron, blocking the spliceosome from removing introns from the sequence, causing an unspliced transcript or an alternatively spliced transcript to arise (Figure 1.2: C).(30) When the aberrantly spliced transcript is subsequently translated, a frame-shift or premature stop codon is generated, thus producing a protein that is partially or completely nonfunctional.(31) Detection of morpholino activity is relatively straightforward. When translation-blocking morpholinos are used, protein levels can be measured using quantitative western blotting techniques, whereas when splice-blocking morpholinos are injected, polymerase chain reaction (PCR) can be conducted on cDNA generated by reverse transcriptase on RNA isolated from zebrafish embryos.(31,32)

To show evidence for the specificity of the morpholino, mRNA rescue experiments are usually performed. In a rescue experiment, mRNA is coinjected with the morpholino at the early cell stage. The sequence can be altered to eliminate the morpholino-binding site or, as is more

commonly the case, mRNA from another organism can be injected. In zebrafish, mRNA of the human homolog is often injected.(33)

Genetic Introduction: DNA Injection and Transposition

In addition to gene knockdown, DNA can also be introduced into the organism for expression. There are 2 ways for inducing the expression of genes of interest: in a transient manner (in which the specified product is only expressed in the intended target fish and for a finite period of time), and in a germ line–integrated manner (in which the desired gene is integrated into the zebrafish genome and can be passed down to progeny).(34,35)

Transient expression is usually done through microinjection of RNA.(36) mRNA encoding for the desired protein is injected into the single-cell stage of a zebrafish embryo. The endogenous cellular machinery then translates the mRNA, expressing the protein in cells presenting the transcript.(36) Transient expression is fleeting; it occurs very early after injection and often lasts only a few hours or days.(36) The promoter used to drive expression and the turnover rate of the mRNA transcript, as well as the protein generated, dictate the longevity of expression.(36)

DNA integration is needed for long-term expression as well as for generating lines of fish that can pass down the introduced genes of interest to their progeny. Genetic integration allows for proteins to be studied at all stages of development—both embryonic and adult—because protein synthesis is under cellular control and can be constantly produced. To introduce a gene for integration, cDNA encoding the gene is cloned onto a plasmid between 2 flanking Tol2 transposition sites (Figure 1.3).(37) This plasmid, as well as RNA coding for the transposase protein, is injected into the single-cell stage of the embryo. Cellular machinery then translates

the transposase protein, which in turn integrates the gene of interest somewhere into the genome through homologous recombination at the Tol2 sites.(37) For genes that are unmarked, it is often useful to include a fluorescent-transgenesis marker with this type of integration.(38) This marker is only expressed when the gene has been transposed, thus making it easy to screen injected embryos for successful integration. To further confirm integration into the zebrafish genome, fin clips can be utilized.(39) This process takes advantage of the regenerative process of the tail fin. A portion of the tail fin can be cut off from zebrafish, and the fin will grow back with no detriment to the organism. DNA can then be isolated from the cells from the clipped fin, and screening for the integrated gene of interest can be accomplished through PCR.(39)

A typical manipulation and unification of both the transient and germ-line integration techniques is to use the yeast Gal4-UAS system first pioneered in *D melanogaster*.(40) Typically, the promoter of interest is cloned in front of the gene encoding for the Gal4 protein and a UAS sequence is placed in front of the desired gene of interest (Figure 1.4). The Gal4 protein driven by the included promoter is only expressed in the cells that typically express that promoter (eg, cardiac myocyte light chain 2 *[cmlc2]* drives protein expression only in cardiac cells in zebrafish).(41,42) Concurrently, the UAS gene is only expressed in cells in which the Gal4 is also concomitantly expressed.(41) Germ-line expression of a Gal4-driven protein can be used to regulate the expression of a variety of UAS-driven specific genes, thus yielding very controlled and exclusive expression of the protein of interest within specific embryonic tissues.

Zebrafish Biochemistry

In addition to genetic manipulation, zebrafish are amenable to a variety of other biochemical assays and techniques. Embryos can be dissociated and subjected to SDS-PAGE

gel electrophoresis to identify target proteins; nucleic acid levels can be monitored through *in situ* hybridization assays.(14,43,44) Similar to tissues from other organisms, both embryos and adult fish can be cryopreserved or paraffin embedded, sectioned, and stained by normal histological methods.(14,45) Zebrafish embryos are also uniquely suited in that the embryo in its entirety is osmotically permeable and, as a result, can be subjected to whole-mount staining.(46)

The best usage of zebrafish though, is fluorescent imaging. Because embryos are optically clear, individual proteins, or cellular components, can be fluorescently labeled and monitored through microscopic imaging in real time.(47) GFP and DsRed were the first and remain the most common fluorescent proteins used for transgenic marking because they are highly stable, moderately resistant to photo-bleaching, and can be detected reasonably simply by a variety of microscopic techniques.(47-49) Since its inception, there are now a number of fluorescent proteins available for use in addition to GFP and DsRed, including mcherry, tomato, and BFP, although some have brighter signals than others.(50,51) In addition, photoconvertible proteins have been created that can be switched from green fluorescence to red fluorescence through laser excitation.(52) Photoconversion is a unique tool that allows for specific dynamics such as protein turnover to be studied.(53) When paired with the transgenic expression systems discussed previously, lines of zebrafish can be generated that exhibit reporter fluorescence in specific regions of choice. As mentioned previously, the *cmlc2* promoter placed in front of green fluorescent protein (GFP), for example, expresses GFP in the heart cells (Figure 1.5).(42)

Zebrafish and Drug Discovery

Recently zebrafish have begun to be used for high-throughput screening assays.(11) At a time when small-molecule discovery and development is at the forefront of biochemical

research, zebrafish provide the means to perform *en masse* small-molecule screens on a living organism.(12,54) Although this is not a new concept (drug screens have previously been conducted on *D melanogaster* and *C elegans*), zebrafish provide the ability to observe the effects on a vertebrate organism, thus yielding a more closely relatable phenotype to the human response than what would be observed with the fruit fly or the nematode worm.(12,55,56)

As the zebrafish genome is also completely sequenced, lines of fish exist that have a known, sequenced, and characterized genetic background, similar to strains of yeast or mice.(24,57)(24,57) Zebrafish typically produce between 200 and 300 embryos per mating pair, which is ideal for screening purposes.(11,58)(11,58) Although adult fish are not conducive to small-molecule treatment because of their size, embryos can survive in as little as 50 μL of water, allowing them to be contained in 96- or 384-well plates without issue.(11)(11) This large-plate set-up allows for small molecules to be dispensed to the embryos through robotic systems, and essential component of the high-throughput process.(58,59)(58,59)

Embryonic screening can be conducted for a variety of different reasons. Because embryos are osmotically permeable, small molecules are able to diffuse through the embryo, thus providing insight into the adsorption, biodistribution, and tissue specificity of a possible therapeutic agent.(11) Toxicity of potential therapeutic agents can also be evaluated, although it is necessary to note that the metabolic processes of zebrafish are not completely understood.(60,61) It is in generalities that a drug's toxicity may be evaluated; the specific mechanisms of metabolic breakdown and the metabolites generated may remain a mystery. By comparing the phenotypes of zebrafish treated with a small molecule with those of zebrafish subjected to morpholino injection or alternate forms of knockdown, off-target effects may be identified for compounds thought to affect specific proteins or pathways.(62)

Although there are some genes present in humans that are not present in fish, and vice versa, there is enough similarity between the 2 organisms that studies conducted in zebrafish can shed a great deal of light on human processes. On a cellular level, the specific intricacies of the mitochondrion can be elucidated utilizing zebrafish.

The Mitochondrion

When looking at both humans and zebrafish on a mitochondrial level, a number of similarities arise. The mitochondrion is a complex organelle that is present in all vertebrate organisms. It is dual-membrane bound, and consists of 4 distinct compartments, or regions: the outer membrane, the intermembrane space, the inner membrane, and the matrix.(63) It is estimated that there are 600 to 1000 proteins present in the mitochondrial proteome, yet only a small percentage of these are encoded by the mitochondrial genome.(64-66)

The Mitochondrial Genome and the Respiratory Chain

Most animal mitochondrial genomes are approximately 16,000 base pairs in length and encode for the same 37 genes: 22 tRNAs, 2 rRNAs, 13 proteins, and 1 untranslated region.(67) The organization and structure is virtually identical between human and zebrafish. Human mitochondrial DNA contains 16,569 base pairs, whereas zebrafish mitochondrial DNA contains 16, 596 base pairs (Figure 1.6).(68,69) When analyzed against one another, there is 61% homology between the 2 sequences, indicating a high level of evolutionary conservation.

All protein genes encoded by the mitochondrial genome are subunits of the complexes of the respiratory chain, the most noted occupation of the mitochondrion. The respiratory chain is responsible for shuttling electrons generated during cellular catabolic processes through a system

of protein complexes, generating energy that can be harnessed as ATP for biosynthetic reactions. (Figure 1.7) Electrons harnessed as NADH are brought to NADH dehydrogenase (Complex I).(70) Complex I comprises 45 polypeptide fragments, and 8 iron-sulfur (Fe-S) clusters.(71) Electrons are initially transferred from NADH to a prosthetic FMN group, through the series of Fe-S clusters, with the final acceptor being coenzyme Q.(72) While this transfer is taking place, the first in a series of hydrogen ion translocations from the matrix to the intermembrane space occurs.(72,73) Coenzyme Q also collects electrons from succinate dehydrogenase (Complex II), a protein complex containing 4 subunits that transfers electrons from succinate, via FAD.(73) Because coenzyme Q is fat soluble, it is uniquely suited to act as a transport between the first 2 complexes to the cytochrome bc_1 complex (Complex III). Complex III uses a shuttling pathway, known as Q-cycling, to ultimately pass electrons from coenzyme Q to cytochrome *c*; again pumping hydrogen ions to the intermembrane space in the process.(74) Cytochrome *c*, another lipid-soluble molecule, then traverses through the membrane, to cytochrome *c* oxidase (Complex IV).(75) In Complex IV, electrons are transferred from cytochrome *c* to the final electron acceptor, molecular oxygen, transporting the final few hydrogen ions for the proton gradient.(76) These protons are then coupled with the ATP synthesis when they are reverse-pumped back into the matrix through ATP synthase (Complex V).(77)

Mitochondrial Protein Translocation

Although the respiratory chain is the most noted aspect of mitochondrial function, many other metabolic processes, such as the citric acid cycle or lipid oxidation, occur there.(78,79) The proteins required for these processes are all encoded within the nucleus, are translated in the cytosol, and need to be translocated into their designated compartments within the

mitochondrion. As a result, a complex system of translocation and assembly apparatuses exist within the various compartments of the mitochondria to aid in sorting all incoming precursor proteins (Figure 1.8). The first complex these pre-proteins encounter is the translocase of the outer membrane (TOM).(80,81) The TOM complex comprises 7 integral membrane proteins (Tom70p, Tom40p, Tom22p, Tom20p, Tom7p, Tom6p, and Tom5p) that aid pre-proteins in crossing the outer membrane.(80-83) Proteins that are destined for integration into the outer membrane are segregated through the sorting and assembly (SAM) mechanism, which comprises 2 proteins, Sam50p and Mas37p (Figure 1.8: A).(84-86)

Proteins destined for the inner membrane and matrix must go through another translocase, the translocase of the inner membrane (TIM). There are 2 TIM complexes in mitochondria: the TIM23 complex and the TIM22 complex. Precursor proteins destined for the matrix contain and *N*-terminal targeting sequence and are funneled through the TIM23 complex (Figure 1.8: C).(80,81) Three integral membrane proteins make up the core of theTIM23 complex: Tim50p, Tim17p, and Tim 23p.(80,81,87) Tim50p acts as a receptor to guide incoming precursors through the Tim23 pore, which comprises Tim17p and Tim23p.(88) Translocation through the TIM23 complex would not be possible without the membrane potential, which is provided by Tim44p, Tim14p, mHsp70, and mGrpE.(89) Together these proteins make up the translocation motor, providing the electrophoretic effect needed to attract the positively charged presequence of the precursor proteins.(90)

Proteins destined for integration within the inner membrane proceed through the TIM22 complex (Figure 1.8, B).(91,92) This complex is also comprised of 3 integral membrane proteins, Tim54p, Tim22p, and Tim18p, and acts as a channel through which precursors are inserted into the inner membrane.(92-94) Because the pre-proteins destined for the membrane

are hydrophobic in nature and do not contain an *N*-terminal targeting sequence, they require assistance in traversing the intermembrane space.(95) These carrier proteins, referred to as the "small Tims," form 6-membered complexes comprising 3 subunits of 2 different proteins each, to act as chaperones. Small Tims Tim8p and Tim13p form a complex, and Tim9p and Tim10p form a complex.(96-98) All of the small Tims share a common twin CX_3C motif; and import of these small proteins requires conservation of all 4 thiols.(99,100) Elimination of any of the 4 cysteine residues results in impaired import and improper assembly into the complex formation.(101)

The intermembrane space is an oxidizing environment, compared to the reducing nature of the cytosol, and is very redox sensitive.(102) Many of the proteins in this compartment contain disulfide bonds necessary for carrying out their respective chemical reactions. Proteins such as Cox17p and Cox19p, subunits of the cytochrome *c* oxidase complex, contain twin CX_9C motifs; similar to the CX_3C motifs of the small Tims.(103,104) These proteins also need to be oxidized to fold into their correct conformations after being imported into the intermembrane space from the TOM complex. A disulfide relay organization (the Mia40p-Erv1p pathway) is needed to maintain the activity of the redox-active proteins, such as the small Tims, as well as to fold other cysteine-rich proteins located within the intermembrane space (Figure 1.9).(105,106)

Once precursor proteins are imported through the TOM complex, they encounter Mia40p in the intermembrane space. Mia40p contains 3 disulfide bonds, 2 of which are in a CX_9C motif and appear to maintain a structural role, and 1 disulfide that exists as a CPC triad, located near the *N*-terminus.(107) Incoming proteins undergo a transient disulfide exchange with Mia40p to become oxidized and folded.(107) The redox-active cysteine pair of Mia40p then needs to be reoxidized to accept more electrons and aid in folding other proteins.

Erv1p conducts the oxidation of Mia40p.(103,104) Erv1p is a sulfhydryl oxidase present in the intermembrane space of mitochondria.(108,109) It is imported via the Mia40-Erv1 pathway itself and subsequently folded into its active conformation.(110) In addition to containing an active FAD domain, Erv1 has 2 redox-active cysteine pairs: amino acids C30-33 and C130-C133 in yeast (*Saccharomyces cerevisiae*).(108,111) The C30-C33 pair is located opposite the active site and is responsible for interacting with substrate proteins.(108) Interestingly, although the C30-C33 pair is required for dimerization, it is not needed for catalytic activity. Although a mutant form of the protein (in which the disulfide is deleted) is able to operate catalytically *in vitro,* it cannot be substituted for the wild-type protein *in vivo*, indicating that the C30-C33 pair is essential for *in vivo* activity.(111)

The C130-C133 pair, situated near the active site, transfers electrons to the FAD moiety and is required for the sulfhydryl oxidase to function.(111) Once the substrate has transferred electrons to Erv1p, the electrons are subsequently shuttled from the C30-C33 pair to the C130-C133 pair, and ultimately to the FAD.(108) Once the electrons have been passed to the FAD, they are shuttled through a myriad of electron acceptors, such as cytochrome *c* (which donates them to the electron transport system) or molecular oxygen (initially forming hydrogen peroxide, which is ultimately converted to water by cytochrome *c* peroxidase).(102,112)

From protein translocation to oxidative phosphorylation, the mitochondrion is a complex organelle that still remains largely a mystery. Our laboratory has been working to produce small-molecule tools to revolutionize mitochondrial study. These small molecules allow for the systematic study of synthetically lethal proteins, previously unassayable by typical genetic means. This type of chemical genetics grants the ability to temporally inhibit a protein to observe the effects. Although much of this work has been done *in vitro*, we show that zebrafish

provide a great platform for conducting these types of studies *in vivo*, and expect that more studies will be done on mitochondrial biology using zebrafish in the future.

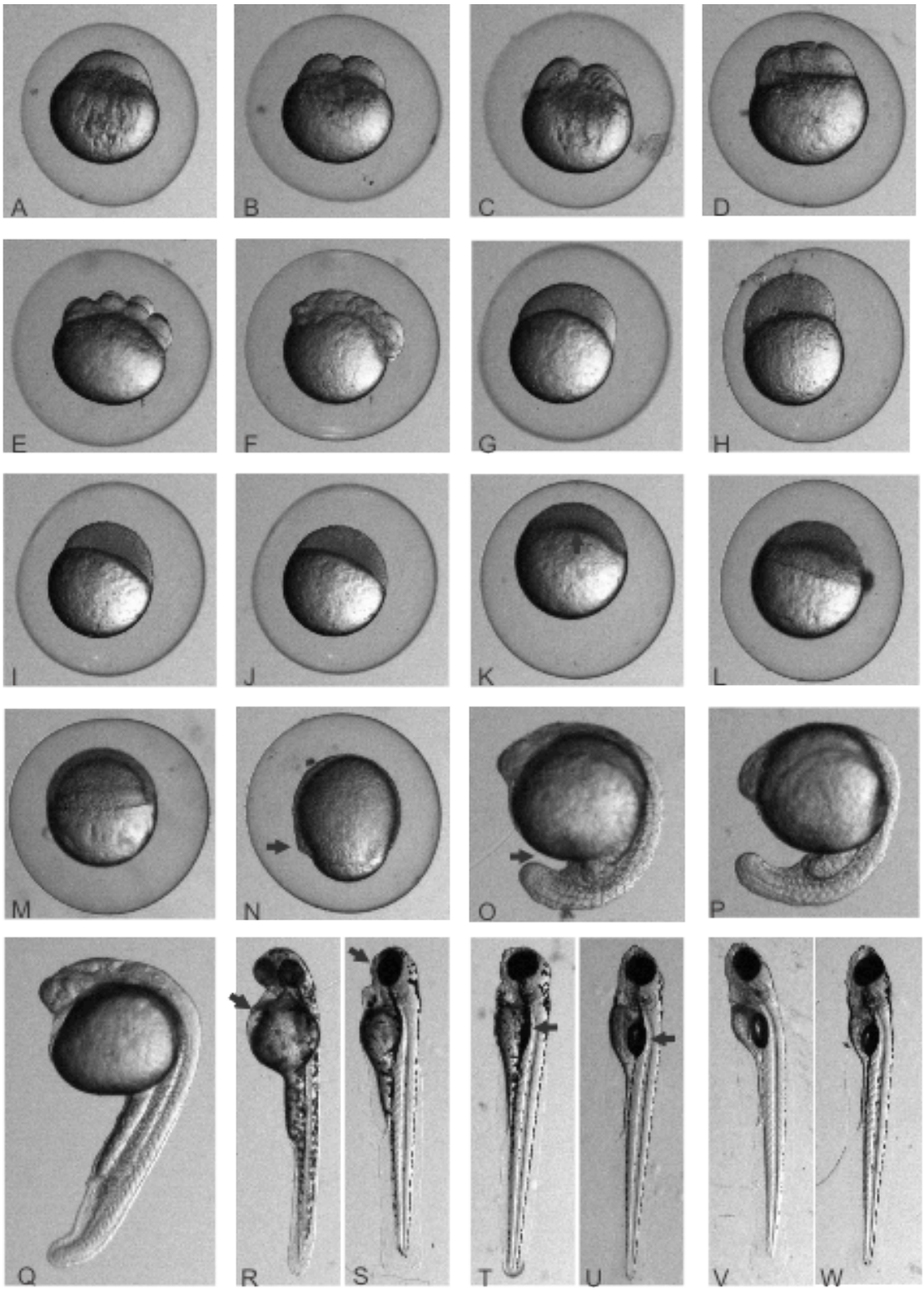
A
B
C
D
E
F
G
H
I
J
K
L
M
N
O
P
Q
R
S
T
U
V
W

Figure 1.1: Stages of embryonic development. A–M are face views. Remaining are left-side views unless where noted with anterior up and dorsal to the left. **A.** 1-cell stage (0.2 h): embryo resides at animal pole (top) and yolk migrates to vegetal pole (bottom). **B.** 2-cell stage (0.75 h). **C.** 4-cell stage (1 h): blastomeres exist as a planar 2 × 2 array. **D.** 8-cell stage (1.25 h): blastomeres exist as a planar 2 × 4 array. **E.** 16-cell stage (1.5 h): blastomeres exist as a planar 4 × 4 array. **F.** 64-cell stage (2 h): blastomeres exist as 3 regular tiers of cells. **G.** 1000-cell stage (3 h): blastula period. The blastodisk appears ball-like and blastomeres reside in 11 tiers. **H.** High stage (3.3 h): beginning of blastodisc flattening. **I.** Oblong stage (3.7 h): flattening becomes elliptical in nature. **J.** Sphere stage (4 h): a flat border exists between yolk and blastodisc, and embryo appears spherical. **K.** Dome stage (4.3 h): embryo stays spherical, but yolk cells bulge inward toward animal pole as epiboly begins (arrow). **L.** 30% epiboly stage (4.7 h): blastodisc thins and spreads uniformly around the yolk. **M.** 50% epiboly stage (5.3 h): blastodisc continues to spread around yolk and remains uniform in thickness. **N.** Bud stage (10 h): right side view, with anterior up and dorsal right. The tail bud becomes visible (arrow). **O.** 16–18 somite stage (~18 h): segmentation period. Extension of the tail begins. **P.** 21–24 somite stage (~20 h): yolk begins to straighten out the posterior of the embryo. **Q.** Prim-5 (24 h): pharyngula period. There are approximately 30 somites, and length of yolk extension equals diameter of yolk ball. **R.** Long-pec stage (48 h): hatching period. Embryo begins to hatch from chorion. Pectoral fins have elongated and heart is clearly visible (arrow). **S.** Protruding-mouth stage (72 h): the mouth is wide open (arrow) and gills have begun to form. **T.** Day 4 (96 h): swim bladder begins to inflate (arrow). **U.** Day 5 (120 h): swim bladder is fully inflated (arrow). **V.** Day 6 (144 h). **W.** Day 7 (168 h). *A-Q imaged at 25x magnification and R-W imaged at 16× magnification using a Leica MZ16F stereoscope*.

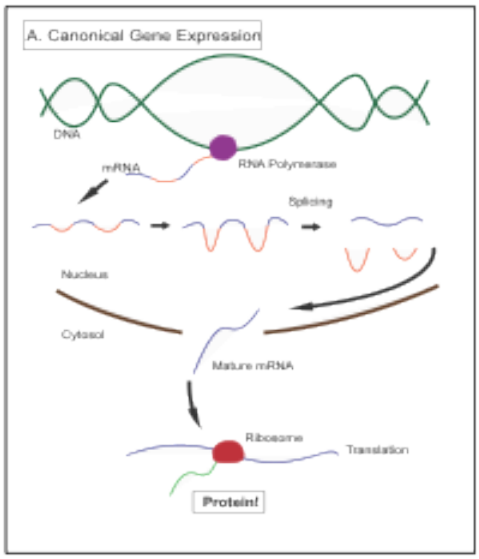

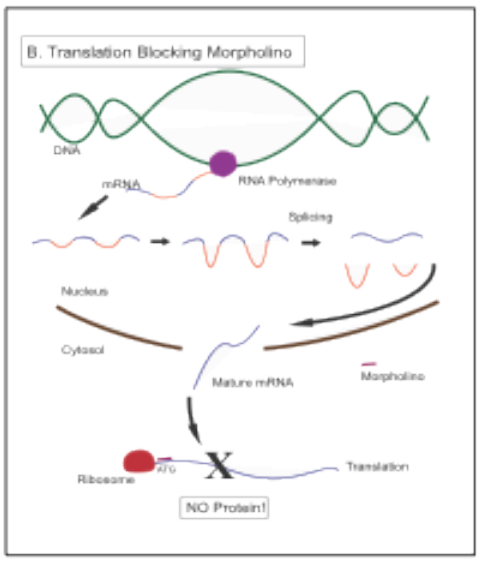

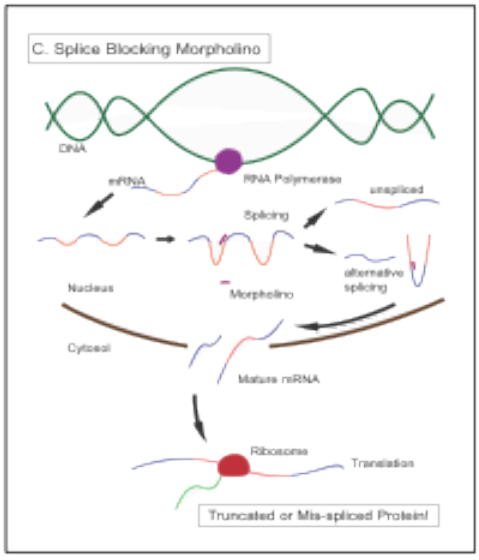

Figure 1.2: Morpholino injection.

A. During normal gene expression, RNA polymerase generates the mRNA transcript of the gene. The introns of the mRNA transcript are then spliced out, generating the mature mRNA. The mRNA is exported to the cytosol, where the ribosome translates the mRNA, synthesizing the protein.

B. When a translation-blocking morpholino is used, transcription and splicing remain unaffected, and the mature mRNA transcript is exported as during normal circumstances. The morpholino then interacts with the mRNA in the cytosol, binding to the ATG start codon after the 5'-UTR, blocking the ribosome from synthesizing the protein.

C. When a splice-blocking morpholino is used, the morpholino binds to the immature mRNA in the nucleus, preventing splicing of a particular intron. The resulting mRNA either remains an unspliced entity at that locus, or alternate splicing occurs. When these mis-spliced transcripts are translated, a truncated or mis-spliced protein can result.

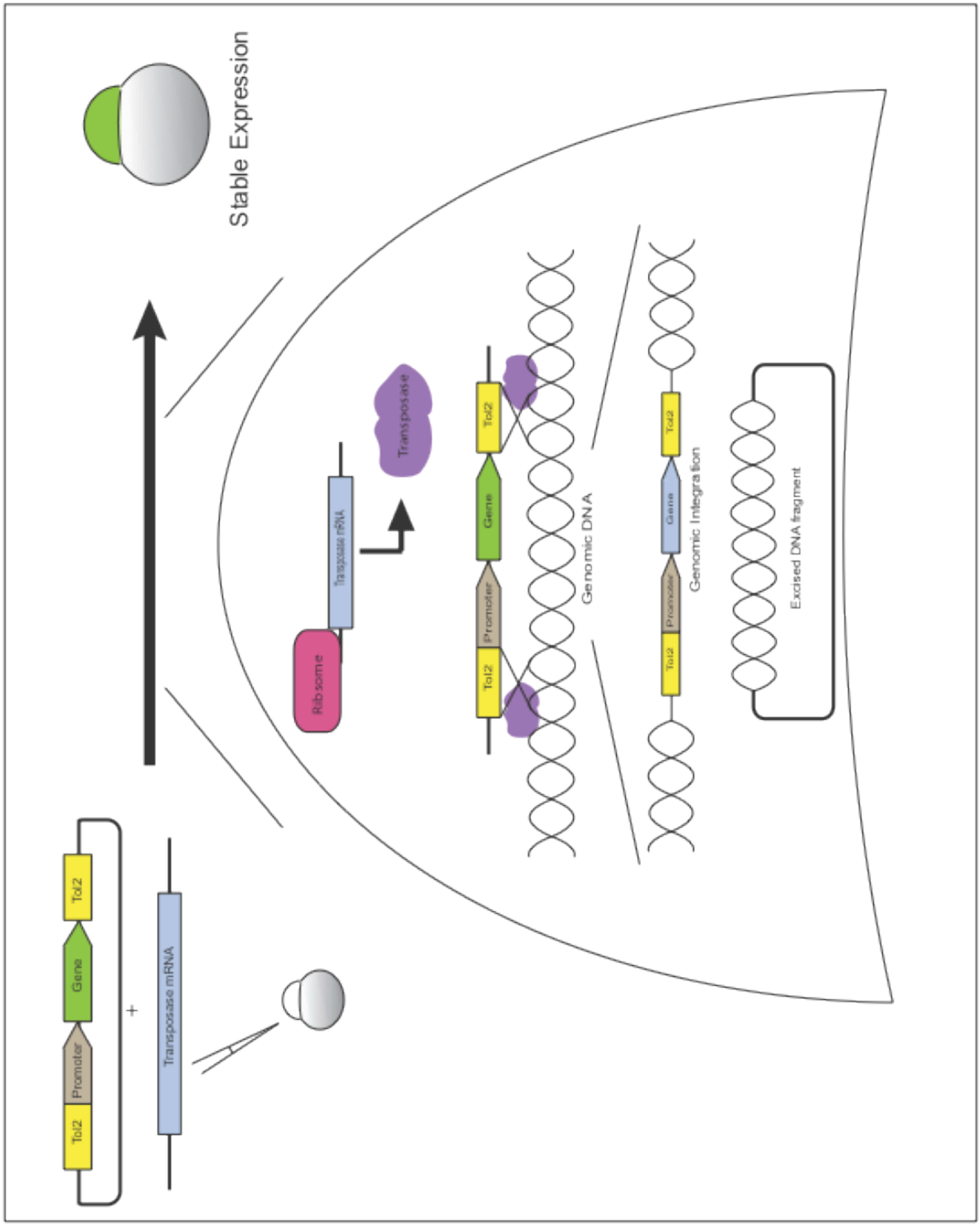
Tol2
Promoter
Gene
Tol2
+
Transposase mRNA
Stable Expression
Ribsome
Transposase mRNA
Transposase
Tol2
Promoter
Gene
Genomic DNA
Tol2
Promoter
Gene
Genomic Integration
Excised DNA fragment

Figure 1.3: The Tol2 method for genetic integration. The desired gene of interest, along with its respective promoter, is cloned between 2 Tol2 transposition insertion sequences. The plasmid and mRNA encoding the transposase protein are then microinjected into the single-cell stage of a developing embryo. The embryo's cellular machinery then translates the mRNA and synthesizes transposase, which integrates the plasmid insert into the genomic DNA through homologous recombination at the Tol2 sites. Insertion can occur many times within a single insertion site, as well as many times throughout the genome, and often results in germ-line transmissibility.

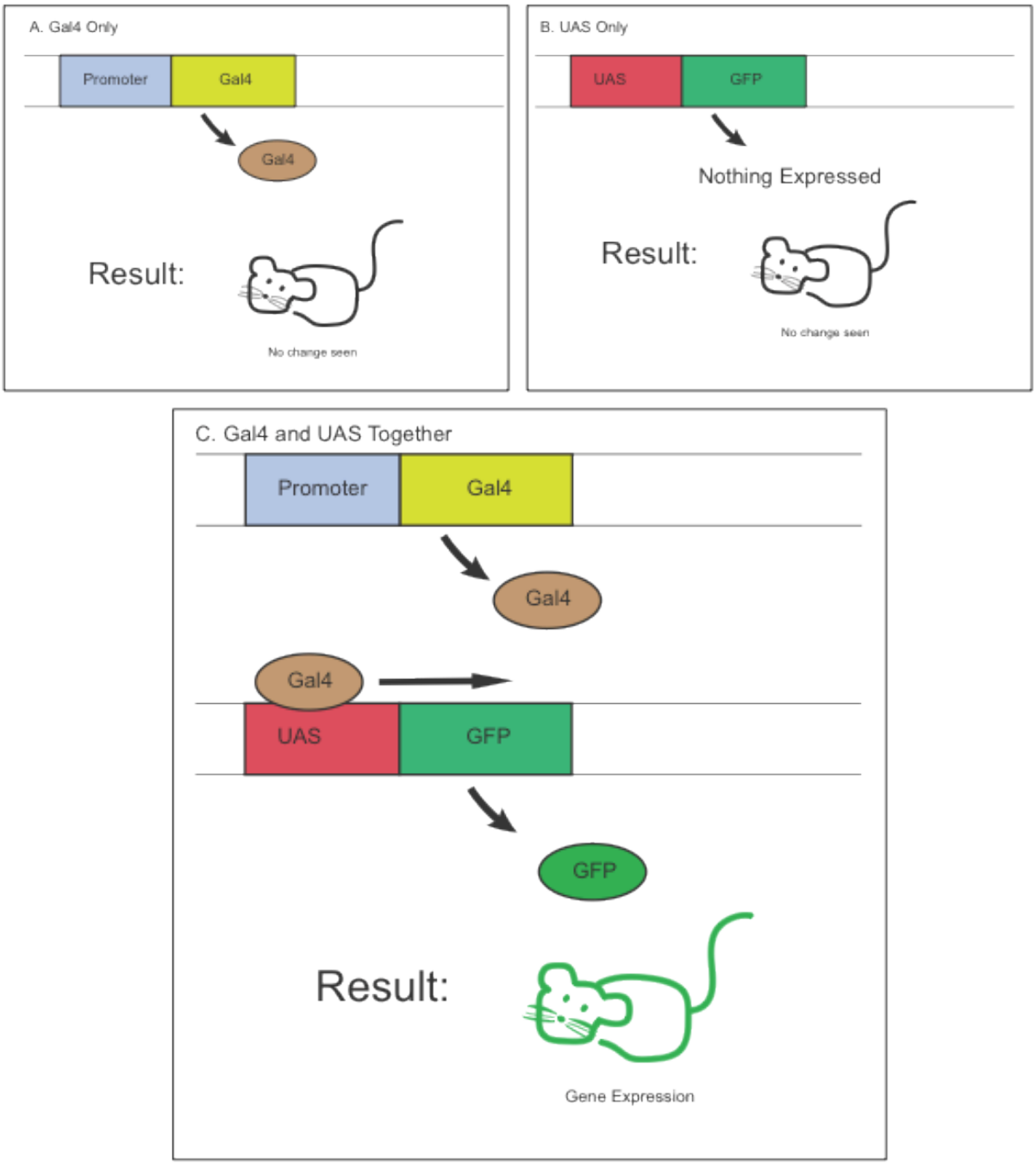
A. Gal4 Only
Promoter
Gal4
Gal4
Result:
No change seen
B. UAS Only
UAS
GFP
Nothing Expressed
Result:
No change seen
C. Gal4 and UAS Together
Promoter
Gal4
Gal4
Gal4
UAS
GFP
GFP
Result:
Gene Expression

Figure 1.4: The Gal4/UAS system. The Gal4/UAS method for protein expression was identified in yeast and utilizes the Gal4 transcription activator protein, which binds to the upstream activator sequence (UAS) enhancer to specifically activate gene expression. **A.** When just the Gal4 protein is introduced, the Gal4 protein is synthesized, but no phenotypic change from wild type is seen. **B.** Similarly, when a gene of interest under the regulation of the UAS enhancer is introduced, the gene cannot be expressed without the transcriptional activator, so no change from wild type is seen. **C.** When both Gal4 and UAS gene are cointroduced, Gal4 is transcribed and translated in cells that express the governing promoter. Gal4 then migrates to and binds the UAS enhancer region, allowing transcription of the gene. In this manner, specific control of gene regulation and activity is achieved.

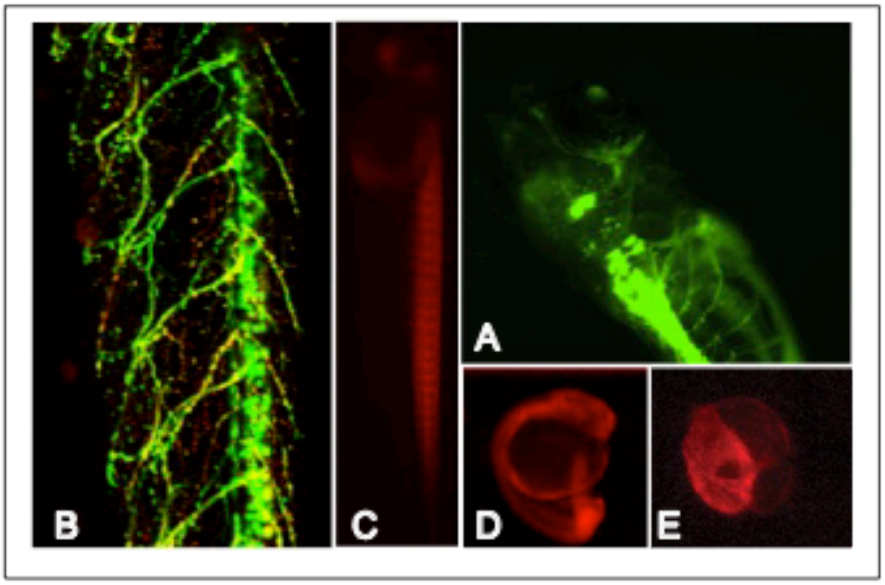

Figure 1.5: Fluorescent lines of zebrafish. Through transgenesis, lines of zebrafish have been generated with fluorescent labeling in different tissues and systems. **A.** Through an enhancer trap screen, a line was generated in which GFP is expressed solely in the motor neurons. **B.** The motor neuron line was enhanced so that mitochondria within the neurons were labeled with DsRed protein. **C.** Zebrafish expressing a mitochondrially targeted DsRed protein (MLS-DsRED) under the α-actin promoter have fluorescent expression only in muscle. **D.** Zebrafish expressing MLS-DsRed under the EF1-α (elongation factor 1-alpha) promoter, have ubiquitous fluorescence. **E.** Zebrafish expressing MLS-DsRed under the cmlc2 (cardiac myocyte light chain 2) promoter have fluorescence only within the heart.

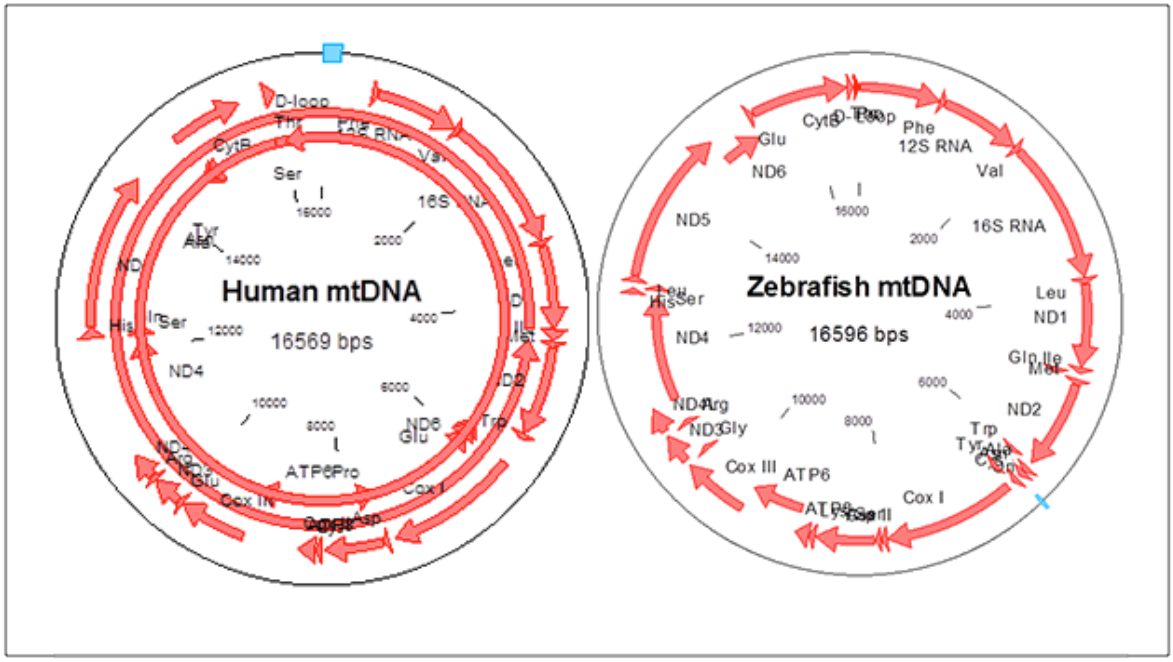

Figure 1.6: Comparison of human and zebrafish mitochondrial genomes. The human and zebrafish mitochondrial genomes are remarkably similar. Both genomes contain 13 protein-encoding genes; 22 tRNAs; 2 rRNAs; and a control region, the D-loop. Although the number of base pairs between the 2 genomes does not differ much, the length of genes encoded is much longer in human mtDNA, causing more overlap between genes to occur.

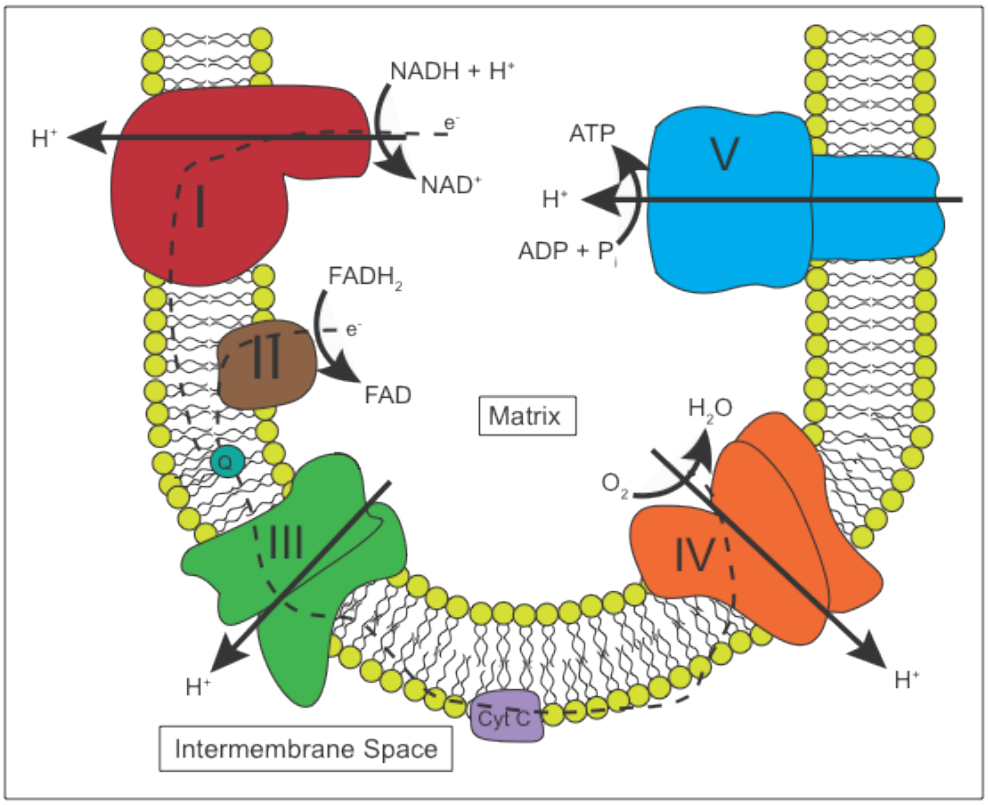

Figure 1.7: The respiratory complexes of the mitochondrion. Electrons shuttled from NADH enter the respiratory chain at Complex I, located in the inner membrane. Electrons are transferred from NADH to coenzyme Q (Q) through a series of iron-sulfur clusters within Complex I, transporting H^+ ions across the membrane from the matrix to the intermembrane space in the process. Similarly, electrons shuttled from $FADH_2$ are transferred to Q through Complex II, although no H+ translocation occurs. Q then travels to Complex III, ultimately transferring electrons to cytochrome *c*, but not before tranlocating more H^+ ions through Q-cycling. Cytochrome *c* then releases the electrons to the final acceptor, O_2, at Complex IV, where more H^+ ions are pumped into the intermembrane space. The translocated protons are then pumped back into the matrix by Complex V, and the energy generated is harnessed to generate ATP from ADP.

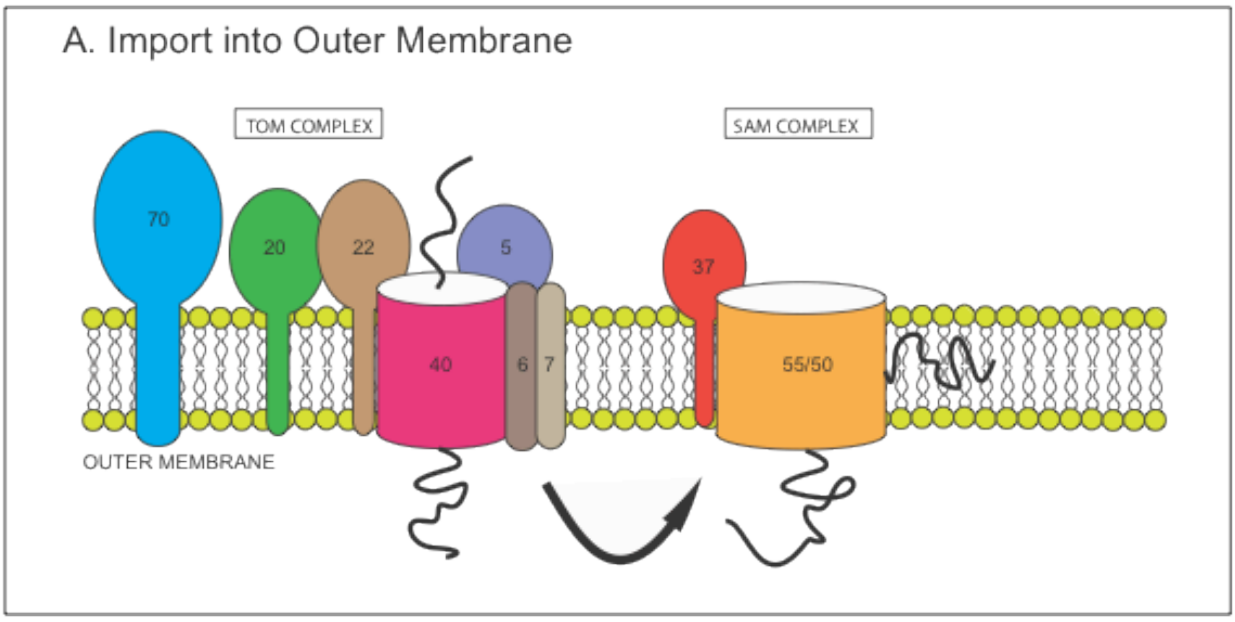
A. Import into Outer Membrane
TOM COMPLEX
SAM COMPLEX
70
20
22
5
37
40
6
7
55/50
OUTER MEMBRANE

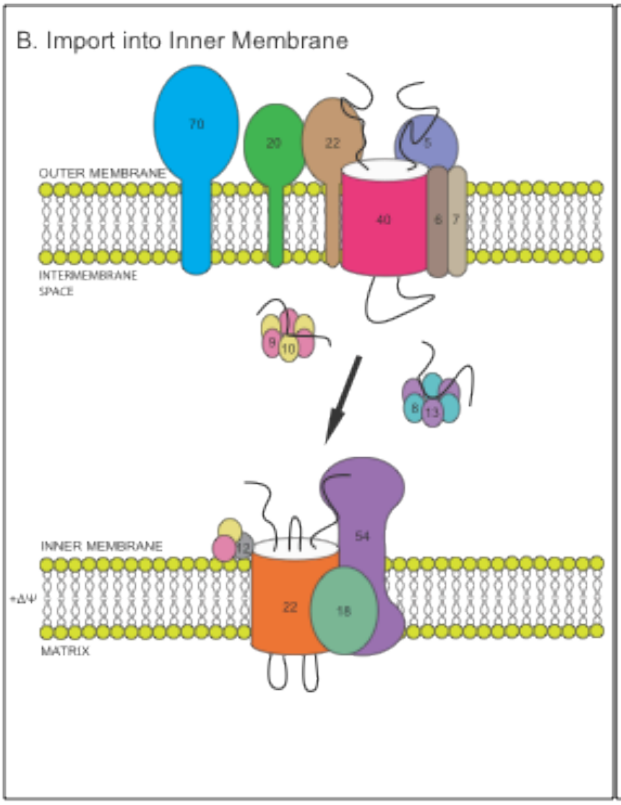
B. Import into Inner Membrane
70
20
22
5
OUTER MEMBRANE
INTERMEMBRANE SPACE
40
6
7
9
10
8
13
INNER MEMBRANE
12
54
22
18
+ΔΨ
MATRIX

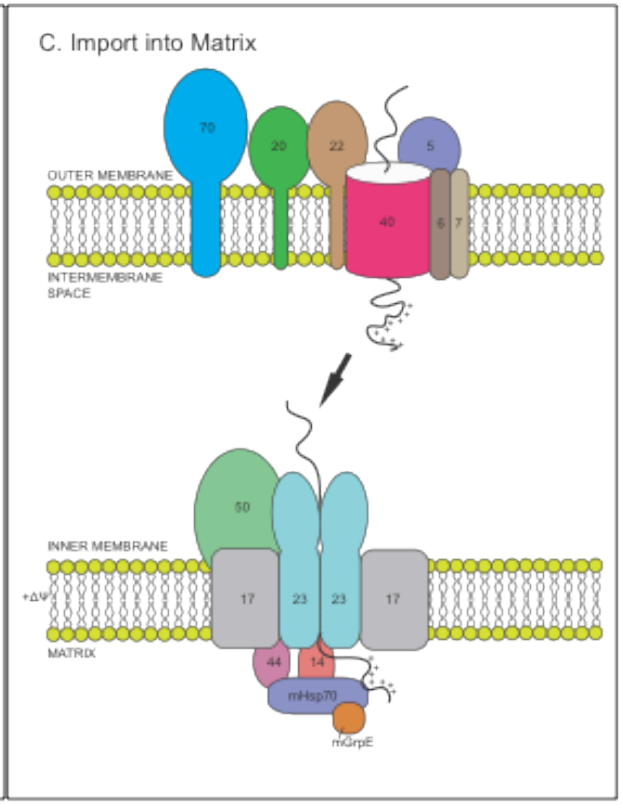
C. Import into Matrix
70
20
22
5
OUTER MEMBRANE
INTERMEMBRANE SPACE
40
6
7
50
INNER MEMBRANE
17
23
23
17
+ΔΨ
MATRIX
44
14
mHsp70
mGrpE

Figure 1.8: Mitochondrial protein import. Protein translocation into the mitochondria progresses through different protein pathways, depending on the final destination. All proteins first progress through the TOM complex. **A.** For proteins destined to remain in the outer membrane, precursors are diverted to the SAM complex, where they are inserted into the membrane. **B.** Proteins targeted for insertion into the inner membrane are accompanied by the small Tim complexes once they exit the Tom40 pore. The small Tims deposit the precursor protein at the TIM22 complex, where insertion into the inner membrane is mediated. **C.** Matrix-targeted proteins contain a positively charged *N*-terminal localization sequence that directs them to the TIM23 complex. Tim23 and Tim17 form a channel for the precursor to travel through into the matrix, where the *N*-terminal targeting sequence is cleaved off upon entry. Translocation for both inner membrane complexes is reliant on a membrane potential ($\Delta\Psi$), which is provided by the translocation motor (Tim44, Tim14, mHsp70, and mGrpE).

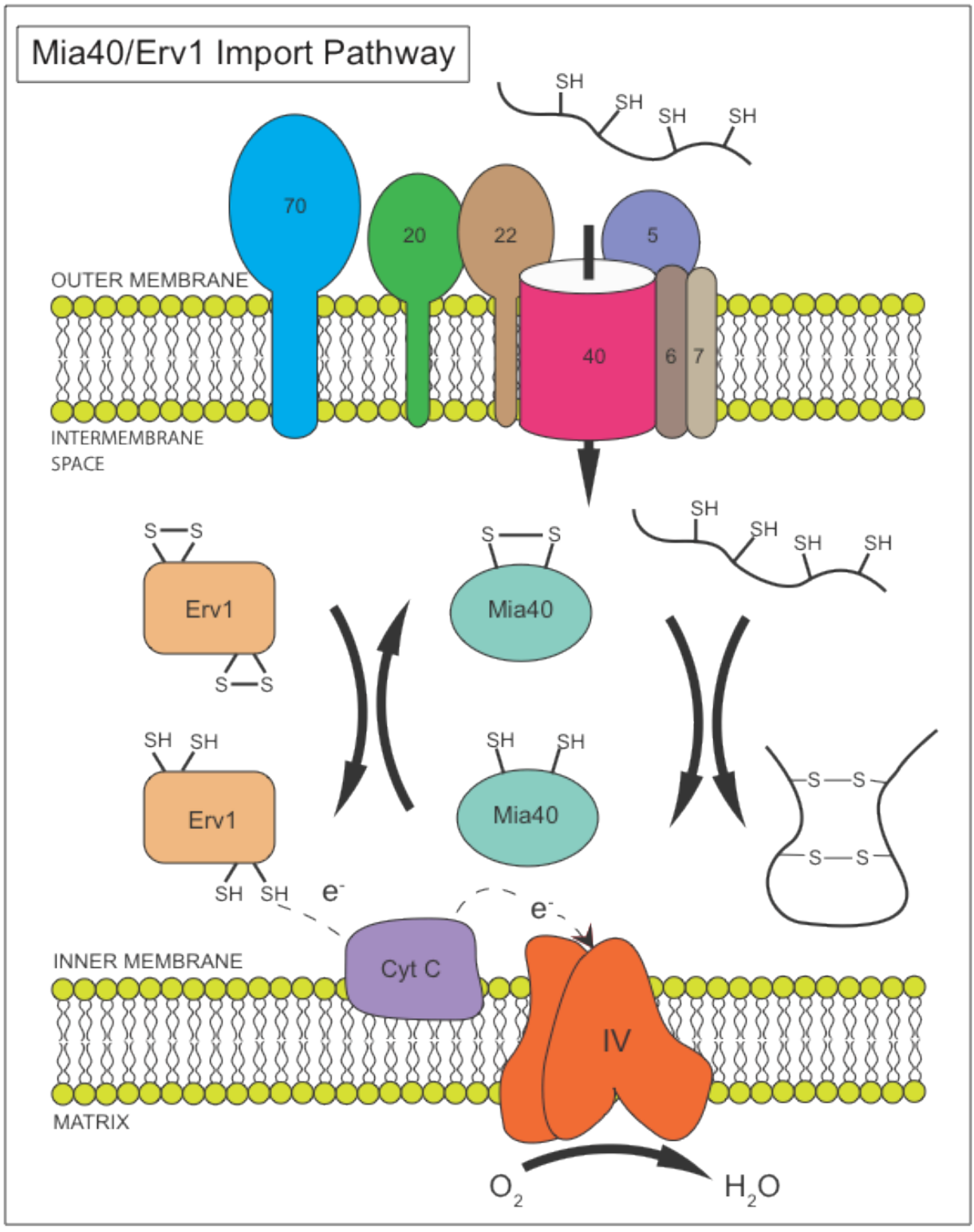
Mia40/Erv1 Import Pathway
SH
SH
SH
SH
70
20
22
5
OUTER MEMBRANE
40
6
7
INTERMEMBRANE
SPACE
S—S
Erv1
S—S
S—S
Mia40
SH
SH
SH
SH
SH
SH
Erv1
SH
SH
SH
SH
Mia40
S—S
S—S
e-
e-
INNER MEMBRANE
Cyt C
IV
MATRIX
O2
H2O

Figure 1.9: The Mia40/Erv1 disulfide relay. Proteins destined for the intermembrane space often contain disulfide bonds that require oxidation for activity. The oxidative folding of these proteins is mediated by Mia40 and Erv1. Precursor proteins first encounter oxidized Mia40 upon exit from the Tom40 pore. Mia40 oxidizes the precursor into its active form, subsequently becoming reduced. Erv1 reoxidizes Mia40 to its active state, becoming reduced. Erv1 becomes reoxidized and active through electron transfer to an acceptor such as cytochrome *c*, which ultimately passes the electrons to O_2, through its mediation with Complex IV.

References

1. Hanahan, D., Wagner, E. F., and Palmiter, R. D. (2007) *Genes Dev* **21**, 2258-2270

2. Waterston, R. H., Lindblad-Toh, K., Birney, E., Rogers, J., Abril, J. F., Agarwal, P., Agarwala, R., Ainscough, R., Alexandersson, M., An, P., Antonarakis, S. E., Attwood, J., Baertsch, R., Bailey, J., Barlow, K., Beck, S., Berry, E., Birren, B., Bloom, T., Bork, P., Botcherby, M., Bray, N., Brent, M. R., Brown, D. G., Brown, S. D., Bult, C., Burton, J., Butler, J., Campbell, R. D., Carninci, P., Cawley, S., Chiaromonte, F., Chinwalla, A. T., Church, D. M., Clamp, M., Clee, C., Collins, F. S., Cook, L. L., Copley, R. R., Coulson, A., Couronne, O., Cuff, J., Curwen, V., Cutts, T., Daly, M., David, R., Davies, J., Delehaunty, K. D., Deri, J., Dermitzakis, E. T., Dewey, C., Dickens, N. J., Diekhans, M., Dodge, S., Dubchak, I., Dunn, D. M., Eddy, S. R., Elnitski, L., Emes, R. D., Eswara, P., Eyras, E., Felsenfeld, A., Fewell, G. A., Flicek, P., Foley, K., Frankel, W. N., Fulton, L. A., Fulton, R. S., Furey, T. S., Gage, D., Gibbs, R. A., Glusman, G., Gnerre, S., Goldman, N., Goodstadt, L., Grafham, D., Graves, T. A., Green, E. D., Gregory, S., Guigo, R., Guyer, M., Hardison, R. C., Haussler, D., Hayashizaki, Y., Hillier, L. W., Hinrichs, A., Hlavina, W., Holzer, T., Hsu, F., Hua, A., Hubbard, T., Hunt, A., Jackson, I., Jaffe, D. B., Johnson, L. S., Jones, M., Jones, T. A., Joy, A., Kamal, M., Karlsson, E. K., Karolchik, D., Kasprzyk, A., Kawai, J., Keibler, E., Kells, C., Kent, W. J., Kirby, A., Kolbe, D. L., Korf, I., Kucherlapati, R. S., Kulbokas, E. J., Kulp, D., Landers, T., Leger, J. P., Leonard, S., Letunic, I., Levine, R., Li, J., Li, M., Lloyd, C., Lucas, S., Ma, B., Maglott, D. R., Mardis, E. R., Matthews, L., Mauceli, E., Mayer, J. H., McCarthy, M., McCombie, W. R., McLaren, S., McLay, K., McPherson, J. D., Meldrim, J., Meredith, B., Mesirov, J. P., Miller, W., Miner, T. L., Mongin, E., Montgomery, K. T., Morgan, M., Mott, R., Mullikin, J. C., Muzny, D. M., Nash, W. E., Nelson, J. O., Nhan, M. N., Nicol, R., Ning, Z., Nusbaum, C., O'Connor, M. J., Okazaki, Y., Oliver, K., Overton-Larty, E., Pachter, L., Parra, G., Pepin, K. H., Peterson, J., Pevzner, P., Plumb, R., Pohl, C. S., Poliakov, A., Ponce, T. C., Ponting, C. P., Potter, S., Quail, M., Reymond, A., Roe, B. A., Roskin, K. M., Rubin, E. M., Rust, A. G., Santos, R., Sapojnikov, V., Schultz, B., Schultz, J., Schwartz, M. S., Schwartz, S., Scott, C., Seaman, S., Searle, S., Sharpe, T., Sheridan, A., Shownkeen, R., Sims, S., Singer, J. B., Slater, G., Smit, A., Smith, D. R., Spencer, B., Stabenau, A., Stange-Thomann, N., Sugnet, C., Suyama, M., Tesler, G., Thompson, J., Torrents, D., Trevaskis, E., Tromp, J., Ucla, C., Ureta-Vidal, A., Vinson, J. P., Von Niederhausern, A. C., Wade, C. M., Wall, M., Weber, R. J., Weiss, R. B., Wendl, M. C., West, A. P., Wetterstrand, K., Wheeler, R., Whelan, S., Wierzbowski, J., Willey, D., Williams, S., Wilson, R. K., Winter, E., Worley, K. C., Wyman, D., Yang, S., Yang, S. P., Zdobnov, E. M., Zody, M. C., and Lander, E. S. (2002) *Nature* **420**, 520-562

3. Emes, R. D., Goodstadt, L., Winter, E. E., and Ponting, C. P. (2003) *Hum Mol Genet* **12**, 701-709

4. Nagy, A. (2003) *Manipulating the Mouse Embryo: A Laboratory Manual*, 3rd ed., Cold Spring Harbor Laboratory Press, Cold Spring Harbor, NY

5. Davis, K., Corrow, D., Davisson, M., Greene, M., Leighton, C., Linnell, S., Lutz, C., Rockwood, S., Soukup, J., Strobel, M., Taft, R., Trepanier, L., Witham, B., and Yeadon, J. (2007) *Breeding Strategies for Maintaining Colonies of Laboratory Mice: A Jackson Laboratory Resource Manual*, The Jackson Laboratory, Bar Harbor, ME

6. Dooley, K., and Zon, L. I. (2000) *Curr Opin Genet Dev* **10**, 252-256

7. Lieschke, G. J., and Currie, P. D. (2007) *Nat Rev Genet* **8**, 353-367

8. Laelle, H. (1977) *J Fish Biol* **10**, 121-174

9. Koerber, A. S., and Kalishman, J. (2009) *J Am Assoc Lab Anim Sci* **48**, 65-75

10. Vatine, G., Vallone, D., Gothilf, Y., and Foulkes, N. S. (2011) *FEBS Lett* **585**, 1485-1494

11. Delvecchio, C., Tiefenbach, J., and Krause, H. M. (2011) *Assay Drug Dev Technol* **9**, 354-361

12. Zon, L. I., and Peterson, R. T. (2005) *Nat Rev Drug Discov* **4**, 35-44

13. Kimmel, C. B., Ballard, W. W., Kimmel, S. R., Ullmann, B., and Schilling, T. F. (1995) *Dev Dyn* **203**, 253-310

14. Westerfield, M. (2000) *The Zebrafish Book. A Guide for the Laboratory Use of Zebrafish (Danio rerio)*, 4th ed., University of Oregon Press, Eugene, OR

15. Stickney, H. L., Barresi, M. J., and Devoto, S. H. (2000) *Dev Dyn* **219**, 287-303

16. Tu, S., and Chi, N. C. (2012) *Differentiation* **84**, 4-16

17. Lawrence, C. (2007) *Aquaculture* **269**, 1-20

18. Shafizadeh, E., Huang, H., and Lin, S. (2002) *Methods Mol Biol* **183**, 225-233

19. Lu, J., Peatman, E., Tang, H., Lewis, J., and Liu, Z. (2012) *BMC Genomics* **13**, 246

20. Venter, J. C., Adams, M. D., Myers, E. W., Li, P. W., Mural, R. J., Sutton, G. G., Smith, H. O., Yandell, M., Evans, C. A., Holt, R. A., Gocayne, J. D., Amanatides, P., Ballew, R. M., Huson, D. H., Wortman, J. R., Zhang, Q., Kodira, C. D., Zheng, X. H., Chen, L., Skupski, M., Subramanian, G., Thomas, P. D., Zhang, J., Gabor Miklos, G. L., Nelson, C., Broder, S., Clark, A. G., Nadeau, J., McKusick, V. A., Zinder, N., Levine, A. J., Roberts, R. J., Simon, M., Slayman, C., Hunkapiller, M., Bolanos, R., Delcher, A., Dew, I., Fasulo, D., Flanigan, M., Florea, L., Halpern, A., Hannenhalli, S., Kravitz, S., Levy, S., Mobarry, C., Reinert, K., Remington, K., Abu-Threideh, J., Beasley, E., Biddick, K., Bonazzi, V., Brandon, R., Cargill, M., Chandramouliswaran, I., Charlab, R., Chaturvedi, K., Deng, Z., Di Francesco, V., Dunn, P., Eilbeck, K., Evangelista, C., Gabrielian, A. E., Gan, W., Ge, W., Gong, F., Gu, Z., Guan, P., Heiman, T. J., Higgins, M. E., Ji, R. R., Ke, Z., Ketchum, K. A., Lai, Z., Lei, Y., Li, Z., Li, J., Liang, Y., Lin, X., Lu, F., Merkulov, G. V., Milshina, N., Moore, H. M., Naik, A. K., Narayan, V. A., Neelam, B., Nusskern, D., Rusch, D. B., Salzberg, S., Shao, W., Shue, B., Sun, J., Wang, Z., Wang, A., Wang, X., Wang, J., Wei, M., Wides, R., Xiao, C., Yan, C., Yao, A., Ye, J., Zhan, M., Zhang, W., Zhang, H., Zhao, Q., Zheng, L., Zhong, F., Zhong, W., Zhu, S., Zhao, S., Gilbert, D., Baumhueter, S., Spier, G., Carter, C., Cravchik, A., Woodage, T., Ali, F., An, H., Awe, A., Baldwin, D., Baden, H., Barnstead, M., Barrow, I., Beeson, K., Busam, D., Carver, A., Center, A., Cheng, M. L., Curry, L., Danaher, S., Davenport, L., Desilets, R., Dietz, S., Dodson, K., Doup, L., Ferriera, S., Garg, N., Gluecksmann, A., Hart, B., Haynes, J., Haynes, C., Heiner, C., Hladun, S., Hostin, D., Houck, J., Howland, T., Ibegwam, C., Johnson, J., Kalush, F., Kline, L., Koduru, S., Love, A., Mann, F., May, D., McCawley, S., McIntosh, T., McMullen, I., Moy, M., Moy, L., Murphy, B., Nelson, K., Pfannkoch, C., Pratts, E., Puri, V., Qureshi, H., Reardon, M., Rodriguez, R., Rogers, Y. H., Romblad, D., Ruhfel, B., Scott, R., Sitter, C., Smallwood, M., Stewart, E., Strong, R., Suh, E., Thomas, R., Tint, N. N., Tse, S., Vech, C., Wang, G., Wetter, J., Williams, S., Williams, M., Windsor, S., Winn-Deen, E., Wolfe, K., Zaveri, J., Zaveri, K., Abril, J. F., Guigo, R., Campbell, M. J., Sjolander, K. V., Karlak, B., Kejariwal, A., Mi, H., Lazareva, B., Hatton, T., Narechania, A., Diemer, K., Muruganujan, A., Guo, N., Sato, S., Bafna, V., Istrail, S., Lippert, R., Schwartz, R., Walenz, B., Yooseph, S., Allen, D., Basu, A., Baxendale, J., Blick, L., Caminha, M., Carnes-Stine, J., Caulk, P., Chiang, Y. H., Coyne, M., Dahlke, C., Mays, A., Dombroski, M., Donnelly, M., Ely, D., Esparham, S., Fosler, C., Gire, H., Glanowski, S., Glasser, K., Glodek, A., Gorokhov, M., Graham, K., Gropman, B., Harris, M., Heil, J., Henderson, S., Hoover, J., Jennings, D., Jordan, C., Jordan, J., Kasha, J., Kagan, L., Kraft, C., Levitsky, A., Lewis, M., Liu, X., Lopez, J., Ma, D., Majoros, W., McDaniel, J., Murphy, S., Newman, M., Nguyen, T., Nguyen, N., Nodell, M., Pan, S., Peck, J., Peterson, M., Rowe, W., Sanders, R., Scott, J., Simpson, M., Smith, T., Sprague, A., Stockwell, T., Turner, R., Venter, E., Wang, M., Wen, M., Wu, D., Wu, M., Xia, A., Zandieh, A., and Zhu, X. (2001) *Science* **291**, 1304-1351

21. Pennisi, E. (2003) *Science* **300**, 1484

22. Volff, J. N. (2005) *Heredity (Edinb)* **94**, 280-294

23. Taylor, J. S., Braasch, I., Frickey, T., Meyer, A., and Van de Peer, Y. (2003) *Genome Res* **13**, 382-390

24. Nasevicius, A., and Ekker, S. C. (2000) *Nat Genet* **26**, 216-220

25. Summerton, J. (1999) *Biochim Biophys Acta* **1489**, 141-158

26. Hudziak, R. M., Barofsky, E., Barofsky, D. F., Weller, D. L., Huang, S. B., and Weller, D. D. (1996) *Antisense Nucleic Acid Drug Dev* **6**, 267-272

27. Summerton, J., and Weller, D. (1997) *Antisense Nucleic Acid Drug Dev* **7**, 187-195

28. Ekker, S. C., and Larson, J. D. (2001) *Genesis* **30**, 89-93

29. Moulton, J. D., and Yan, Y. L. (2008) *Current Protocols in Molecular Biology* **83**, 26.28.21–26.28.29

30. Schmajuk, G., Sierakowska, H., and Kole, R. (1999) *J Biol Chem* **274**, 21783-21789

31. Draper, B. W., Morcos, P. A., and Kimmel, C. B. (2001) *Genesis* **30**, 154-156

32. Bill, B. R., Petzold, A. M., Clark, K. J., Schimmenti, L. A., and Ekker, S. C. (2009) *Zebrafish* **6**, 69-77

33. Eisen, J. S., and Smith, J. C. (2008) *Development* **135**, 1735-1743

34. Lin, F., Liu, Q., Li, M., Li, Z., Hong, N., Li, J., and Hong, Y. (2012) *Int J Biol Sci* **8**, 882-890

35. Kennedy, B. N., Vihtelic, T. S., Checkley, L., Vaughan, K. T., and Hyde, D. R. (2001) *J Biol Chem* **276**, 14037-14043

36. Nüsslein-Volhard, C., and Dahm, R. (2002) *Zebrafish: A Practical Approach*, 1st ed., Oxford University Press, Oxford, UK

37. Clark, K. J., Urban, M. D., Skuster, K. J., and Ekker, S. C. (2011) *Methods Cell Biol* **104**, 137-149

38. Kwan, K. M., Fujimoto, E., Grabher, C., Mangum, B. D., Hardy, M. E., Campbell, D. S., Parant, J. M., Yost, H. J., Kanki, J. P., and Chien, C. B. (2007) *Dev Dyn* **236**, 3088-3099

39. Amsterdam, A., Burgess, S., Golling, G., Chen, W., Sun, Z., Townsend, K., Farrington, S., Haldi, M., and Hopkins, N. (1999) *Genes Dev* **13**, 2713-2724

40. Fischer, J. A., Giniger, E., Maniatis, T., and Ptashne, M. (1988) *Nature* **332**, 853-856

41. Scheer, N., and Campos-Ortega, J. A. (1999) *Mech Dev* **80**, 153-158

42. Huang, C. J., Tu, C. T., Hsiao, C. D., Hsieh, F. J., and Tsai, H. J. (2003) *Dev Dyn* **228**, 30-40

43. Thisse, C., and Thisse, B. (2008) *Nat Protoc* **3**, 59-69

44. Link, V., Shevchenko, A., and Heisenberg, C. P. (2006) *BMC Dev Biol* **6**, 1

45. Wendl, T., Lun, K., Mione, M., Favor, J., Brand, M., Wilson, S. W., and Rohr, K. B. (2002) *Development* **129**, 3751-3760

46. Ransom, D. G., Haffter, P., Odenthal, J., Brownlie, A., Vogelsang, E., Kelsh, R. N., Brand, M., van Eeden, F. J., Furutani-Seiki, M., Granato, M., Hammerschmidt, M., Heisenberg, C. P., Jiang, Y. J., Kane, D. A., Mullins, M. C., and Nusslein-Volhard, C. (1996) *Development* **123**, 311-319

47. Finley, K. R., Davidson, A. E., and Ekker, S. C. (2001) *Biotechniques* **31**, 66-70, 72

48. Amsterdam, A., Lin, S., and Hopkins, N. (1995) *Dev Biol* **171**, 123-129

49. Zhu, H., and Zon, L. I. (2004) *Methods Cell Biol* **76**, 3-12

50. Shaner, N. C., Campbell, R. E., Steinbach, P. A., Giepmans, B. N., Palmer, A. E., and Tsien, R. Y. (2004) *Nat Biotechnol* **22**, 1567-1572

51. Ko, S. K., Chen, X., Yoon, J., and Shin, I. (2011) *Chem Soc Rev* **40**, 2120-2130

52. Wacker, S. A., Oswald, F., Wiedenmann, J., and Knochel, W. (2007) *Dev Dyn* **236**, 473-480

53. Pham, A. H., McCaffery, J. M., and Chan, D. C. (2012) *Genesis*

54. Bowman, T. V., and Zon, L. I. (2010) *ACS Chem Biol* **5**, 159-161

55. Chang, S., Bray, S. M., Li, Z., Zarnescu, D. C., He, C., Jin, P., and Warren, S. T. (2008) *Nat Chem Biol* **4**, 256-263

56. Petrascheck, M., Ye, X., and Buck, L. B. (2009) *Ann N Y Acad Sci* **1170**, 698-701

57. Sprague, J., Bayraktaroglu, L., Bradford, Y., Conlin, T., Dunn, N., Fashena, D., Frazer, K., Haendel, M., Howe, D. G., Knight, J., Mani, P., Moxon, S. A., Pich, C., Ramachandran, S., Schaper, K., Segerdell, E., Shao, X., Singer, A., Song, P., Sprunger, B., Van Slyke, C. E., and Westerfield, M. (2008) *Nucleic Acids Res* **36**, D768-772

58. Hong, C. C. (2009) *Methods Mol Biol* **486**, 43-55

59. Hao, J., Williams, C. H., Webb, M. E., and Hong, C. C. (2010) *J Vis Exp*

60. Hill, A. J., Teraoka, H., Heideman, W., and Peterson, R. E. (2005) *Toxicol Sci* **86**, 6-19

61. Wheeler, G. N., and Brandli, A. W. (2009) *Dev Dyn* **238**, 1287-1308

62. Ito, T., Ando, H., Suzuki, T., Ogura, T., Hotta, K., Imamura, Y., Yamaguchi, Y., and Handa, H. (2010) *Science* **327**, 1345-1350

63. Daum, G., Bohni, P. C., and Schatz, G. (1982) *J Biol Chem* **257**, 13028-13033

64. Sickmann, A., Reinders, J., Wagner, Y., Joppich, C., Zahedi, R., Meyer, H. E., Schonfisch, B., Perschil, I., Chacinska, A., Guiard, B., Rehling, P., Pfanner, N., and Meisinger, C. (2003) *Proc Natl Acad Sci U S A* **100**, 13207-13212

65. Taylor, S. W., Fahy, E., Zhang, B., Glenn, G. M., Warnock, D. E., Wiley, S., Murphy, A. N., Gaucher, S. P., Capaldi, R. A., Gibson, B. W., and Ghosh, S. S. (2003) *Nat Biotechnol* **21**, 281-286

66. Reinders, J., Zahedi, R. P., Pfanner, N., Meisinger, C., and Sickmann, A. (2006) *J Proteome Res* **5**, 1543-1554

67. Anderson, S., Bankier, A. T., Barrell, B. G., de Bruijn, M. H., Coulson, A. R., Drouin, J., Eperon, I. C., Nierlich, D. P., Roe, B. A., Sanger, F., Schreier, P. H., Smith, A. J., Staden, R., and Young, I. G. (1981) *Nature* **290**, 457-465

68. Alexeyev, M. F., Ledoux, S. P., and Wilson, G. L. (2004) *Clin Sci (Lond)* **107**, 355-364

69. Broughton, R. E., Milam, J. E., and Roe, B. A. (2001) *Genome Res* **11**, 1958-1967

70. Schultz, B. E., and Chan, S. I. (2001) *Annu Rev Biophys Biomol Struct* **30**, 23-65

71. Carroll, J., Fearnley, I. M., Skehel, J. M., Shannon, R. J., Hirst, J., and Walker, J. E. (2006) *J Biol Chem* **281**, 32724-32727

72. Bourges, I., Ramus, C., Mousson de Camaret, B., Beugnot, R., Remacle, C., Cardol, P., Hofhaus, G., and Issartel, J. P. (2004) *Biochem J* **383**, 491-499

73. Tomitsuka, E., Hirawake, H., Goto, Y., Taniwaki, M., Harada, S., and Kita, K. (2003) *J Biochem* **134**, 191-195

74. Gao, X., Wen, X., Esser, L., Quinn, B., Yu, L., Yu, C. A., and Xia, D. (2003) *Biochemistry* **42**, 9067-9080

75. Capaldi, R. A., Darley-Usmar, V., Fuller, S., and Millett, F. (1982) *FEBS Lett* **138**, 1-7

76. Fernandez-Vizarra, E., Tiranti, V., and Zeviani, M. (2009) *Biochim Biophys Acta* **1793**, 200-211

77. Boyer, P. D. (1997) *Annu Rev Biochem* **66**, 717-749

78. Owen, O. E., Kalhan, S. C., and Hanson, R. W. (2002) *J Biol Chem* **277**, 30409-30412

79. Di Mauro, S., Trevisan, C., and Hays, A. (1980) *Muscle Nerve* **3**, 369-388

80. Pfanner, N., Craig, E. A., and Honlinger, A. (1997) *Annu Rev Cell Dev Biol* **13**, 25-51

81. Neupert, W. (1997) *Annu Rev Biochem* **66**, 863-917

82. Dietmeier, K., Honlinger, A., Bomer, U., Dekker, P. J., Eckerskorn, C., Lottspeich, F., Kubrich, M., and Pfanner, N. (1997) *Nature* **388**, 195-200

83. Honlinger, A., Bomer, U., Alconada, A., Eckerskorn, C., Lottspeich, F., Dietmeier, K., and Pfanner, N. (1996) *EMBO J* **15**, 2125-2137

84. Kozjak, V., Wiedemann, N., Milenkovic, D., Lohaus, C., Meyer, H. E., Guiard, B., Meisinger, C., and Pfanner, N. (2003) *J Biol Chem* **278**, 48520-48523

85. Paschen, S. A., Waizenegger, T., Stan, T., Preuss, M., Cyrklaff, M., Hell, K., Rapaport, D., and Neupert, W. (2003) *Nature* **426**, 862-866

86. Wiedemann, N., Kozjak, V., Chacinska, A., Schonfisch, B., Rospert, S., Ryan, M. T., Pfanner, N., and Meisinger, C. (2003) *Nature* **424**, 565-571

87. Yamamoto, H., Esaki, M., Kanamori, T., Tamura, Y., Nishikawa, S., and Endo, T. (2002) *Cell* **111**, 519-528

88. Geissler, A., Chacinska, A., Truscott, K. N., Wiedemann, N., Brandner, K., Sickmann, A., Meyer, H. E., Meisinger, C., Pfanner, N., and Rehling, P. (2002) *Cell* **111**, 507-518

89. Gaume, B., Klaus, C., Ungermann, C., Guiard, B., Neupert, W., and Brunner, M. (1998) *EMBO J* **17**, 6497-6507

90. Geissler, A., Krimmer, T., Bomer, U., Guiard, B., Rassow, J., and Pfanner, N. (2000) *Mol Biol Cell* **11**, 3977-3991

91. Rehling, P., Model, K., Brandner, K., Kovermann, P., Sickmann, A., Meyer, H. E., Kuhlbrandt, W., Wagner, R., Truscott, K. N., and Pfanner, N. (2003) *Science* **299**, 1747-1751

92. Sirrenberg, C., Bauer, M. F., Guiard, B., Neupert, W., and Brunner, M. (1996) *Nature* **384**, 582-585

93. Kerscher, O., Holder, J., Srinivasan, M., Leung, R. S., and Jensen, R. E. (1997) *J Cell Biol* **139**, 1663-1675

94. Kerscher, O., Sepuri, N. B., and Jensen, R. E. (2000) *Mol Biol Cell* **11**, 103-116

95. Koehler, C. M. (2004) *Annu Rev Cell Dev Biol* **20**, 309-335

96. Paschen, S. A., Rothbauer, U., Kaldi, K., Bauer, M. F., Neupert, W., and Brunner, M. (2000) *EMBO J* **19**, 6392-6400

97. Adam, A., Endres, M., Sirrenberg, C., Lottspeich, F., Neupert, W., and Brunner, M. (1999) *EMBO J* **18**, 313-319

98. Koehler, C. M., Merchant, S., Oppliger, W., Schmid, K., Jarosch, E., Dolfini, L., Junne, T., Schatz, G., and Tokatlidis, K. (1998) *EMBO J* **17**, 6477-6486

99. Koehler, C. M., Leuenberger, D., Merchant, S., Renold, A., Junne, T., and Schatz, G. (1999) *Proc Natl Acad Sci U S A* **96**, 2141-2146

100. Lutz, T., Neupert, W., and Herrmann, J. M. (2003) *EMBO J* **22**, 4400-4408

101. Roesch, K., Curran, S. P., Tranebjaerg, L., and Koehler, C. M. (2002) *Hum Mol Genet* **11**, 477-486

102. Dabir, D. V., Leverich, E. P., Kim, S. K., Tsai, F. D., Hirasawa, M., Knaff, D. B., and Koehler, C. M. (2007) *EMBO J* **26**, 4801-4811

103. Allen, S., Balabanidou, V., Sideris, D. P., Lisowsky, T., and Tokatlidis, K. (2005) *J Mol Biol* **353**, 937-944

104. Mesecke, N., Terziyska, N., Kozany, C., Baumann, F., Neupert, W., Hell, K., and Herrmann, J. M. (2005) *Cell* **121**, 1059-1069

105. Chacinska, A., Pfannschmidt, S., Wiedemann, N., Kozjak, V., Sanjuan Szklarz, L. K., Schulze-Specking, A., Truscott, K. N., Guiard, B., Meisinger, C., and Pfanner, N. (2004) *EMBO J* **23**, 3735-3746

106. Rissler, M., Wiedemann, N., Pfannschmidt, S., Gabriel, K., Guiard, B., Pfanner, N., and Chacinska, A. (2005) *J Mol Biol* **353**, 485-492

107. Grumbt, B., Stroobant, V., Terziyska, N., Israel, L., and Hell, K. (2007) *J Biol Chem* **282**, 37461-37470

108. Fass, D. (2008) *Biochim Biophys Acta* **1783**, 557-566

109. Lee, J., Hofhaus, G., and Lisowsky, T. (2000) *FEBS Lett* **477**, 62-66

110. Gabriel, K., Milenkovic, D., Chacinska, A., Muller, J., Guiard, B., Pfanner, N., and Meisinger, C. (2007) *J Mol Biol* **365**, 612-620

111. Hofhaus, G., Lee, J. E., Tews, I., Rosenberg, B., and Lisowsky, T. (2003) *Eur J Biochem* **270**, 1528-1535

112. Bihlmaier, K., Mesecke, N., Terziyska, N., Bien, M., Hell, K., and Herrmann, J. M. (2007) *J Cell Biol* **179**, 389-395

Chapter 2: Modeling the *In Vivo* Drug Response of Identified Small-Molecule Inhibitors of Mitochondrial Function Using Zebrafish

Abstract

Zebrafish are uniquely suited for monitoring the *in vivo* drug response to small-molecule therapeutics. Conducting studies using embryos provides a vertebrate, whole-organism view, which is unattainable with *in vitro*, *in cellulo*, and invertebrate study. Assays can be performed rapidly, and efficiently, providing information regarding all aspects of compound discovery, from target verification to characterization and toxicity studies. Many compounds currently available arose from studies utilizing zebrafish. Here we describe the work done to characterize 2 inhibitors of mitochondrial function identified in the laboratory. MitoBloCKs-2 and -6 have been shown to behave specifically within the mitochondrion, interacting with targeted aspects of mitochondrial biology and behavior. Through the work done with zebrafish, we show that these drugs affect particular aspects of embryo development, providing validation for the MitoBloCK compounds as tools for targeted *in vivo* study, as well as providing information as to the importance and role of mitochondria during embryonic development.

Introduction

Role of Zebrafish in Small-Molecule Development

With the introduction of high-throughput screening (HTS), the rate of identifying small molecules capable of modifying biological processes, or providing therapeutic help for disease, rapidly increased.(1) Early methods included *in vitro* and *in cellulo* assays, and although these assays do have size and speed advantages, drugs identified from them often failed when introduced to animal models, possibly because of metabolic breakdown, inability to permeate cellular membranes and reach target tissues, and off-target toxicity concerns.(1,2) Small-molecule screens have been performed in simple model systems previously, such as *Drosophila melanogaster* or *Caenorhabditis elegans*; however, these invertebrate organisms still differ from humans and other larger animals in a multitude of ways.(3,4) Screening compounds in zebrafish provides an efficient way to elucidate these concerns in a vertebrate model. Zebrafish have the unique ability to fit into many aspects of the drug discovery pipeline. They can be used in the very beginning, during lead compound discovery using high-throughput methods; for target verification once potential hit compounds have been identified; for drug optimization; and for characterization during the adsorption, distribution, metabolism, excretion, and toxicity (ADMET) studies.

HTS Discovery. Zebrafish are ideally suited for initial HTS discovery: they produce large numbers of identical embryos per mating, they are optically clear and osmotically permeable (allowing molecules to freely diffuse into the organism), and through sequencing it has been proven that there is a great deal of genetic synteny between zebrafish and humans.(1,5,6) With a multitude of new lines available that that are transgenic and contain

fluorescently labeled tissues, the possibilities for monitoring *in vivo* responses to small-molecule treatment in new and more intricate ways are endless. The Z-tag system (Zymogen) was automated to create a screen for antiangiogenesis drugs in fish with fluorescently labeled blood vessels, identifying a previously unknown compound with antiangiogenic properties.(7) Through a similar screen, a drug for prostate cancer was discovered using zebrafish, further proving their utility as a research animal, even though they do not contain a prostate.(8)

Target Verification. Because of their amenability to molecular biology and genetic studies, zebrafish can be used for rapid confirmation of hit compounds. For example, zebrafish testing illustrated the *in vivo* proof that thalidomide interacted with the cereblon protein previously identified *in vitro*.(9) The authors were able to recapitulate the phenotype seen with thalidomide treatment through morpholino knockdown of cereblon, thus proving the teratogenic properties of the drug were due to its interaction with the protein.

ADMET Studies. Traditionally used as a marker of environmental toxicity, zebrafish are rapidly becoming a hallmark of dose-dependent toxicity.(10,11) Drug delivery to zebrafish embryos is easily accomplished because exposure can occur through simple osmosis. Most toxicity analysis done to date has been pharmaceutical in nature, such as looking at the effects of the antirheumatism drug diclofenac, or Amiodarone, which targets heart arrhythmias, although research has started to include the effects on nonpharmacological substances, such as ethanol and acetaldehyde, and their subsequent role on development.(12-14)

Structure-Activity Relationships (SARs). Following drug characterization, SAR studies usually accompany development as a way of dissecting the activity of a compound through substituent modification. Zebrafish provide a means to rapidly screen SARs for phenotype as well as toxicologic effects. This technique was used to modify the drug

dorsomorphin, which was originally characterized to combat bone morphogenetic protein (BMP), which causes improper dorsal-ventral patterning.(15) Dorsomorphin also caused vascular endothelial growth factor problems, preventing its use as a therapeutic.(16) Through SAR studies in zebrafish, researchers were able to identify a modified compound that retains its BMP-inhibitory properties without any vascular endothelial growth factor issues.(16)

Small-Molecule Screens of Mitochondrial Proteins

Previous work performed in the laboratory utilized both *in vitro* screening using recombinantly purified protein and an *in vivo* study conducted in *Saccharomyces cerevisiae* to identify small-molecule compounds that arrest import of varying components of mitochondrial import.

MitoBloCK-2

MitoBloCK-2, an indazole derivative, was isolated by a former graduate student during a chemical genetic screen conducted in yeast to determine inhibitors of mitochondrial protein translocation, namely, the inhibition of the small Tim proteins, Tim9p and Tim10p (data unpublished). When characterizing the method of import impairment, it was surprising to see that MitoBloCK-2 was able to inhibit the import of substrates of the TIM22 pathway and the TIM23 pathway, as well as the import of the TOM40 translocon of the outer membrane. This was startling because each of these pathways is specific, and little overlap occurs between their respective substrate components. Upon further scrutiny, it was noticed by Coomassie staining and other assays for mitochondrial integrity that the basal levels of mitochondrial proteins were actually markedly decreased in the presence of MitoBloCK-2. Interestingly, trypan blue staining

confirmed that the plasma membrane remained intact in HeLa cells, nor did it appear that the membrane of the endoplasmic reticulum was disrupted, which indicated that only the mitochondrial membrane was affected in the presence of MitoBloCK-2.

When SAR assays were performed on MitoBloCK-2, a hydroxyl group was deemed the cause of the impairment. When functional substitutions were conducted on the phenyl ring, in which the 5'-hydroxyl moiety was replaced by a 5'-O-methyl, the integrity of the mitochondrial membrane was maintained during treatment, and import proceeded as normal (Figure 2.1). Mitochondrial integrity appeared sound after treatment with the SAR compounds (data not shown).

MitoBloCK-6

MitoBloCK-6 was identified during an *in vitro* screen designed to isolate modulators of Erv1p oxidase activity. An *in vitro* reconstitution assay was designed using recombinantly purified yeast Erv1p and a nonphysiologic substrate DTT. When the assay proceeded without disruption, DTT would be oxidized by Erv1p, thus generating H_2O_2 from O_2 when Erv1p was reoxidized. The amount of H_2O_2 generated would then be measured using Amplex Red and horseradish peroxidase in a fluorometric assay. As H_2O_2 was produced, the fluorescent signal of the Amplex Red would increase, thus giving a quantifiable way for measuring Erv1p activity. When a small molecule inhibited Erv1p, the fluorescent signal would be decreased accordingly. This screen resulted in the identification of the small-molecule MitoBloCK-6 (Manuscript in submission, data not shown).

It was seen through *in vitro* reconstitution assays that treatment with MitoBloCK-6 impaired import of Erv1p itself, as well as other substrate proteins imported via the Mia40/Erv1

import pathway, such as Mia40p (Figure 2.2: B–C). Proteins not involved with this pathway showed no change in their ability to be imported upon MB-6 treatment (Figure 2.2: D). Mitochondrial integrity assays indicated that MitoBloCK-6 did not disrupt the mitochondrial membrane, unlike MitoBloCK-2, nor did it uncouple the electron transport chain. Subsequent studies using mammalian mitochondria showed that MitoBloCK-6 was also able to inhibit import of, and by, ALR, the vertebrate homolog of Erv1p.

In Vivo Zebrafish Assays

After isolating and characterizing our compounds in yeast and mammalian tissue culture systems (data not shown), we devised an assay using zebrafish to ascertain whether the activity witnessed in the *in vitro* and *in cellulo* assays would be retained in higher organized systems, and what overall *in vivo* response the small molecules would elicit when introduced into a vertebrate organism. Using zebrafish, I determined what the effect of MitoBloCK-2 and MitoBloCK-6 would be on developing zebrafish embryos. With these small molecules as tools I was able to highlight what role these specific aspects of mitochondrial biology may provide during development, roles that were previously unable to be studied because of their embryonic lethal nature.

Results

MitoBloCK-2

To ascertain which concentration of MitoBloCK-2 was best suited for our studies, many drug concentrations were tested and the resultant phenotype observed. Time-synchronized

developing embryos were treated with buffer, 1% DMSO control, or MitoBloCK-2 at 3 hours post fertilization (hpf) and allowed to develop undisturbed for 3 days at 28.5°C before data analysis. The time point of 3 hpf was chosen because that is the stage during which the embryos undergo a final round of synchronous cell division before beginning asynchronous development. Three days was chosen because this was the maximal time in which embryos could survive in the drug, thus allowing us to maximize any developing phenotype while still maintaining embryo viability.

Treatment with 1 μM MitoBloCK-2 resulted in prominent spinal curvature morphology at 3 days post fertilization (dpf) (Figure 2.3). Even treatment at concentrations on the nanomolar level produced a pronounced phenotype, illustrating the potency of MitoBloCK-2 (Figure 2.3: B). At concentrations higher than 2.5 μM, the embryos were unable to sustain viability (data not shown). When looking closely at cardiac development and morphology, a wild-type heart is dual chambered and loops in on itself. Blood is pumped in through the bottom ventricle and exits the heart out through the top atrium. Treatment with MitoBloCK-2, however, caused the heart to be malformed (Figure 2.3: J). The chambers are either enlarged or improperly looped, so the heart appeared stringy in nature.

As mentioned previously, import assays showed that treatment with 2 SAR molecules JMS-A-140-1 (SAR-140) and JMS-A-146-1 (SAR-146), restored import to control levels seen with 1% DMSO treatment (Figure 2.4). When zebrafish embryos were treated with the maximal concentration of 2.5 μM of SAR-140 and SAR-146, compared to MitoBloCK-2 treatment, we see no difference in body axis formation or development compared to wild-type and control-treated embryos (Figure 2.4: D–E). Additionally, the hearts of the SAR-treated embryos appear to be normal in size and are looped properly, indicating that the SAR compounds have no effects

in vivo, both specific effects as seen with MitoBloCK-2 and possible off-target effects (Figure 2.4: N–O).

MitoBloCK-6

Assays performed with MitoBloCK-6 were conducted similarly to those performed with MitoBloCK-2. After testing a variety of concentrations, it was deemed that 2.5-μM and 5-μM treatment provided a reliable phenotype. Again, time-synchronized developing embryos were treated with buffer, 1% DMSO control, or MitoBloCK-6 at 3 hpf and allowed to develop undisturbed at 28.5°C for 3 days before data analysis.

Treatment with MitoBloCK-6 resulted in improper somite formation and body curvature compared with vehicle control treatment (Figure 2.5: B). In addition, treatment with MitoBloCK-6 resulted in an improperly looped heart, as well as a loss of fluorescent signal, indicating compromised development (Figure 2.5: H). Upon closer inspection, it was noted that MitoBloCK-6–treated hearts had difficulty circulating blood throughout the embryo, resulting in a heart rate with slower beats per minute (bpm) compared with untreated and vehicle control–treated embryos (Figure 2.5: J). This effect was further confirmed through staining with o-dianisidine, which binds to heme groups. O-dianisidine staining showed prolific staining below the bottom chamber of the heart where blood enters, and little stain along the vasculature, indicating cardiac deficiency resulting in blood pooling before entering the heart (Figure 2.5: E).

Because MitoBloCK-6 targets a known protein within the mitochondrion, we wanted to confirm that the effects seen were a direct result of inhibition of ALR and not simply off-target effects of drug treatment. To do this we designed a morpholino specific to zebrafish ALR. The morpholino was injected at a concentration of 4 ng into the single-cell stage of a zebrafish

embryo and then embryos were allowed to develop undisturbed until 2 dpf. Embryos were imaged at 2 dpf rather than 3 dpf because of concerns about morpholino longevity. After 2 days, a similar phenotype was observed with morpholino treatment as with MitoBloCK-6 treatment, indicating that the effects seen with MitoBloCK-6 treatment are truly the result of specific knockdown of ALR.

Discussion

The work here illustrates the true power of using zebrafish as a model for drug response simulation in a vertebrate system. Conducting the same experiment using another vertebrate model, like mouse, would require a series of complex prenatal injections into the mother, or some sort of oral system in which the drug is ensured to travel through the mother's system untouched and reach the developing pups. This can be costly and time consuming, with no guarantee of strong and worthwhile delivery. Zebrafish bypass all of these caveats. Embryos are fertilized externally, allowing for rapid collection and treatment, ensuring that drug can be administered at the very earliest of stages. Small molecules can freely diffuse through the proteinaceous chorion to reach the embryo; therefore, drug delivery is simple and efficient. Their optical clarity allows for effective observation and imaging of phenotypic response, and the ease with which biochemical assays can be performed on them ensures quantifiable results.

MitoBloCK-2 treatment illustrates a phenotype seen before when mitochondrial function is impaired.(17,18) The similarity garnered here between other documented knockdown of mitochondrial function and MitoBloCK-2, which disrupts the mitochondrial membrane, gives credence to the specificity of our targeted response and further verifies previous work suggesting that MitoBloCK-2 only acts on mitochondria and does not disrupt other membranes within the

organism. The fact that zebrafish are so remarkably sensitive to MitoBloCK-2 treatment, that concentrations on the nanomolar scale were capable of curtailing development, suggests how important mitochondria are to the accurate and correct development of these aspects of embryogenesis.

Protecting the 5'-hydroxyl of MitoBloCK-2 with a methyl group completely abrogated the function of the 2 SAR compounds *in vivo*, further validating the results ascertained during the *in vitro* experiments. Simply changing the one moiety resulted in the restoration of the wild-type phenotypic response, suggesting that no other part of the molecule shows any activity *in vivo*. It is interesting that a single scaffold can be completely inert *in vivo* with one substitution, and potentially very active with another, all by changing a single moiety. If this technology could somehow be controlled *in vivo*, one could potentially target a small molecule to a desired protein, and then incapacitate it,; either throughout the entire organism or within a specific region or tissue. The implications this method could have for both research tools as a whole, as well as disease therapeutics, would be tremendous.

MitoBloCK-6 treatment showed distinct differences in phenotype compared to MitoBloCK-2. Although both drugs resulted in spinal curvature, defects in somatogenesis, and cardiac defects, MitoBloCK-6 also resulted in distinct circulatory deficiencies. MitoBloCK-6 treatment yielded improperly looped cardiac muscles that were unable to circulate blood through the embryo properly. As a result, blood pooling was seen around the lower chamber of the heart. This strong cardiac phenotype suggests that mitochondria play a crucial role in cardiac development. This is unsurprising; mitochondria are the major source of energy in the cell, and during embryonic development, as with any organism, the heart plays a crucial role in viability. Additionally, other studies examining proteins involved in mitochondrial import showed that

knockdown of import proteins can cause the heart to form on the opposite side of the embryo's body (data unpublished).

Comparing the phenotype of chemical treatment with that of the morpholino injection provides a frame of reference for the specificity of the small molecule for its designated target protein. Morpholinos are designed to be sequence-specific as well as species-specific. They are designed not to cross-react and affect other proteins when injected into an organism. Injection with the ALR morpholino showed a similar phenotype to treatment with MitoBloCK-6, illustrating that the specificity first exemplified *in vitro* is retained *in vivo.*

Materials and Methods

Zebrafish Lines. Zebrafish displaying fluorescent hearts were derived from transgenic TL fish expressing a mitochondrially targeted dsRed regulated by a cardiac myocyte light chain 2 *(cmlc2)* promoter to make it heart-specific. O-dianisidine staining was conducted in albino lines that were generated from crosses of wild-type TL and Tü. Morpholino injections were performed in wild-type AB.

Zebrafish Husbandry. Zebrafish lines were maintained in a 14-hour-light/10-hour-dark cycle and mated for 1 hour to obtain synchronized embryonic development. Embryos were grown in E3 buffer (5 mM sodium chloride, 0.17 mM potassium chloride, 0.33 mM calcium chloride, 0.33 mM magnesium sulfate) at 28.5°C.

Zebrafish Drug Treatment Assay. Zebrafish were mated for 1 hour to obtain synchronized embryonic development. Embryos were grown to 3 hpf in E3 buffer (5 mM sodium chloride, 0.17 mM potassium chloride, 0.33 mM calcium chloride, 0.33 mM magnesium sulfate) and then incubated with buffer, 1% DMSO, or drug for 3 days at 28.5°C. Following treatment, embryos were imaged using a Leica S8APO microscope at 1.575× magnification or Leica MZ16F fluorescent stereoscope (TexasRed filter set) at 5× magnification. Albino embryos were stained with o-dianisidine (40% (v/v) ethanol, 0.01 M sodium acetate, 0.65% hydrogen peroxide, 0.6 mg/mL o-dianisidine) and incubated for 15 minutes in complete darkness. Embryos were then washed with E3 buffer to remove residual stain and stereoscopically imaged under white light using a Leica S8APO microscope at 1.575× magnification. Images were resized to 300 dpi without resampling using Adobe Photoshop.

Zebrafish Morpholino Studies. Wild-type AB embryos were microinjected at the single-cell stage with 4 ng of an ATG morpholino targeted to zebrafish ALR protein (5'-GAGGGTTGCCAGATCTCTGTTAAAT) (GeneTools, Inc.) Zebrafish were allowed to develop undisturbed to 2 dpf and imaged similarly to drug-treated embryos. Images were resized to 300 dpi without resampling using Adobe Photoshop.

Figures

Figure 2.1: Import of AAC in the presence of MitoBloCK-2 and structure-activity relationship (SAR) compounds. Radiolabeled precursor was imported into GA74A (wild-type) mitochondria. Mitochondria at a concentration of 100 µg/mL were incubated with DMSO vehicle control or drug (1% DMSO final concentration) for 15 minutes at 25°C. *In vitro* transcription/translation product was then added to each reaction. At designated time points, aliquots were removed and stopped with cold buffer and trypsin. All aliquots were incubated for 15 minutes in stop buffer before being subjected to centrifugation. Pellets were then carbonate-extracted for 30 minutes on ice. After carbonate extraction, mitochondria were resuspended in reducing sample buffer and resolved on a 12% SDS-PAGE. Gels were dried and then exposed to film for 6 hours. Resultant film indicated that in the presence of MitoBloCK-2 and SAR compound JMS-A-151-1, import of AAC was impaired, but in the presence of SAR compounds JMS-A-140-1 and JMS-A-146-1, import was unaffected and comparable to vehicle control treatment. *Figure adapted with permission from Samuel A. Hasson.*

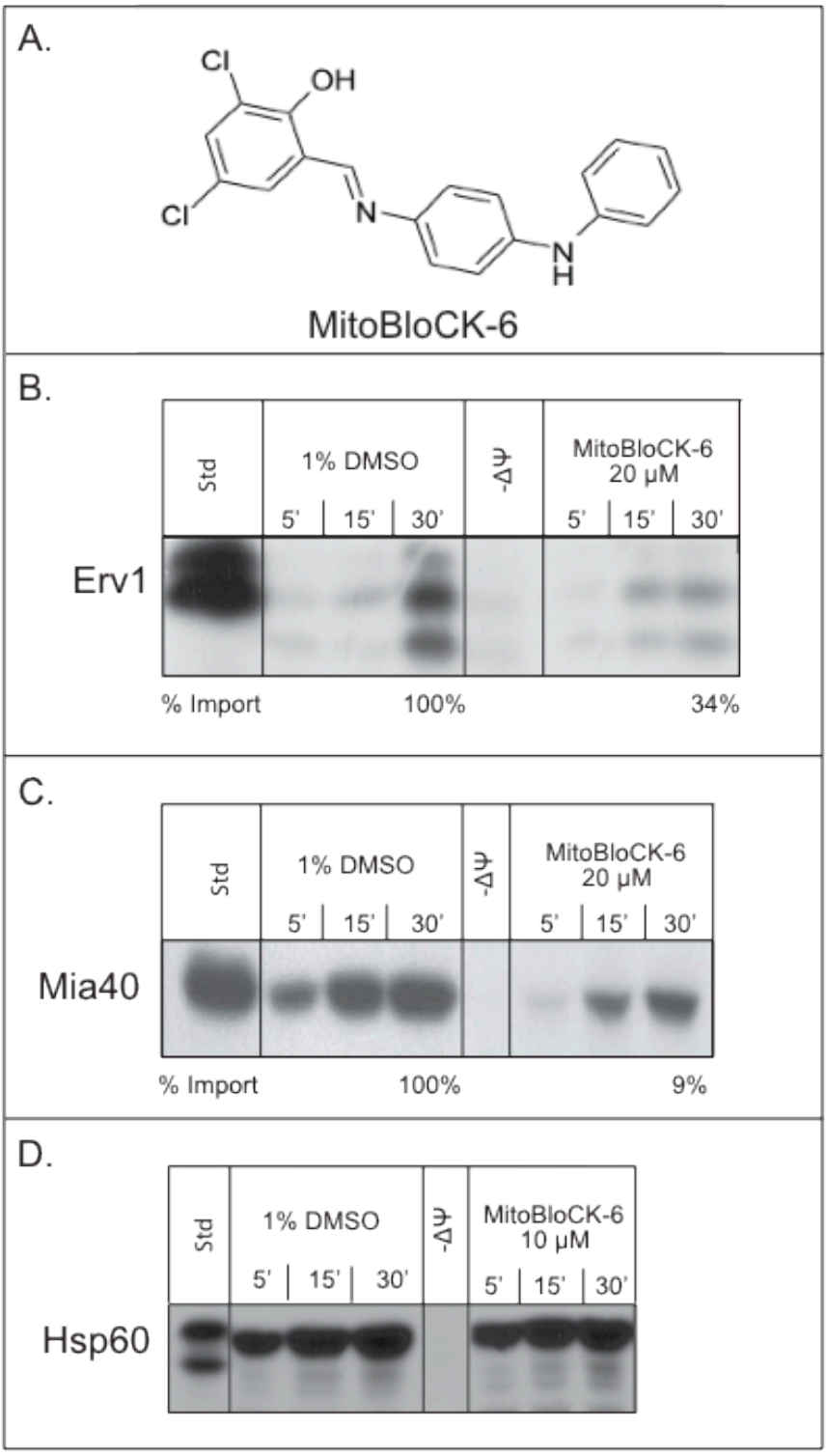
A.
Cl
OH
Cl
N
N
H
MitoBloCK-6
B.
Std
1% DMSO
-ΔΨ
MitoBloCK-6
20 μM
5'
15'
30'
5'
15'
30'
Erv1
% Import
100%
34%
C.
Std
1% DMSO
-ΔΨ
MitoBloCK-6
20 μM
5'
15'
30'
5'
15'
30'
Mia40
% Import
100%
9%
D.
Std
1% DMSO
-ΔΨ
MitoBloCK-6
10 μM
5'
15'
30'
5'
15'
30'
Hsp60

Figure 2.2: MitoBloCK-6 effect on precursor import. A. Chemical structure of MitoBloCK-6. **B–D.** In a procedure similar to that outlined in Figure 2.1, wild-type mitochondria were incubated in the presence of 1% DMSO vehicle control or drug. After incubation period, *in vitro* transcription/translation precursor was added to the reaction. Aliquots were taken at time points and the reaction stopped. Pellets were carbonate-extracted and loaded on and SDS-PAGE gel. Gels were dried and exposed to film. **B and C.** Precursors involved in the Mia40/Erv1 import pathway (Erv1 and Mia40) saw a marked reduction in import into mitochondria. **D.** Import of precursors that do not utilize the Mia40/Erv1 pathway (Hsp60) was unaffected by MitoBloCK-6 treatment. *Figure adapted with permission from Deepa V. Dabir.*

	1% DMSO	MitoBloCK-2 0.1 µM	MitoBloCK-2 1.0 µM	MitoBloCK-2 2.5 µM
Unstained	A 	B 	C 	D 
Stained with O-Dianisidine	E 	F 	G 	H 

1% DMSO	MitoBloCK-2 2.5 µM
I 	J 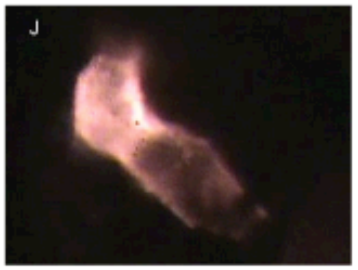

Figure 2.3: MitoBloCK-2 treatment. Embryos were treated with either 1% DMSO vehicle control or different concentrations of MitoBloCK-2 beginning at 3 hpf. Once treated, embryos were left undisturbed for 3 days. **A–D.** Treatment with MitoBloCK-2 resulted in spinal curvature at concentrations as low as 0.1 μM and as high as 2.5 μM. Embryos treated at concentrations higher than 2.5 μM were not viable. **E–H.** Staining with o-dianisidine which stains red blood cells, also showcased cardiac phenotype (arrows). **I–J.** Treatment with MitoBloCK-2 also resulted in cardiac formation defects.

1% DMSO
MitoBloCK-2
1.0 µM
MitoBloCK-2
2.5 µM
JMS-S-140-1
2.5 µM
JMS-A-146-1
2.5 µM
Unstained
Stained with
O-Dianisidine
A
B
C
D
E
F
G
H
I
J
K
L
M
N
O

Figure 2.4: MitoBloCK-2 SAR treatment. Treatment with the SAR analogs JMS-A-140-1 and JMS-A-146-1 do not exhibit the effects seen upon MitoBloCK-2 treatment. MitoBloCK-2 treatment results in spinal curvature and cardiac myopathy (**B, C, L, M)**, but treatment with the 2 SAR analogs results (**D, E, N, O**) in the same phenotype as the DMSO control (**A, K)**. Embryos were also stained with o-dianisidine, which binds to heme groups, marking red blood cells (**F-J)**.

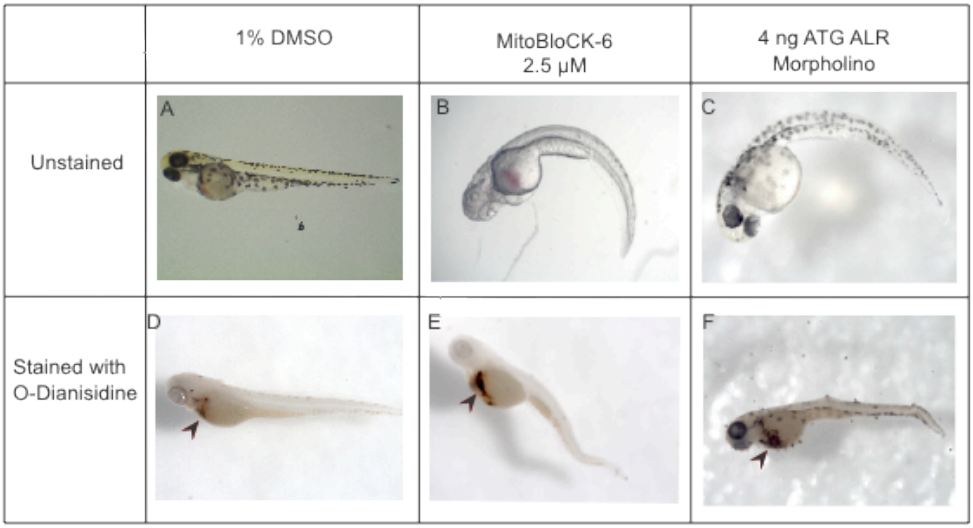

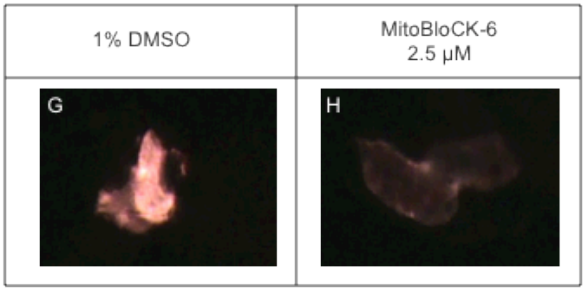

I.

Heart Rate in Presence of MitBloCK-6	
Untreated	198 ± 17
2.5 µM MitoBloCK-6	110 ± 16
5 µM MitoBloCK-6	95 ± 9
4ng ATG ALR Morpholino	150 ± 20

Figure 2.5: MitoBloCK-6 treatment. MitoBloCK-6 treatment resulted in defects in somitogenesis as well as circulatory deficiencies. Embryos were treated at 3 hpf with 1% DMSO control or MitoBloCK-6. MitoBloCK-6 fish exhibited spinal curvature (**B**), compared to control treatment (**A**), as well as cardiac morphology problems, exhibited by blood pooling below the ventricle in MitoBloCK-6–treated embryos compared with DMSO control (**D, E**, arrow). Additionally, florescence was lost, indicating problems during development. (**N**) Embryos injected with 4 ng of a translation-blocking morpholino against ALR also exhibited a similar spinal curvature (**C**) as well as blood pooling below the ventricle (**F**, arrow). (**I**) The heart rates of MitoBloCK-6 treated fish and morpholino-injected fish were markedly reduced compared with untreated controls, further indicating cardiac problems.

References

1. Delvecchio, C., Tiefenbach, J., and Krause, H. M. (2011) *Assay Drug Dev Technol* **9**, 354-361

2. Zon, L. I., and Peterson, R. T. (2005) *Nat Rev Drug Discov* **4**, 35-44

3. Chang, S., Bray, S. M., Li, Z., Zarnescu, D. C., He, C., Jin, P., and Warren, S. T. (2008) *Nat Chem Biol* **4**, 256-263

4. Petrascheck, M., Ye, X., and Buck, L. B. (2009) *Ann N Y Acad Sci* **1170**, 698-701

5. Hong, C. C. (2009) *Methods Mol Biol* **486**, 43-55

6. Barbazuk, W. B., Korf, I., Kadavi, C., Heyen, J., Tate, S., Wun, E., Bedell, J. A., McPherson, J. D., and Johnson, S. L. (2000) *Genome Res* **10**, 1351-1358

7. Tran, T. C., Sneed, B., Haider, J., Blavo, D., White, A., Aiyejorun, T., Baranowski, T. C., Rubinstein, A. L., Doan, T. N., Dingledine, R., and Sandberg, E. M. (2007) *Cancer Res* **67**, 11386-11392

8. Wang, C., Tao, W., Wang, Y., Bikow, J., Lu, B., Keating, A., Verma, S., Parker, T. G., Han, R., and Wen, X. Y. (2010) *Eur Urol* **58**, 418-426

9. Ito, T., Ando, H., Suzuki, T., Ogura, T., Hotta, K., Imamura, Y., Yamaguchi, Y., and Handa, H. (2010) *Science* **327**, 1345-1350

10. Scholz, S., Fischer, S., Gundel, U., Kuster, E., Luckenbach, T., and Voelker, D. (2008) *Environ Sci Pollut Res Int* **15**, 394-404

11. McGrath, P., and Li, C. Q. (2008) *Drug Discov Today* **13**, 394-401

12. Hallare, A. V., Kohler, H. R., and Triebskorn, R. (2004) *Chemosphere* **56**, 659-666

13. Fushimi, S., Wada, N., Nohno, T., Tomita, M., Saijoh, K., Sunami, S., and Katsuyama, H. (2009) *Aquat Toxicol* **95**, 292-298

14. Reimers, M. J., Flockton, A. R., and Tanguay, R. L. (2004) *Neurotoxicol Teratol* **26**, 769-781

15. Yu, P. B., Hong, C. C., Sachidanandan, C., Babitt, J. L., Deng, D. Y., Hoyng, S. A., Lin, H. Y., Bloch, K. D., and Peterson, R. T. (2008) *Nat Chem Biol* **4**, 33-41

16. Hao, J., Ho, J. N., Lewis, J. A., Karim, K. A., Daniels, R. N., Gentry, P. R., Hopkins, C. R., Lindsley, C. W., and Hong, C. C. (2010) *ACS Chem Biol* **5**, 245-253

17. Song, Y., Selak, M. A., Watson, C. T., Coutts, C., Scherer, P. C., Panzer, J. A., Gibbs, S., Scott, M. O., Willer, G., Gregg, R. G., Ali, D. W., Bennett, M. J., and Balice-Gordon, R. J. (2009) *PLoS One* **4**, e8329

18. Khuchua, Z., Yue, Z., Batts, L., and Strauss, A. W. (2006) *Circ Res* **99**, 201-208

Chapter 3: Elucidating Mitochondrial Dynamics During Early-Stage Axonal Growth and Development in Zebrafish Embryos

Abstract

Neuron growth and formation during embryogenesis has been well characterized. With increasing focus being drawn to the field of mitochondrial dynamics because of links being found between mitochondrial dysfunction and neurodegenerative disorders, significant interest has arisen in cellular trafficking within neurons. Of particular interest are the motor neurons, the cells required for muscle control. In the work described here, we characterize mitochondrial presence and dynamics within the motor neurons of developing zebrafish embryos, describing trafficking patterns and movement at the various stages. By comparing the information gathered here with development seen when mitochondrial biology is impaired, we can determine what potential roles mitochondrial proteins may have in motor neuron development.

Introduction

Zebrafish and Neuronal Study

Zebrafish have been studied as a hallmark model for vertebrate developmental biology for many years. Because zebrafish can produce 200 to 300 eggs in a single clutch, the embryos are transparent and develop externally with veritable synchrony; they are ideal for studying developmental processes beginning as early as fertilization.(1,2) Embryos can also be genetically manipulated to observe cellular process; even the minute movements of individual proteins and signaling factors can be observed through fluorescent labeling in the optically clear organism.(3) With a major focus of medicine shifting onto neurological disorders with links to mitochondrial dysfunction, such as Parkinson's disease and Alzheimer's disease, the development and function of the nervous system is beginning to be more closely examined.(4-6) Given that the nervous system is so complex, and essential for viability, much is still unknown about the inner mechanisms of neurons.

The Vertebrate Nervous System

The vertebrate nervous system comprises primarily the brain; spinal cord; and peripheral ganglia, or nerve cells.(7) There are numerous types of neurons, including sensory neurons, which respond to stimulus from the sensory faculties and send signals to the spinal cord and brain; motor neurons, which receive signals from the brain to control muscle contractions and glandular secretions; and interneurons, which connect neurons to each other within the spinal cord and brain.

A neural cell has 3 segments: the cell body (where the bulk of the cell mass is located), the dendrites, and the axon (Figure 3.1).(7) Dendrites are thin protrusions that arise from the cell body and project radially, often extending for a few centimeters and branching multiple times along the way, giving rise to a vast branching network. Although a cell body can give rise to many dendrites, it can only generate 1 axon. Axons, like dendrites, are cellular extensions of the cell body, but they are much thicker in nature and grow much longer. Human axons can be up to 1 meter in length, and in some species they can be even longer. Axons also have many branch points along their length; some axons can branch hundreds of times before their termination. For protection as well as to aid in signal conduction, the axons of motor neurons are covered by the myelin sheath, a fibrous layer produced by Schwann cells (Figure 3.1).

Neurons are unlike other cells in many ways. Most notably, neurons do not undergo cell division; rather, a type of stem cell generates them, and neurogenesis is virtually nonexistent once the organism reaches adulthood.(8) Additionally, neurons have the ability to communicate signals through the presence of synapses. Synapses are junctions between nerve cell components responsible for transmitting signals from the brain to the desired target. Synaptic signaling usually occurs from the axon of one neuron to the dendrite of another, but signaling can proceed in alternate fashions as well.

Axonal Growth

Because vertebrate organisms can be very complex, the axonal network needs to be extremely precise to guarantee maximal control over, and communication with, all cellular processes. Because each neuron only produces 1 axon, and because axons can extend very long distances from the cell body, each axon and axonal projection needs to be precisely placed.

During development, axons traverse through their environment through the growth cone. The growth cone is located at the tip of the axon and expresses filopodia responsible for sensing signaling factors of the surrounding area and responding accordingly. Signals such as cell adhesion molecules (CAMs) influence the direction and rate of axonal growth and can be classified into 4 categories: contact-attracting, contact-repulsing, long-range chemoattracting, and long-range chemorepulsing.(9) In this manner, axons are able to grow and retract, spreading out and integrating into the environment by interacting with, and responding to, the various signaling components.

Axonal growth during development is well characterized, but the extent to which, and mechanisms through which, the cellular components are trafficked within the growing axons, namely the mitochondria, is largely unknown. To this end, we set out to ascertain where mitochondria are located, and how they behave in developing motor neurons during the early growth process in embryonic zebrafish.

Results

Axon Growth: 1dpf

Motor neurons develop in the spinal column, from the anterior end (head) to posterior end of the zebrafish (tail); as a result, the anterior axons appear more developed than the posterior axons (Figure 3.2: A). Each new "row" along the spinal column contains 2 cell bodies, each growing laterally along the body curvature to the dorsal and the ventral sides simultaneously. The axons of 3 sequential cell bodies intertwine to form a large bundle that then grows as a unit longitudinally through the embryo.

The majority of axon growth seen at 1 dpf is longitudinal axonal projection away from the cell body (Figure 3.2). By 24 hours, the cell bodies have formed along the length of the spinal column and the developing axons are in the bundles of 3 axons each. The growth cones of the axons extend in an overall outward motion from the dorsal side of the embryo to the ventral side of the embryo, following the line of the dorsoventral axis. The actual growth cone moves in a combination of anterograde (extending away from the cell body) and retrograde (contracting toward the cell body) movement as it senses chemical cues from the environment as well as from other projecting axons. Small branch points of growth can be seen to begin developing at this stage.

The mitochondria present in the motor neurons at 1 dpf are concentrated predominantly in the cell body of the axon (Figure 3.2: B). Almost no fluorescent signal can be detected in the axonal projections themselves, indicating that either very few or no mitochondria have traveled into the projection itself. Although all of the fluorescence is concentrated in the cell body, it is unclear whether the mitochondria exist as a cluster of individual mitochondria or as 1 large fused mitochondrion or mitochondrial network.

Axon Growth:2 dpf

At 2 dpf, the axons are still short, thick, longitudinal projections along the dorsoventral axis of the embryo (Figure 3.3). The growth cone is still proceeding away from the cell body overall, but the anterograde and retrograde movement is still visible as the axons respond to surrounding signals. Projections deviating from branch points along the longitudinal line become more pronounced at the ends of the developing axons.

The mitochondria of each neuronal cell can be detected in large groups throughout the entire axonal projection at this stage (Figure 3.3: B). Given the size of the mitochondrially localized, fluorescent signal seen scattered throughout the axonal projection, we anticipate that the mitochondria exist, and travel, as fused groups of mitochondria as they migrate radially outward from the cell body. Interestingly, over the imaging time frame, very little movement can be seen in the projection itself, indicating that migration of the mitochondria down the axon is very slow at this stage. In contrast, a plethora of movement can be seen along the neurons that make up the spinal column (Figure 3.4).

Axon Growth: 3 dpf

At 3 dpf, small projections are beginning to branch along the entire length of the axon, rather than just at the distal end near the growth cone (Figure 3.5: A). Most growth seen at this point is lateral growth of the branches as they spread throughout the body of the zebrafish. These projections grow in a similar manner to the expansion of the singular axon; the growth cone extends and retracts as it moves through the surroundings, encountering other branching axons. Developing projections repel one another, ensuring that no neuron branch occupies the same space as another.

The mitochondria are beginning to spread more diffusely throughout the entire axon at this stage, and have begun to migrate into the branches growing off the main axon trunk (Figure 3.5: B). As was seen at day 2, very little movement could be detected from the mitochondria present in the axonal projections (Figure 3.6), indicating that movement along the axons and in the branches is still very slow at day 3, but activity along the spinal column remains present and fast-paced (Figure 3.6).

Axon Growth: 4 dpf

At 4 dpf, small, secondary and tertiary projections can be seen along the branches of the axonal projection (Figure 3.7: A). The majority of growth at this stage is still lateral growth of the extending primary and secondary branches. The trunk of the axon does not appear to show much change in growth because the overall width of the embryo is not changing much during this time period.

Mitochondria appear to be smaller, and perhaps exist as individual entities at this stage, rather than the larger groups visualized at the earlier time points (Figure 3.7: B). Interestingly, at 4 dpf we can detect the individual, rapid movement of mitochondria in the axonal projections (Figure 3.8: A). Indeed, at 4 dpf we can detect the most movement of mitochondria within the axonal projections. As expected, movement is still detected along the spinal cord, with many mitochondria traversing the field during this time (Figure 3.8: B).

Axon Growth: 5 dpf

At 5 dpf, the axons are very thin, and little growth is detected over the experiment length. The axons appear as a web, traversing the expanse of the "empty" space seen between the axonal bundles first observed at 1 dpf (Figure 3.9: A). The smaller primary and secondary branches seem to bisect the regions between these bundles into virtually even sectors, and no branches appear to overlap a region.

By 5 dpf, mitochondria seem spread uniformly throughout the main projection and the peripheral branches (Figure 3.9: B). The mitochondria are also rather stationary along the axon length and in the primary and secondary branches, although a small amount of movement can

still be detected (Figure 3.10). At 5 dpf, we can also detect fully developed mitochondrial networks along the projections, rather than just the existence of individual or large, fused groups of mitochondria (Figure 3.11, inset).

Axon Growth: 6+ dpf

At 6 dpf and beyond, the physical axon morphology remains virtually identical to that seen at 5 dpf (Figure 3.12). Any growth observed coincided with the overall growth and development of the zebrafish. The majority of the branches needed to reach developing muscles have been formed, so no change in branch formation or location can really be detected from 5 to 6 dpf. Similarly, the mitochondrial networks observed at 5 dpf are still easily visible at 6 dpf and beyond. There is little sporadic movement of the mitochondria along the axons, but migration is still observed regularly along the spinal region (Figure 3.13).

Discussion

As mentioned previously, although the development process of motor neurons in early zebrafish embryos is very well documented and characterized, little is known about the location and trafficking of a large number of cellular components. Of particular interest to our research was the movement and behavior of mitochondria within these developing neurons. At 1 dpf, the mitochondria could be observed predominantly in the cell body, with little observable signal seen in the axonal projections. This changes as the organism develops over time: the mitochondria migrate along the axonal projection, eventually spreading out to cover the entirety of the primary axon as well as all of the peripheral branches.

It is interesting to compare mitochondrial location and placement with observable embryo movement during development. At 1 dpf, the embryo is still in its chorion, and the only motion observed is the spontaneous wiggle of the tail. If the embryo is removed from the chorion, it is still only able to writhe its tail back and forth; it is unable to swim. At 2 dpf, the embryo is able to swim, but only in a straight line in a singular direction. Movement is often the result of a perceived external stimulus; when undisturbed the embryo will often remain stationary. From 3 dpf onward, motion of the embryo becomes more controlled, more frequent, and less of a direct result of external stimulation. Embryos will still flee from a perceived threat, but they also swim frequently and continuously when there is no external impetus.

This increase in both frequency and control of movement directly correlates to the migration of mitochondria and formation of a mitochondrial network in motor neurons. At stages in which embryonic movement is minimal and limited (1 through 3 dpf), mitochondria are in a primitive point of migrating along the developing axonal network. Transmitting signals that control motion response, both along a singular axon branch as well as between neighboring axons, is energetically costly; as a result, motion may be restricted to the spontaneous reaction to the firing of neurons (the "fight-or-flight" response).

As mitochondria migrate through the axon in later stages of development, forming networks and sparking movement of individual mitochondria within the projections (4 dpf onward), the embryo develops the ability to swim multidirectionally. This stands to reason: with the mitochondria that generate the majority of energy for a cell spread throughout the entire axon, the energy production required to transmit the signals that control finite motion throughout the motor neuron network is also spread through the axon, within close proximity to firing

synapses. Motion is not restricted to spontaneous reactions and the "fight-or-flight" response, but becomes a regular and essential component of the ability to survive.

Through characterizing the development of the zebrafish embryonic motor neuron, and how the mitochondria behave at the various stages for development, we created a basis of reference for monitoring axonal behavior and response. By comparing the canonical behavior during development with the observations garnered when a protein involved in mitochondrial biology is modified, we can determine what potential roles the proteins of interest may play in motor neuron development.

Materials and Methods

Zebrafish Lines

The line of zebrafish expressing green fluorescent neurons with red fluorescent mitochondria was generated by modifying a line of fish identified during a GFP enhancer trap screen, conducted at the University of Tübingen. The Gal4-GFP cassette location was mapped to intron 1 of the *gnaI2* gene on chromosome 6, and is regulated by either the *gnaI2* or *inka1b* enhancer. Zebrafish expressing the enhancer GFP were injected with a UAS-MLS-DsRed in pCS2+. The MLS-DsRed construct was created by fusing the coxVIIIa mitochondrial targeting sequence in front of the DsRed protein, and cloning the fusion protein into the pCS2+ vector. This construct was then microinjected into zebrafish embryos at the 1-cell stage, along with transposase RNA, and integrated into the host genome using homologous recombination around the Tol2 locus.

Zebrafish Husbandry

Zebrafish lines were maintained in a 14-hour-light/10-hour-dark cycle and mated for 1 hour to obtain synchronized embryonic development. Embryos were grown in E3 buffer (5 mM sodium chloride, 0.17 mM potassium chloride, 0.33 mM calcium chloride, 0.33 mM magnesium sulfate) for 1 to 7 days at 28.5°C.

Confocal Microscopy: Axon Growth Experiments

Zebrafish embryos were anesthetized in 0.01% tricaine and embedded in a sealed chamber using 1.2% low-melt agarose. Larvae were imaged for 12 hours using a 20× air

objective. Stacks were scanned every 20 minutes in 0.71-μm intervals. Imaging was performed with 4 to 6 larvae per session on a LSM 510 confocal microscope (Zeiss) with an automated stage, using Multitime software. Larvae viability was maintained at 28.5°C throughout the time course using a stage heater. Maximum intensity projections of confocal stacks were generated using Zeiss LSM software, and further processed using Image J.(10)

Confocal Microscopy: Mitochondrial Movement Experiments

Zebrafish embryos were anesthetized in 0.01% tricaine and embedded in a sealed chamber using 1.2% low-melt agarose. Larvae were imaged for 5 minutes using a 40× oil objective and 3× optical zoom. Stacks were scanned in rapid succession every second over a 1-μm section volume. Imaging was performed on a LSM 510 confocal microscope (Zeiss) with an automated stage, using Multitime software. Larvae viability was maintained at 28.5°C throughout the time course using a stage heater. Maximum intensity projections of confocal stacks were generated using Zeiss LSM software, and further processed using Image J.(10)

Figures

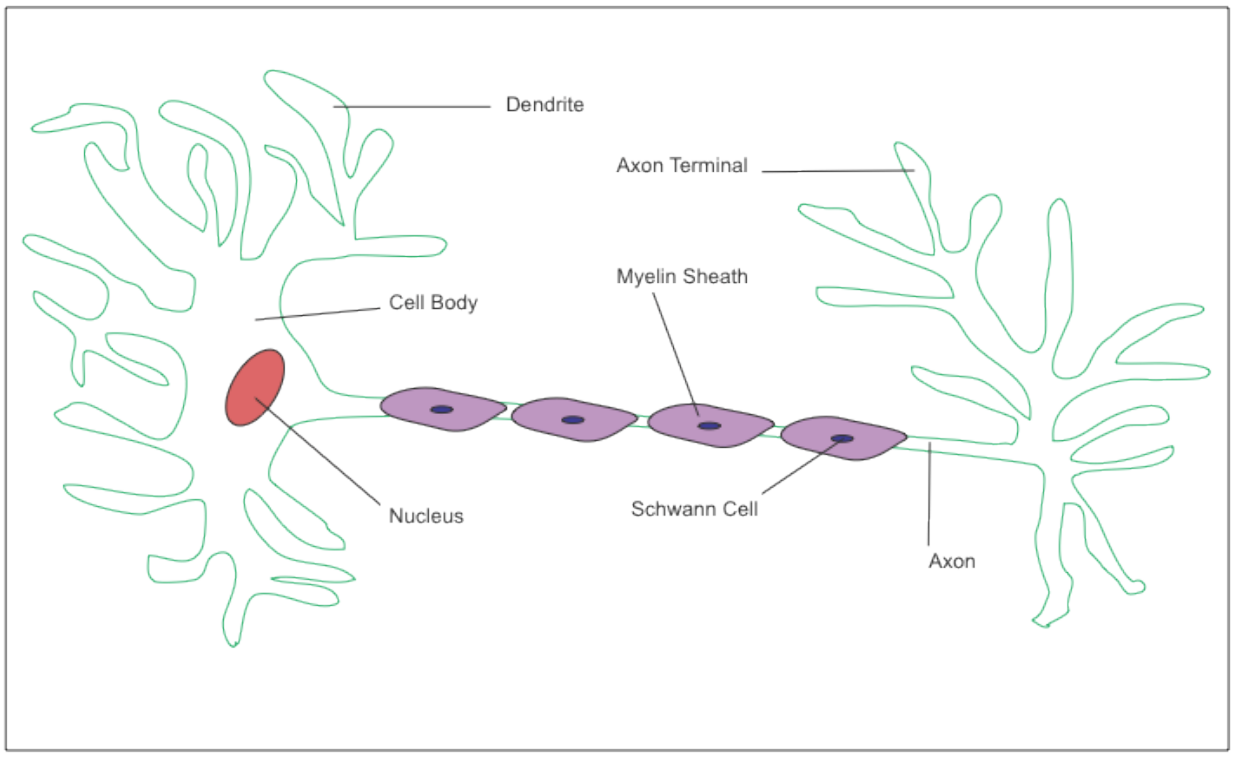

Figure 3.1: A neuron. A neuron cell comprises 3 distinct regions: the dendrites, the cell body, and the axon. Although a neuron has more than 100 dendrites, each cell body produces only 1 axon. Axons project radially away from the cell body, and can branch into many termini along the way. For protection, and to enhance signal conduction, axons are covered by a fibrous layer of myelin.

Axon Development: 1 dpf

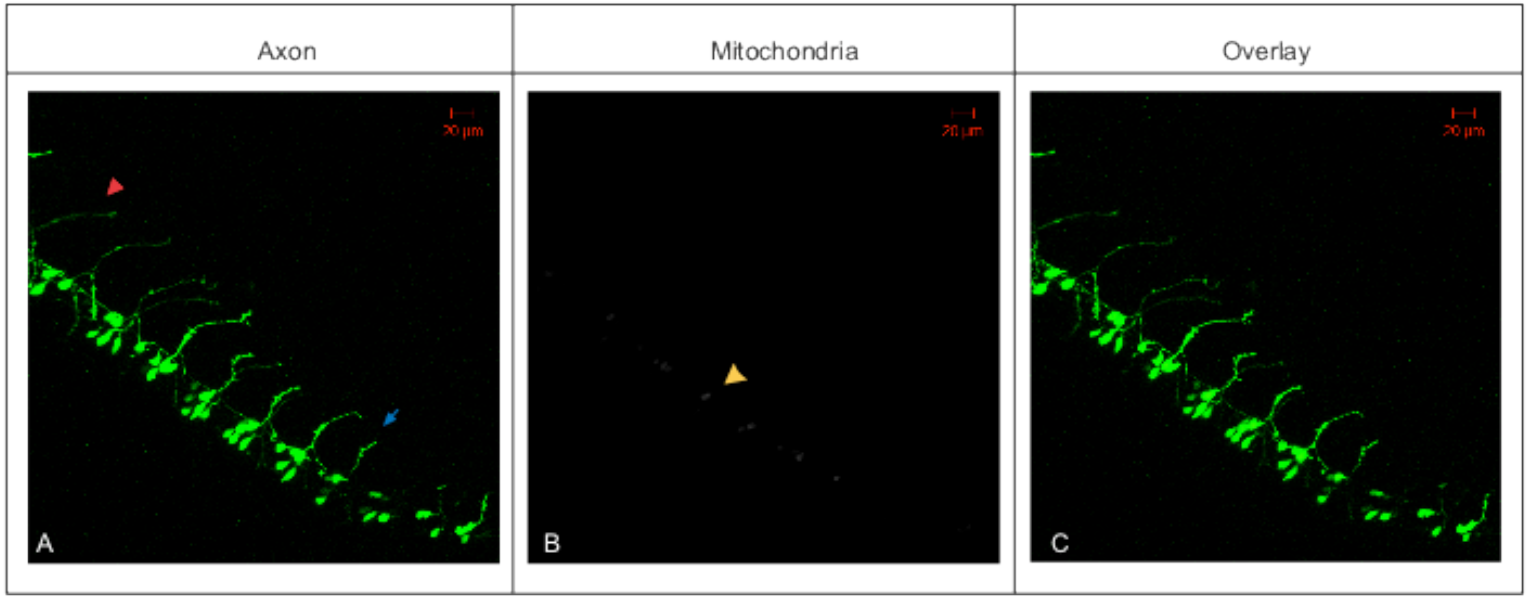

Figure 3.2: Axonal development at 1 dpf. At 1 dpf, axons are growing longitudinally away from the cell body. Axons develop from anterior (**A**, red arrow) to posterior (**A**, blue arrow) so projections closer to the tail are shorter in length. Branches are beginning to form at the axon termini. **B.** Mitochondria are predominantly clustered within the cell body (arrow). No signal is detectable along the projection.

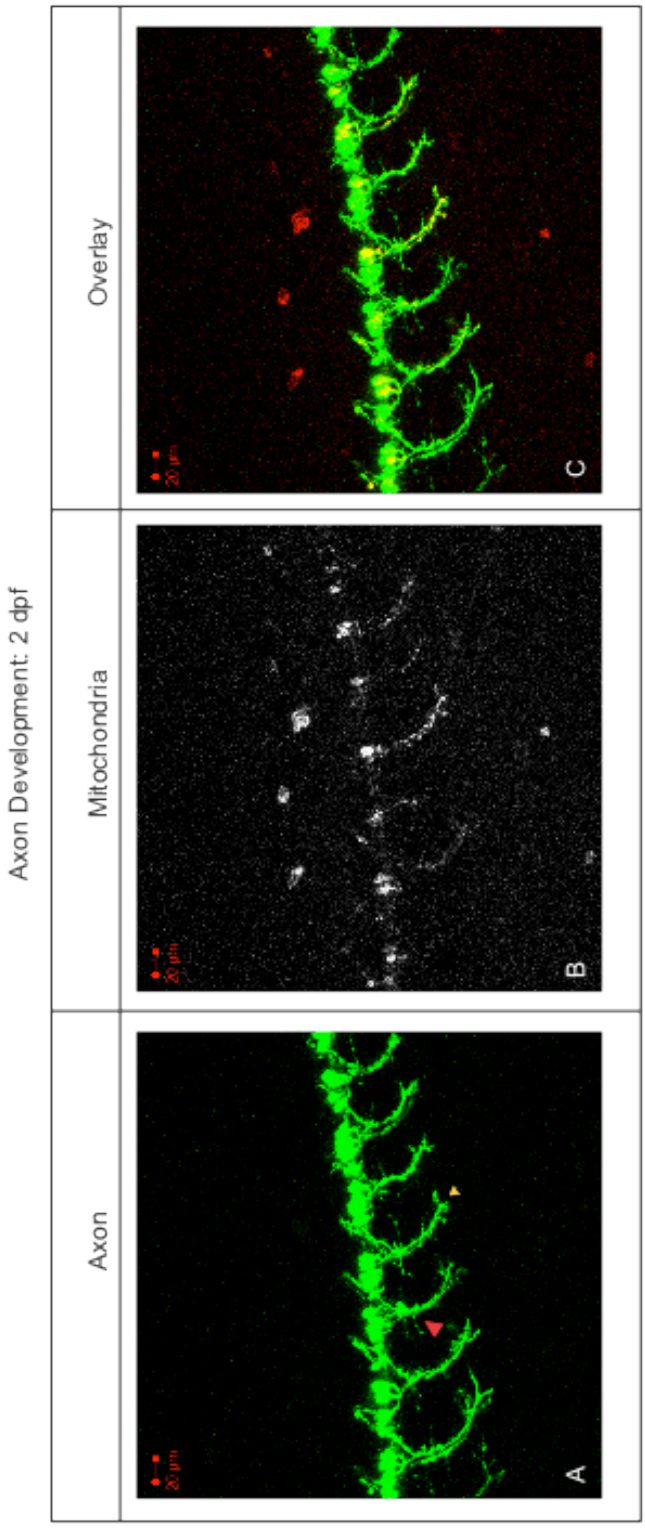
Axon Development: 2 dpf
Axon
Mitochondria
Overlay
A
B
C
20 µm

Figure 3.3 Axonal development at 2 dpf. **A.** Axons are continuing to project away from the cell body, and branch points can be seen at the axon termini (yellow arrow) as well as beginning to develop along the length of the axon (red arrow). **B.** Mitochondria are spread throughout the axonal projection. Fluorescence appears as large blocks, scattered throughout the entire axon, indicating that mitochondria travel as clusters as they migrate.

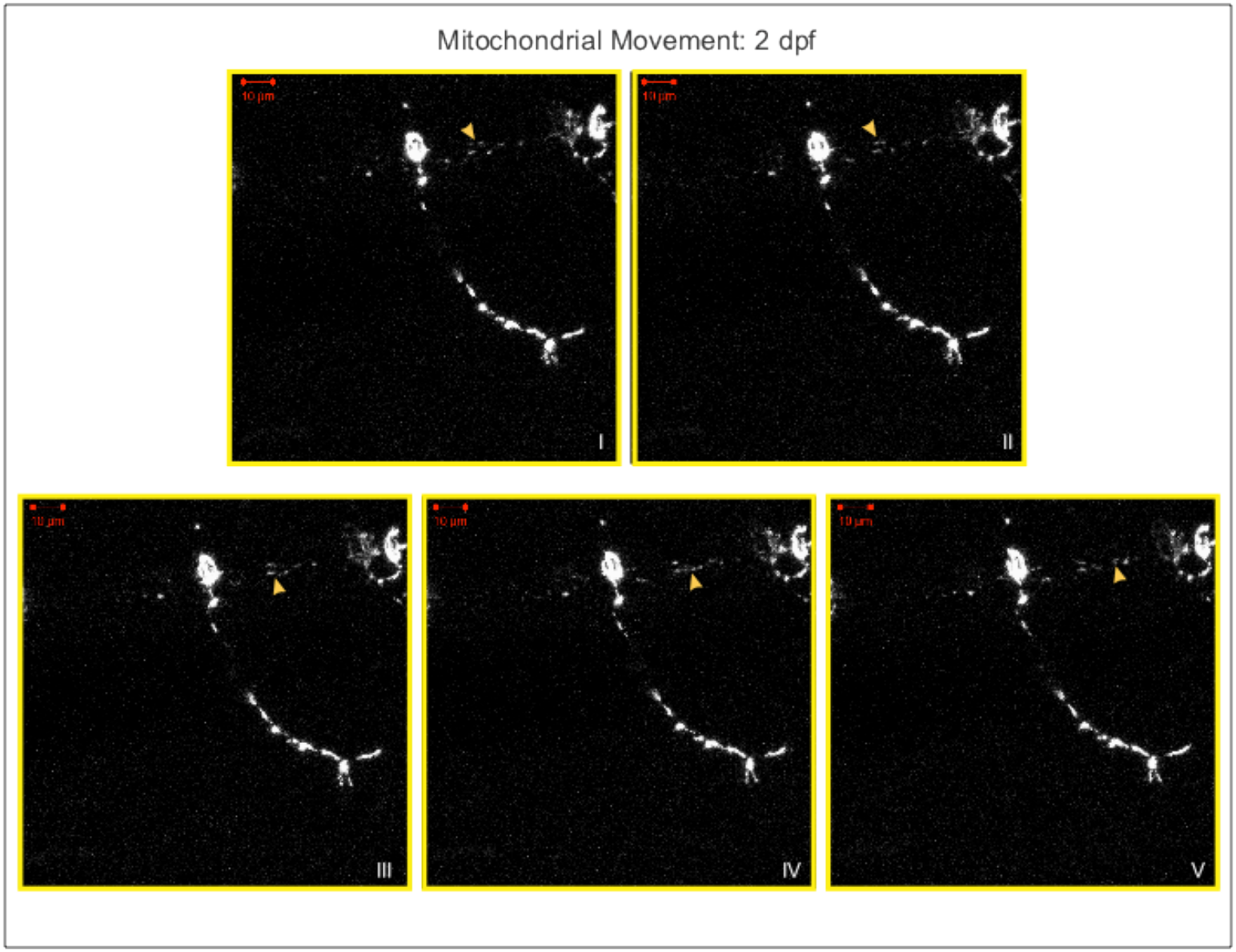
Mitochondrial Movement: 2 dpf
10 µm
I
10 µm
II
10 µm
III
10 µm
IV
10 µm
V

Figure 3.4: Mitochondrial movement at 2 dpf. Very little movement can be witnessed in the projections at 2 dpf, indicating that mitochondrial progress is slow. Motion can be detected in the spinal column at this stage (arrows).

Axon Development: 3 dpf

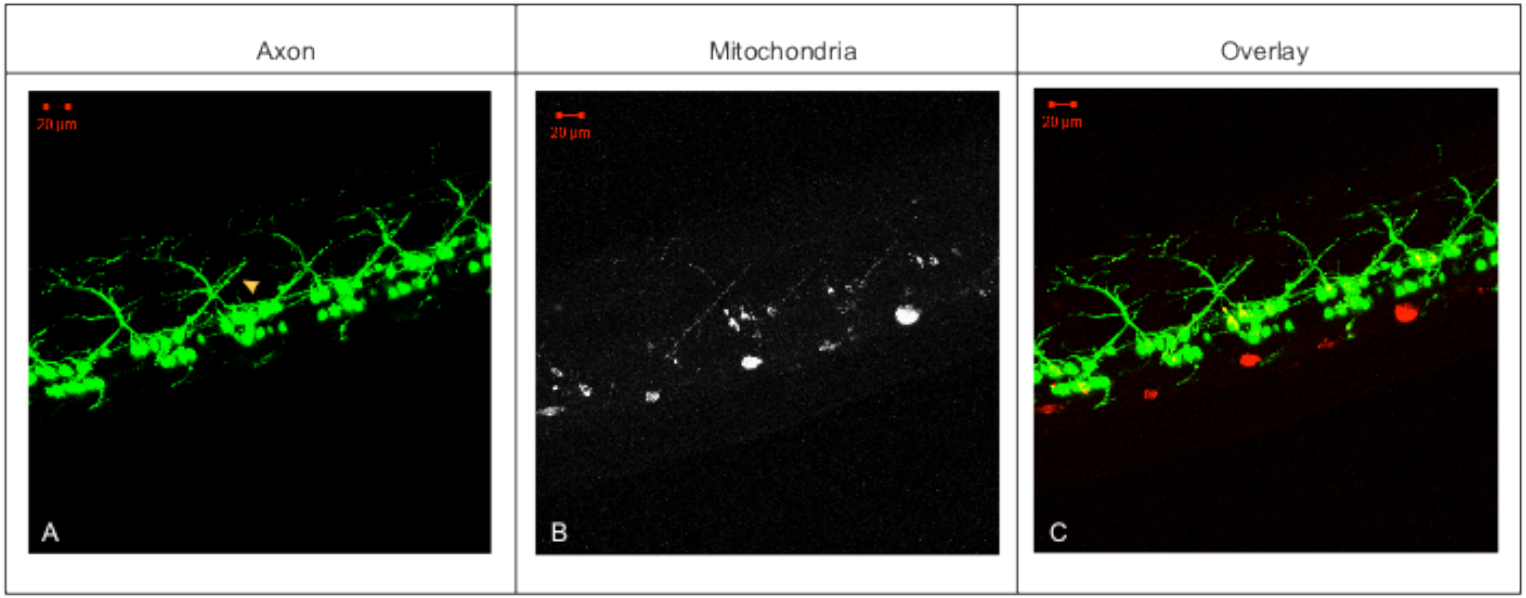

Figure 3.5: Axonal development at 3 dpf. **A.** Projections are distinct throughout the entire length of the axon, and are not just concentrated at distal ends. (arrow) **B.** Mitochondria are smaller and can be seen migrating within the newly developed peripheral branches.

3 dpf Mitochondrial Movement
I
II
III
IV
V
10 µm

Figure 3.6: Mitochondrial movement at 3 dpf. Mitochondrial movement can be detected along the spinal column (arrows), but not in the projection (thick, white segment in center of image set), indicating that the mitochondria are still progressing very slowly.

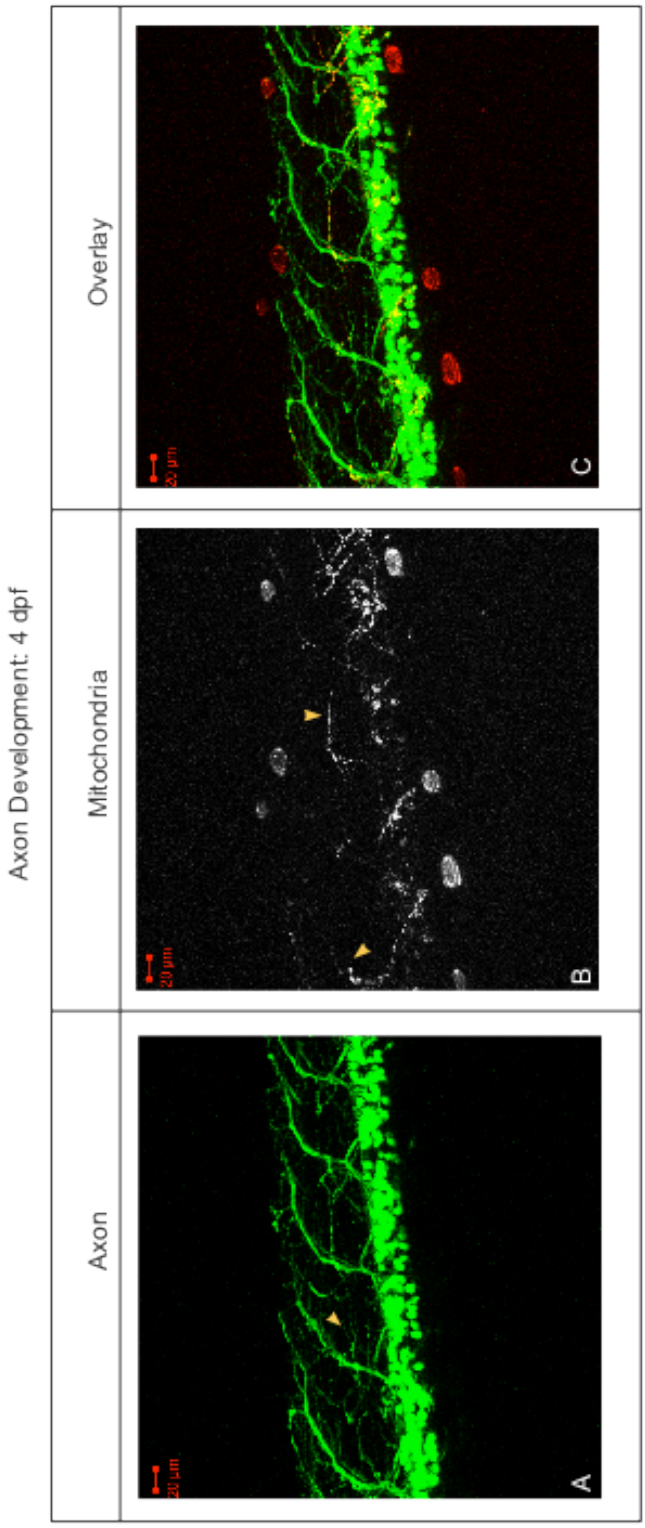
Axon Development: 4 dpf
Axon
Mitochondria
Overlay
20 µm
20 µm
20 µm
A
B
C

Figure 3.7: Axonal development at 4 dpf. **A.** Tertiary branches can be seen off of the secondary branch points (arrow). **B.** Mitochondria appear to be individual entities, and are present throughout the entire axon, as well as in the peripheral projections (arrows).

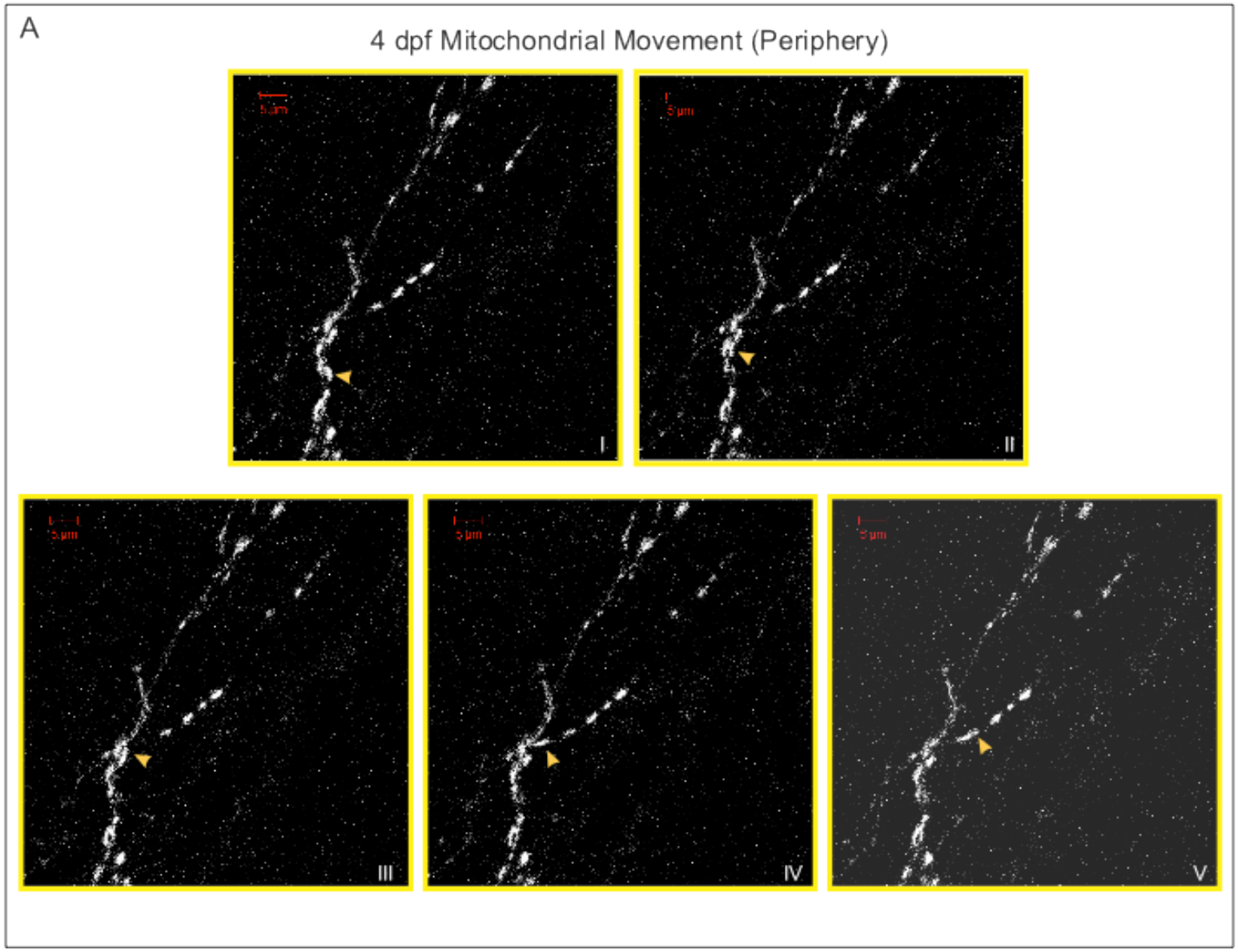
A
4 dpf Mitochondrial Movement (Periphery)
I
II
III
IV
V

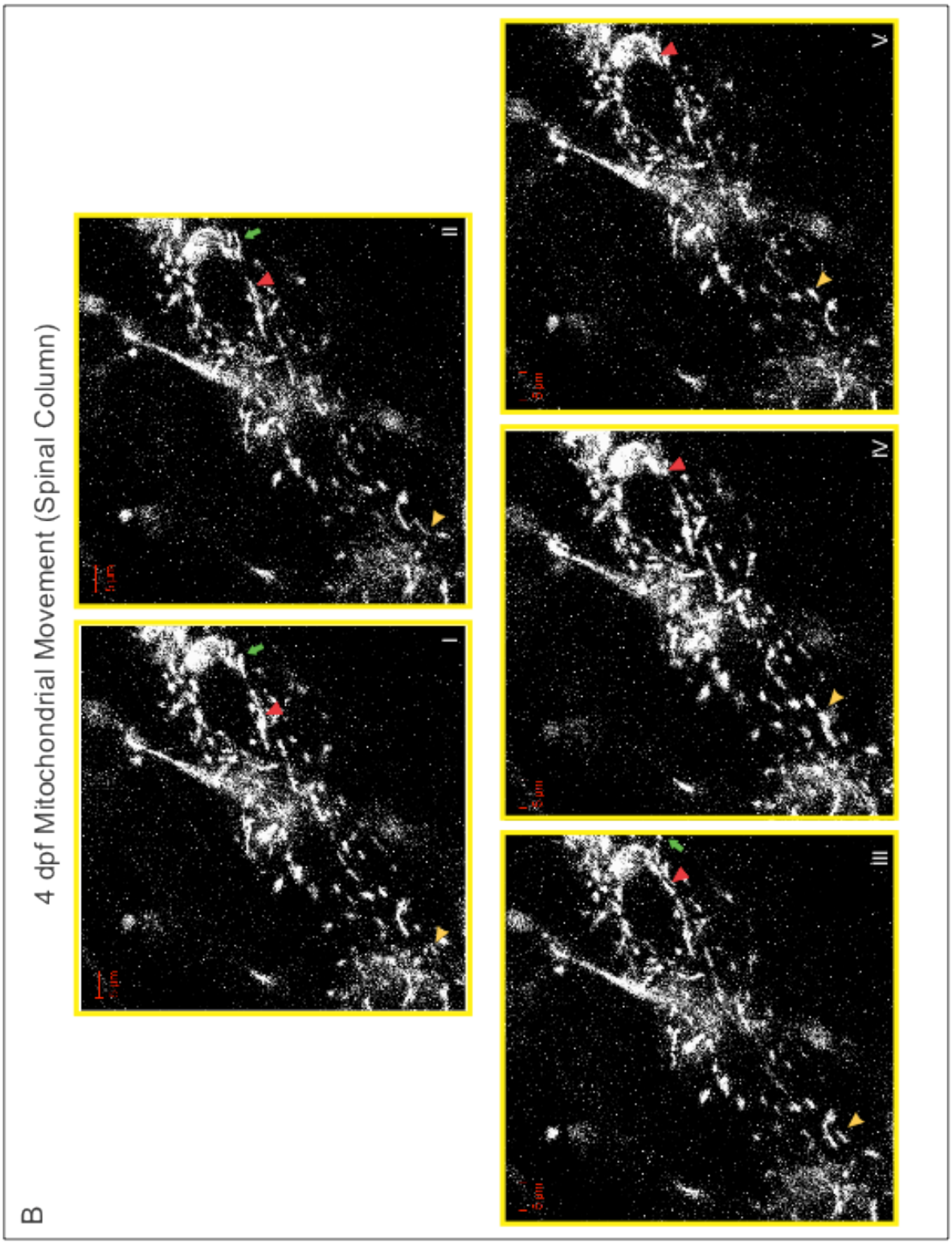
B
4 dpf Mitochondrial Movement (Spinal Column)
I
II
III
IV
V

Figure 3.8: Mitochondrial movement at 4 dpf. Movement can be detected in both peripheral branches, as well as along the spinal column. **A.** Movement of a singular mitochondrion through a peripheral branch point (arrow). **B.** Many mitochondria can be visualized traversing the spinal column. Each colored arrow follows the path of 1 mitochondrion.

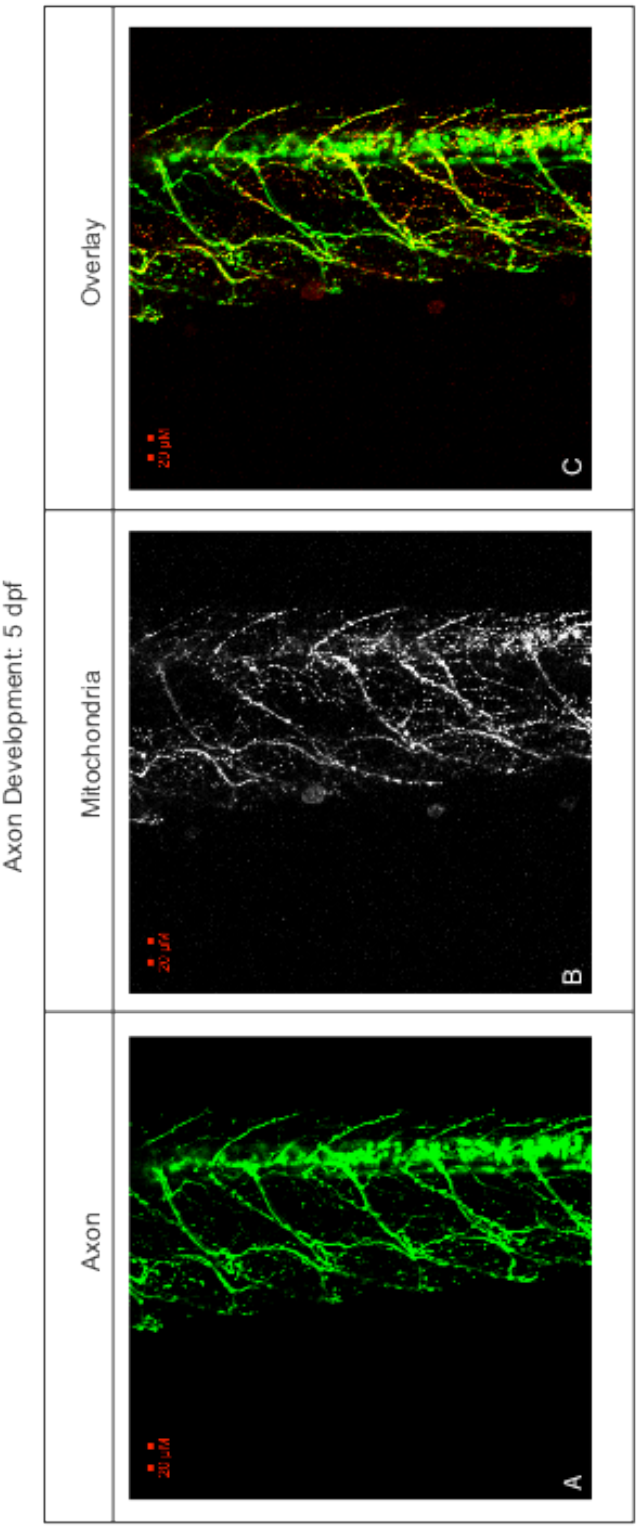
Axon Development: 5 dpf
Axon
Mitochondria
Overlay
A
B
C
20 µM

Figure 3.9: Axonal development at 5 dpf. **A.** Axons appear as a web throughout the entire body of the zebrafish. **B.** Mitochondria are spread uniformly throughout axon length and all peripheral projections.

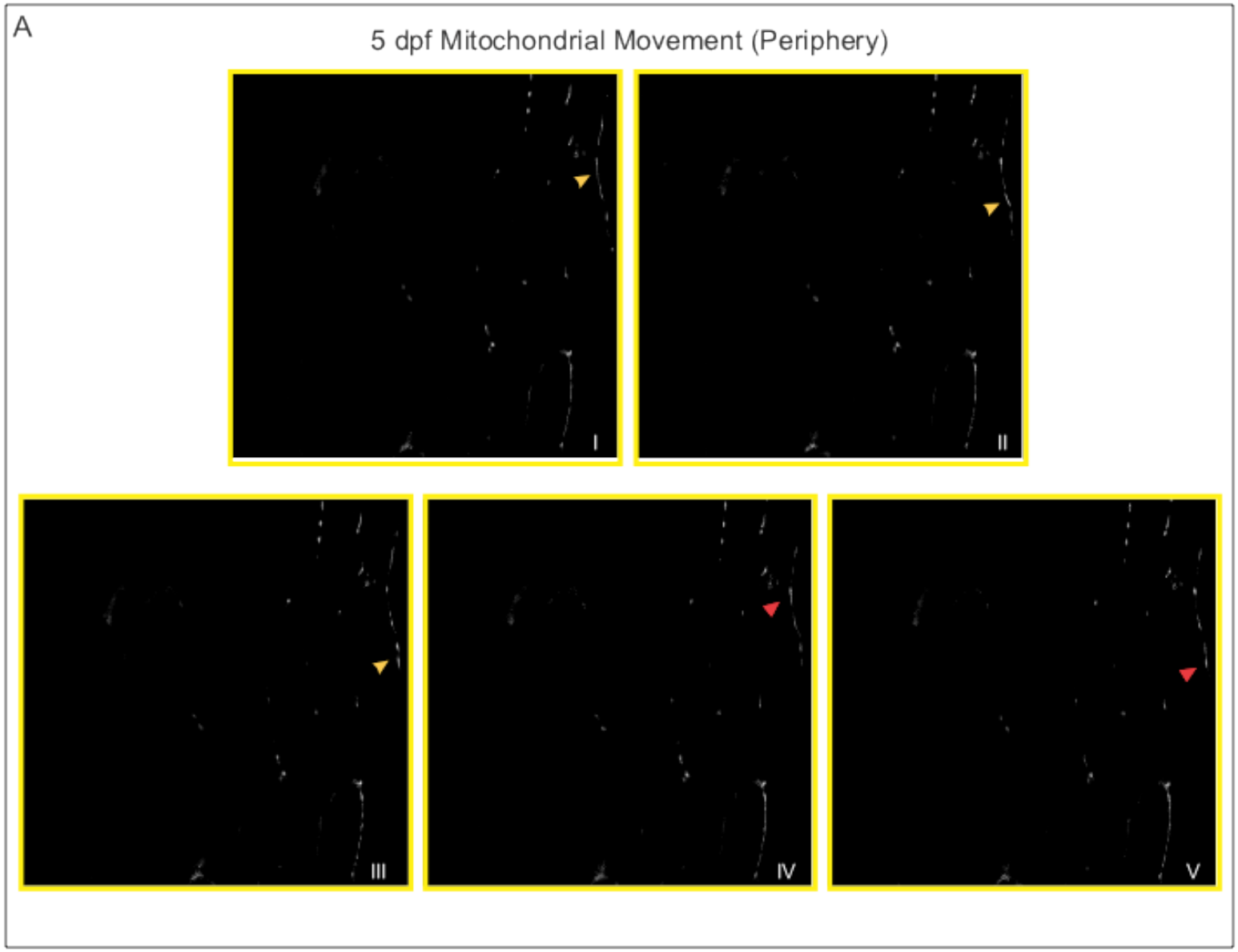
A
5 dpf Mitochondrial Movement (Periphery)
I
II
III
IV
V

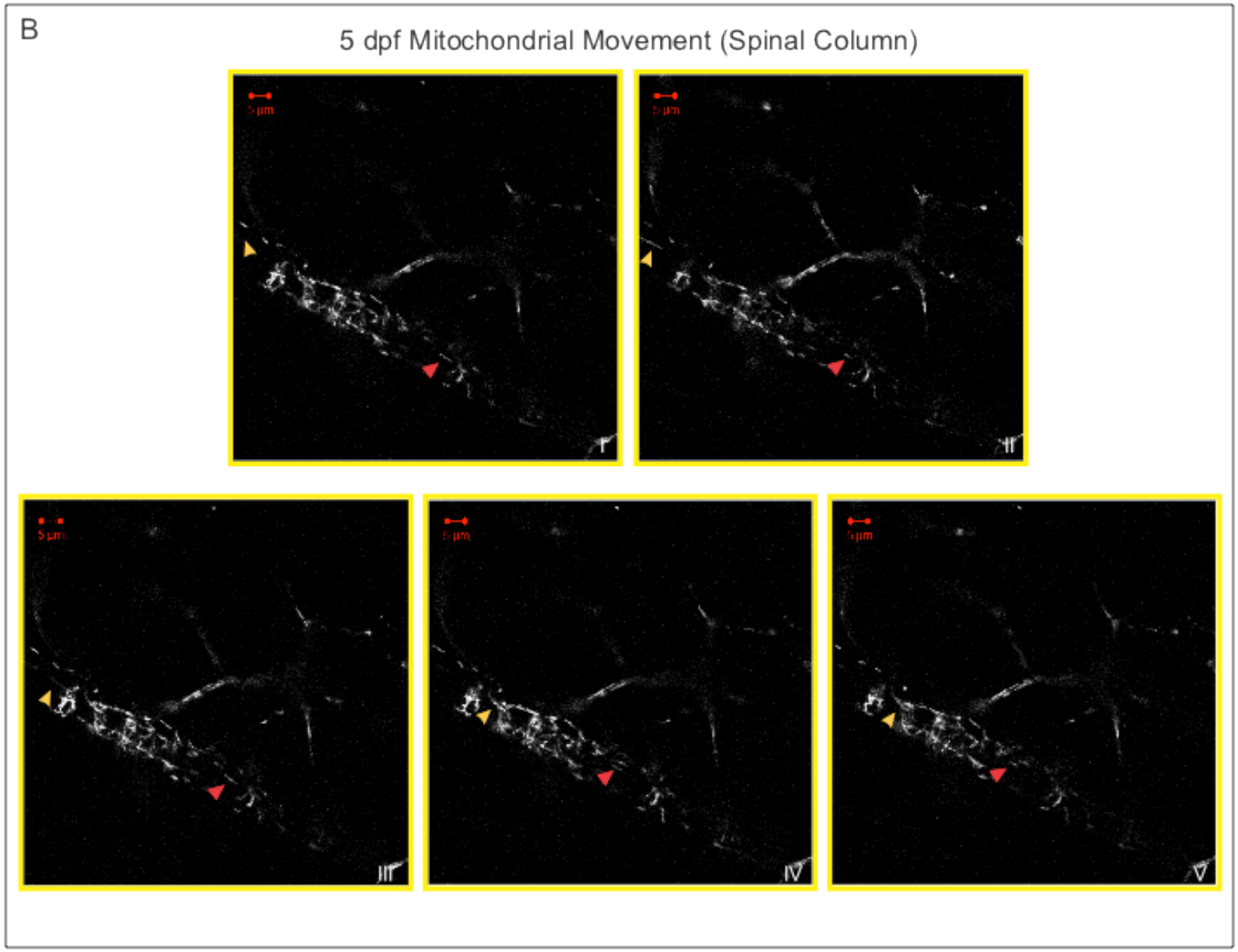
B
5 dpf Mitochondrial Movement (Spinal Column)
5 µm
I
II
III
IV
V

Figure 3.10: Mitochondrial movement at 5 dpf. **A.** Movement in peripheral projections is restricted; most mitochondria remain stationary. **B.** Movement remains in the spinal column, to a greater extent than in peripheral projections, but is not as rapid as in 4 dpf.

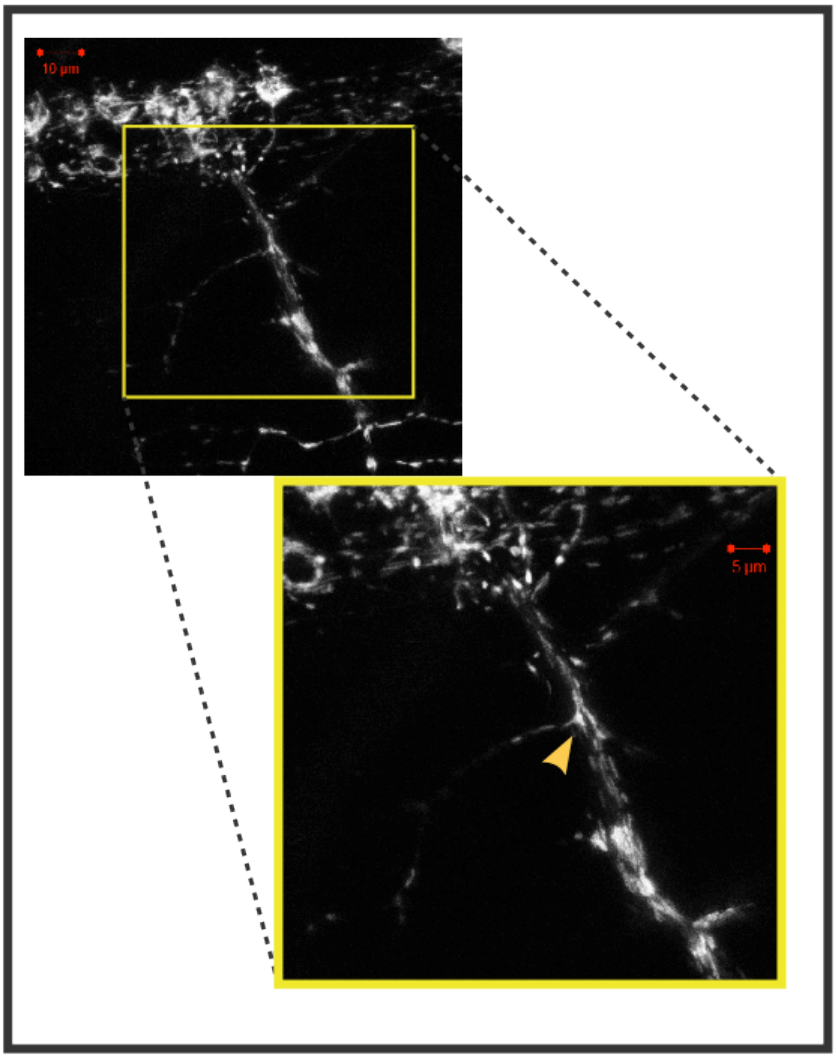

Figure 3.11: Mitochondrial networks. Mitochondrial networks can be detected in projections at 5 dpf. Mitochondria undergo fusion and fission as a means of traveling through a projection.

Axon Growth at 6 dpf

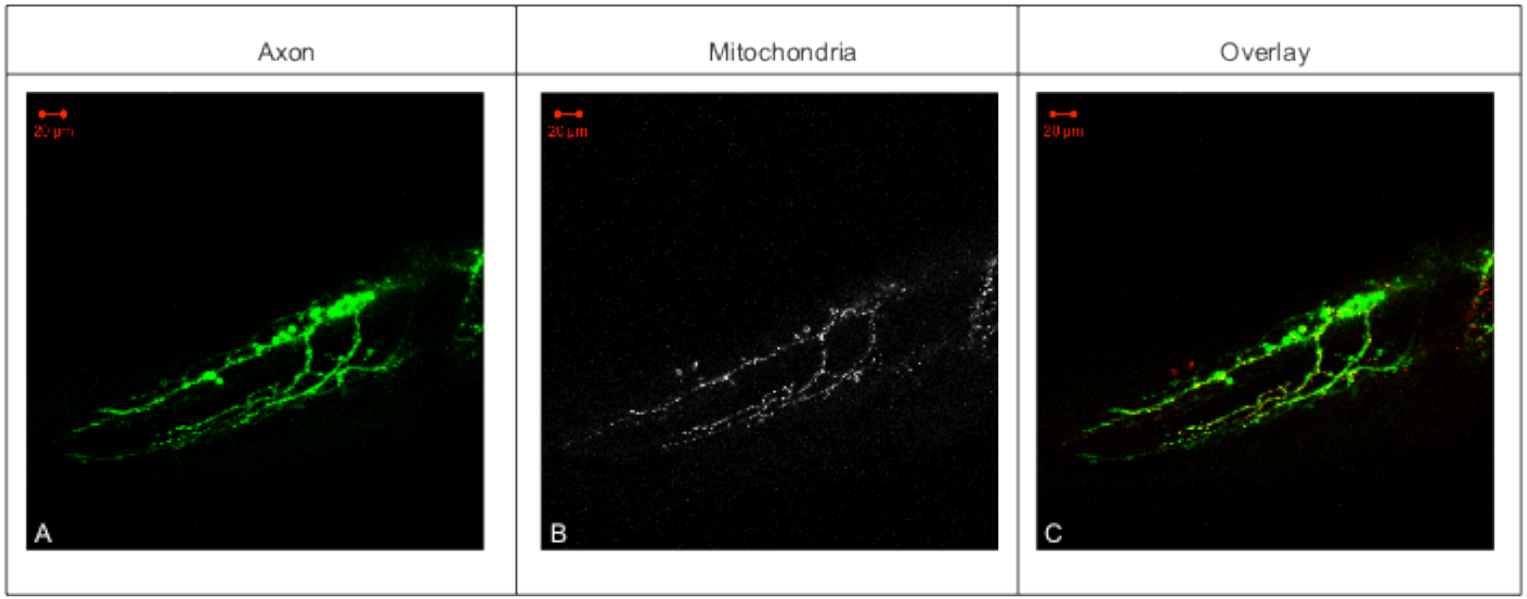

Figure 3.12: Axonal development at 6 dpf. Axon morphology appears identical to 5 dpf, with no great change in branch formation or number. Projections to tail are fully elongated.

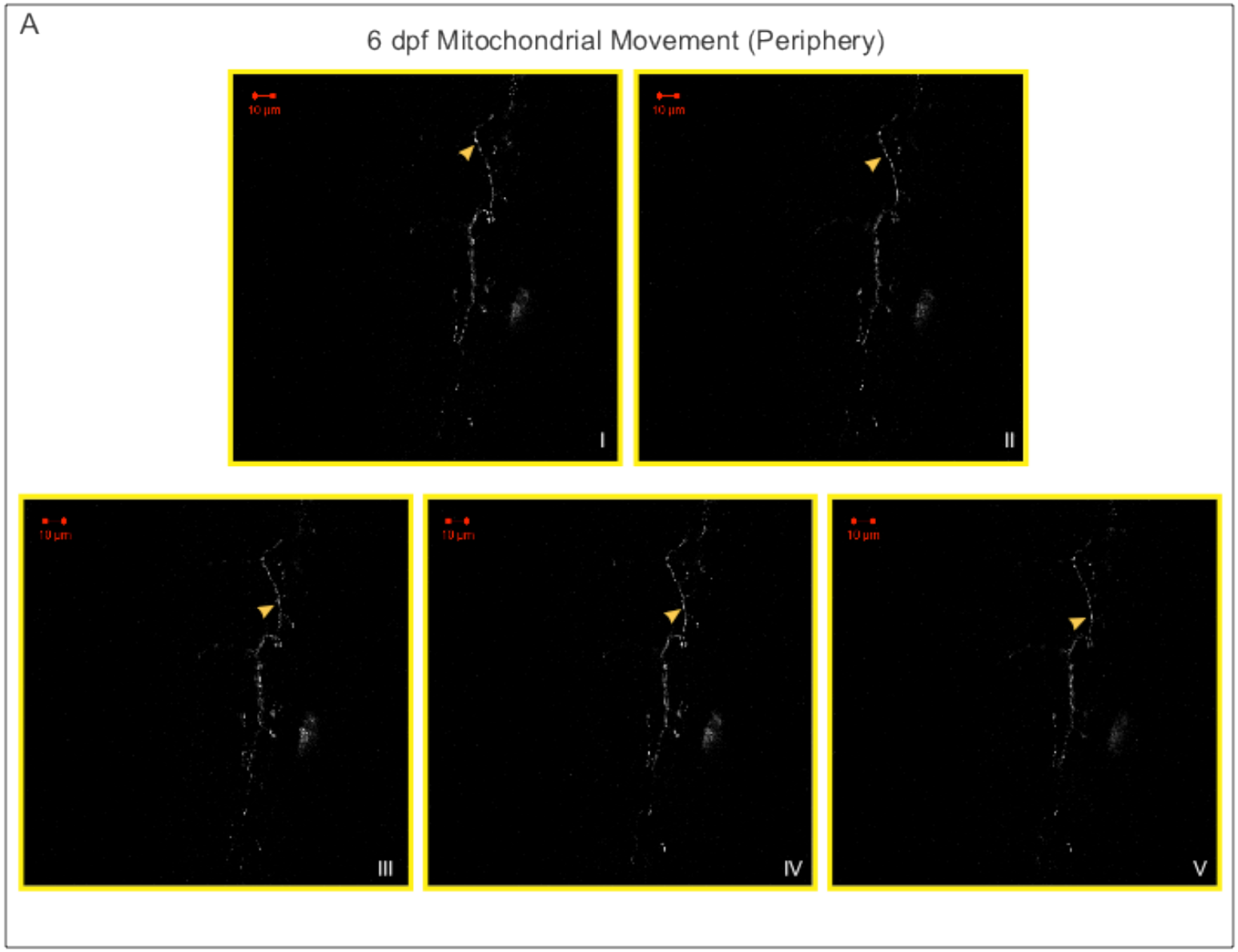
A
6 dpf Mitochondrial Movement (Periphery)
10 µm
I
10 µm
II
10 µm
III
10 µm
IV
10 µm
V

B
6 dpf Mitochondrial Movement (Spinal Column)
I
II
III
IV
V
10 µm

Figure 3.13: Mitochondrial movement at 6 dpf. A. Movement along periphery is limited to small migrations. **B.** Movement still occurs regularly along length of spinal column.

References

1. Delvecchio, C., Tiefenbach, J., and Krause, H. M. (2011) *Assay Drug Dev Technol* **9**, 354-361

2. Hong, C. C. (2009) *Methods Mol Biol* **486**, 43-55

3. Finley, K. R., Davidson, A. E., and Ekker, S. C. (2001) *Biotechniques* **31**, 66-70, 72

4. Trancikova, A., Tsika, E., and Moore, D. J. (2012) *Antioxid Redox Signal* **16**, 896-919

5. Martin, L. J. (2012) *Prog Mol Biol Transl Sci* **107**, 355-415

6. Calkins, M. J., Manczak, M., Mao, P., Shirendeb, U., and Reddy, P. H. (2011) *Hum Mol Genet* **20**, 4515-4529

7. Pough, F. H., Janis, C. M., and Heiser, J. B. (2009) *Vertebrate Life*, 8th ed., Pearson Benjamin Cummings, San Francisco, CA

8. Nowakowski, R. S. (2006) *Proc Natl Acad Sci U S A* **103**, 12219-12220

9. Goodman, C. S. (1996) *Annu Rev Neurosci* **19**, 341-377

10. Schneider, C. A., Rasband, W. S., and Eliceiri, K. W. (2012) *Nat Methods* **9**, 671-675

Chapter 4: Inhibiting ALR Affects Axonal Growth and Mitochondrial Movement in the Motor Neurons of Zebrafish

Abstract

Over the past decade, neurodegenerative diseases such as Parkinson's disease and Huntington's disease have been found to contain pathological links to mitochondrial dysfunction. Additionally, many known mitochondrial myopathies, such as Leigh's syndrome, have neurodegenerative components. For these reasons, we treated embryos with MitoBlock-6, a known small-molecule inhibitor of ALR and protein translocation, to observe its effects on motor neuron development and mitochondrial dynamics. Treatment with MitoBlock-6 caused a significant decrease in axon growth, and branching, compared with controls, along with a decrease in mitochondrial motility in axonal projections with prolonged treatment. Together, these data suggest that inhibition of ALR, an essential protein of the intermembrane space, not only affects mitochondrial import, but also axonal development and mitochondrial movement within developing motor neurons. These effects illustrate the importance of studying mitochondrial biology *in vivo*, a methodology that tools such as MitoBlock-6 can greatly enhance.

Introduction

Within the past decade, many neurodegenerative diseases have been linked to problems with mitochondrial function. Neurological disorders such as Parkinson's disease, Alzheimer's disease, and Huntington's disease, have all been found to have a mitochondrial component. Many known mitochondrial myopathies such as Leigh's syndrome or MELAS syndrome (mitochondrial encephalomyopathy, lactic acidosis, and stroke-like episodes) have a neurodegenerative component to their pathology, so it stands to reason that other neurodegenerative disorders would have mitochondrial deficiencies as well.(1,2)

Recently, it was discovered that a hereditary early-onset form of Parkinson's disease is caused by mutations in PINK1 and Parkin.(3) PINK1, a serine/threonine kinase residing in the outer mitochondrial membrane, is responsible for recruiting Parkin to depolarized mitochondria. Activation of the PINK1/Parkin pathway leads to clearance of damaged mitochondria.(4) In neurons where this pathway is inactive because of mutations, clearance of mitochondria is impaired, and the neurons may become prone to degeneration and degradation. Additionally, drugs that inhibit Complex I of the respiratory chain have been shown to produce Parkinson's like symptoms in humans and animal models.(5)

The link between Alzheimer's disease and mitochondria is a new and tenuous one, but there are certain aspects that point to, at the very least, a mitochondrial response. Beta-amyloid (Aβ), the fibril-forming protein responsible for plaque formation, has been shown to be able to localize to the mitochondrion.(6) Additionally, neuronal cultures treated with media from other cells expressing mutant forms of amyloid precursor protein (APP,) the precursor to Aβ, had an increase of mitochondrial fission, a loss of dendrites, and eventually cell death.(7) Although

specifics regarding the mitochondrial role in Alzheimer's degeneration remain elusive, there appears to be a link.

Mutant Huntingtin, the protein responsible for causing Huntington's disease has been shown to interact with dynamin-related protein 1 (Drp1), which is required for mitochondrial division. The interaction between Drp1 and mutant Huntingtin results in abnormal dynamics, and defective anterograde movement, along with synaptic deficiencies.(8,9) In patients and mouse Huntington's disease models, expression of the mutant protein led to elevated lactate levels, a decreased membrane potential, and Complex II respiratory problems.(10)

Amyotrophic lateral sclerosis (ALS) showcases mitochondrial dysfunction specifically within the motor neurons.(11) The familial form of ALS is caused by mutations within superoxide dismutase 1 (SOD1). SOD1 exists in both the cytosol and in the mitochondria. Patients with ALS mutations in SOD1 experience mitochondrial dysfunction and degradation, and ultimately motor neuron degeneration.

Because of these connections between neurons and mitochondria, we decided to test what effects our MitoBlock-6 inhibitor had on mitochondrial function and neuron development within zebrafish embryos. Because ALR is responsible for importing and successfully folding a myriad of proteins involved in all aspects of mitochondria biology, we hypothesized that knocking down its function would have a detrimental effect on axonal development and mitochondrial dynamics.

Results

FCCP: 2 dpf

To ensure that treatment with MitoBloCK-6 was distinct from general uncoupling of mitochondria, 2 days post fertilization (dpf) zebrafish embryos were treated with varying concentrations of FCCP for 1 hour before imaging. At 150 nM, development stalled, and embryos entered a suspended animation–like state. There was a slight growth of the body axis over the time course, but the axons remained unaltered throughout the experiment, which was conducted with a maintained presence of FCCP (Figure 4.1: A). If treatment was elongated to 24 hours before imaging, embryos staged to 1 dpf, the developmental stage at which treatment began (data not shown). At a higher concentration of 500 nM, the mitochondria collapsed and the axons fragmented, but the typical embryo death morphology did not follow, as evidenced by the continued presence of the body outline (Figure 4.1: B).

MitoBloCK-2: 2 dpf

Embryos were treated with E3 buffer, 1% DMSO, or 2.5 μM MitoBloCK-6 at 24 hours post fertilization, and allowed to incubate undisturbed at 28.5°C for an additional 24 hours. Embryos were then mounted in a sealed chamber with the continued presence of MitoBloCK-6, and imaged for 12 hours. Compared to the DMSO control, MitoBloCK-6 treatment resulted in a significant decrease in axon growth (Figure 4.2: B). DMSO-treated axons grew an average of 29.1 μm over the time course, whereas MitoBloCK-6–treated axons grew an average of 17.6 μm. Comparing morphology, axons treated with DMSO grew as the fish axis elongated, and began branching by the end of the experiment. Axons treated with MitoBloCK-6 also grew and

elongated in a similar manner to those in DMSO treatment, and did not exhibit any of the stalled characteristics witnessed with FCCP treatment. However, they also appeared stunted in length, and are markedly less branched than those under DMSO treatment by the end of the time course (Figure 4.2: B).

As mentioned previously, axons develop from anterior to posterior, so each axon projection must be compared individually when analyzing developmental changes. With DMSO treatment, axon 6 (counting anterior from tail) had an average of 7 branch points, with a mean length of 22.4 μm, whereas an axon in MitoBloCK-6 had an average of only 3 branch points, with a mean length of 18.6 μm. Similarly, axon 3 had an average of 4 branch points with a mean length of 13.2 μm in DMSO treatment, but only 2 branch points with a mean length of 9.9 μm (Figure 4.5: I). Although the ratio does not change much in terms of branching from older axon (axon 6) to newer axon (axon 3), there is a dramatic difference in the ratio of branch length.

To ascertain whether the difference in length was due to a lack of growth or a change in the ratio of anterograde (away from cell body extension) to retrograde (toward the cell body retraction), the specific velocities and the direction of growth at each time point were quantified. With DMSO treatment, axons appear to engage in more gross anterograde movement compared with MitoBloCK-6 treatment (Figure 4.6: A). Axons in the presence of MitoBloCK-6 spent more time either stationary, or moving in a retrograde direction. Further analysis examining the specific velocities showed slight differences in growth patterns, but no further information could be gleaned (Figure 4.6: B).

MitoBloCK-2: 1 dpf

To further explore the effects of MitoBloCK-6, we modified the experiment to monitor growth at 1 dpf. Embryos were again treated with E3 buffer, 1% DMSO, or 2.5 μM MitoBloCK-6, and embryos were treated for 24 hours, in keeping with the 2-dpf data. Interestingly, the phenotype was not as strong as that seen at 2 dpf. DMSO treatment resulted in an average growth of 41.2 μm, whereas MitoBloCK-6 treatment resulted in an average growth of 34.1 μm (Figure 4.3). Comparing morphology, we again see the same growth and elongation pattern for DMSO treatment as that of the 2-dpf data. The projections appear normal and evenly spaced along the length of the zebrafish (Figure 4.3: A). With MitoBloCK-6 treatment, however, the neurons look "stump-like," sickly, and disorganized (Figure 4.3: B). Although branching is only beginning at 1 dpf, we still quantified the occurrences. DMSO treatment resulted in more branches on average than MitoBloCK-6 treatment, as was seen at 2 dpf, although there were admittedly smaller differences in number between the 2 treatments (Figure 4.5: II). The branches that did form, however, had no discernible difference in length. When comparing the specific velocities for DMSO and MitoBloCK-6 treatment, we again saw that DMSO treatment resulted in axons that spent more time growing anterograde, and MitoBloCK-6 treatment resulted in axons that remained stationary. Contrary to the 2-dpf data, DMSO treatment resulted in more retrograde movement than MitoBloCK-6 treatment (Figure 4.6: C). Once again, in keeping with the 2-dpf data, the detailed specific velocity quantification did not provide any further insight (Figure 4.6: D).

ALR Morpholino: 2 dpf

To establish whether the effects seen by MitoBloCK-6 treatment were due to specific knockdown of ALR, and not a result of off-target effects incurred occasionally by small-molecule treatment, we injected a morpholino designed to target the zebrafish ALR protein exclusively. Four nanograms of a translation-blocking morpholino was injected into the single-cell stage of embryos. Embryos were then imaged at 2 dpf. The results for these studies were similar to those acquired during MitoBloCK-6 treatment; however, they were not as strong. Morpholino treatment resulted in similar growth morphology compared with uninjected embryos, and had virtually the same average growth as well (Figure 4.4). Axons in morpholino-injected fish, however, looked shorter and less branched, as if they were developmentally delayed compared with those left untreated (Figure 4.4: B). Morpholino-injected zebrafish also has a slight difference in branch number compared with untreated fish, but there was a marked difference in the length of the axon branches at all 3 points of calculation (Figure 4.5: III). Velocity comparisons between morpholino-injected embryos and untreated embryos were virtually identical, although morpholino-injected fish had slightly more retrograde movement and slightly less anterograde movement compared with untreated embryos (Figure 4.6: E).

Mitochondrial Movement and MitoBloCK-6 Treatment

We had previously characterized the movement of mitochondria within the motor neurons during development. To establish whether treatment with MitoBloCK-6 would have any effect on mitochondrial trafficking, we treated embryos with MitoBloCK-6 at 24 hpf and allowed them to develop in the drug undisturbed at 28.5°C until 4 dpf. Twenty-four hours post fertilization was chosen in keeping with our previous data. Additionally, embryos can only

remain viable in MitoBloCK-6 for 3 days, and 4 dpf was shown to have the most mitochondrial movement. To establish a point of reference, and to ensure that MitoBloCK-6 was not behaving as a membrane potential uncoupler, embryos were treated with 150 nM FCCP for 1 hour before imaging, and then kept in FCCP during the time series. Treatment with FCCP resulted in almost a full cessation of mitochondrial movement (Figure 4.7).

Unlike FCCP treatment, MitoBloCK-6 treatment did allow for mitochondrial trafficking within the axon (Figure 4.9). Twenty-six movies were analyzed from zebrafish treated with 1% DMSO, with a total of 827 mitochondria quantified. Similarly, 36 movies were analyzed from zebrafish treated with MitoBloCK-6, with a total of 1171 mitochondria being quantified. Data were normalized for comparison. The percentage of mitochondria trafficked did not differ remarkably from DMSO treatment (Figure 4.8), nor was there a change in the percentage moving anterograde versus retrograde; however, the distance and velocity with which the mitochondria move was drastically altered (Figure 4.10). MitoBloCK-6 treatment resulted in a majority of the mitochondria moving very slowly, most slower than 1 μM/s. DMSO treatment, however, had a large percentage of mitochondria moving between 1 and 2 μM/s.

Discussion

As more neuronal diseases and disorders are found with links to mitochondrial proteins, the role of the mitochondrion within this system becomes an important question. Understanding what part mitochondria play in the key pathways of the affected systems could elucidate where the disease-causing problems leading to neurodegeneration are deviating.

We showed that with MitoBloCK-6 treatment, axonal growth decreased significantly in 2-day-old embryos. Additionally, development was disrupted and axons became stunted and less

branched. Lastly, it appeared that treatment with MitoBloCK-6 caused a decrease in growth by altering elongation patterns; axons in the presence of the drug spent more time in a stationary position rather than lengthening or retracting as is normally seen. Taken together, these data suggest that by inhibiting ALR, we are blocking the translocation of unidentified proteins required for neuronal growth, or perhaps by inhibiting the import of other mitochondrial proteins, we are disrupting cellular energetics within the neuron. However, because the phenotype observed with MitoBloCK-6 did not mirror that seen with FCCP treatment, which uncouples the respiratory chain and prohibits ATP production, the latter option does not seem to be the whole story. Given that the data produced at 1 dpf followed similar trends as that at 2 dpf, but had softer differences between the empirical values of the 2 treatments, we can postulate that protein import via the ALR pathway is more widely essential at 2 dpf. Perhaps protein levels are higher at 2 dpf than at 1 dpf, thus providing a starker contrast when inhibition occurs, or perhaps the level of mitochondrial protein import is simply greater at 2 dpf. There is also the possibility that certain neuron-specific proteins are only just beginning to be synthesized and imported around 24 hpf, and as a result, the phenotype observed is simply not as strong.

Unfortunately, the morpholino injections did not prove to be compelling. Although the trends for growth and branching were present, it appeared as if normal growth had resumed by 2 dpf. Because morpholinos are transient objects and their effects wear off as cellular metabolism eventually degrades them, this is not surprising. The effects of MitoBloCK-6 are reversible within a small treatment window (data not shown); once removed and washed away, protein import resumes as normal. An analogous effect seems to be the case with morpholino treatment; thus, growth rates appear identical to control embryos, but the axons appear delayed.

Interestingly, in addition to growth defects, MitoBloCK-6 seemed to have an effect on mitochondrial trafficking within the motor neurons. The percentage of mitochondria that remain motile was similar to that seen with control treatment; however, the velocity with which the mitochondria move dramatically decreased. It was observed during earlier studies that mitochondria migrate with the axon as it elongates. If that movement is slowed, it could explain why the axons spend more time in a stationary position during the growth time courses. Elongation may not be able to continue very far, or very long, without mitochondria present and migrating simultaneously.

Through these studies we have shown the importance of mitochondria within the neuronal system. Although we do not believe that ALR is directly required for axonal growth and development, we have shown that if ALR is inhibited, not only is import into the intermembrane space affected, but growth and development are as well. These secondary effects make studying the role of mitochondria *in vivo* crucial. Developing tools to dissect these connections could lead to a new understanding of intracellular relationships and possibly new discoveries in the field of neuronal biology.

Future Directions

Further work in these studies is to investigate the specific mechanism by which MitoBloCK-6 is disrupting zebrafish development. Previous experiments conducted by the laboratory have suggested that disruption of ALR could generate reactive oxygen species (ROS) due to its link with cytochrome *c* and molecular oxygen (data not shown). Rendering ALR non-functional causes a build-up of free electrons, which could generate ROS. Studies are currently ongoing to ascertain whether co-treatment with antioxidants such as n-acteyl cysteine would ameliorate the phenotype garnered by MitoBloCK-6 treatment. Should this prove effective, treatment with compounds known to generate ROS, such as hydrogen peroxide or paraquat, will be conducted to recapitulate the phenotype observed with MitoBloCK-6 treatment. Studies are also being designed to over-express ALR in zebrafish neurons in an attempt to induce excessive growth. Additionally, the motor proteins involved with mitochondrial trafficking will be investigated to determine if there is a link between them and ALR, due to the observation that ALR inhibition decreases the velocity of mitochondrial movement. Determining how ALR inhibition causes the observed phenotype could help elucidate the role mitochondrial disruption plays in neurodegenerative disorders.

The methodology described here will also be used for future assays looking at alternative disease-causing proteins localized within the mitochondria. Current research is beginning examining small molecule affectors of mitochondrial proteins linked to Parkinson's disease as well as Alzheimer's disease. Using similar procedures, and zebrafish that are completely transparent as adults; the role of mitochondria, mitochondrial protein import, and mitochondrial trafficking will be examined for these targets, with the ultimate goal to generate an adult model amenable for study.

Materials and Methods

Zebrafish Lines

Zebrafish expressing green fluorescent neurons with red fluorescent mitochondria (MitoMotor) were generated by modifying a line identified during a GFP enhancer trap screen, conducted at the University of Tübingen. The Gal4-GFP cassette location was mapped to the first intron of the *gnaI2* gene on chromosome 6, and is regulated by either the *gnaI2* or *inka1b* enhancer. Zebrafish expressing the enhancer GFP were injected with a UAS-MLS-DsRed in pCS2+. The MLS-DsRed construct was created by fusing the coxVIIIa mitochondrial targeting sequence in front of the DsRed protein, and cloning the fusion protein into the pCS2+ vector. This construct was then microinjected into zebrafish embryos at the single-cell stage, along with transposase RNA, and integrated into the host genome using homologous recombination around the Tol2 locus.

Zebrafish Husbandry

Zebrafish lines were maintained in a 14-hour-light/10-hour-dark cycle and mated for 1 hour to obtain synchronized embryonic development. Embryos were grown in E3 buffer (5 mM sodium chloride, 0.17 mM potassium chloride, 0.33 mM calcium chloride, 0.33 mM magnesium sulfate) at 28.5°C.

Zebrafish FCCP Assay

Zebrafish were mated for 1 hour to obtain synchronized embryonic development. For 2-dpf imaging series; embryos were grown to 24 hpf in E3 buffer (5 mM sodium chloride, 0.17 mM potassium chloride, 0.33 mM calcium chloride, 0.33 mM magnesium sulfate) and incubated

with 150 nM or 500 nM FCCP for 1 hour before imaging. Following treatment, embryos were imaged using a LSM 510 confocal microscope (Zeiss).

Zebrafish Drug Treatment Assay

Zebrafish were mated for 1 hour to obtain synchronized embryonic development. For 2-dpf imaging series; embryos were grown to 24 hpf in E3 buffer (5 mM sodium chloride, 0.17 mM potassium chloride, 0.33 mM calcium chloride, 0.33 mM magnesium sulfate) and incubated with buffer, 1% DMSO or 2.5 μM MitoBloCK-6 for an additional 24 hours at 28.5°C. Following treatment, embryos were imaged using a LSM 510 confocal microscope (Zeiss).

Zebrafish Morpholino Studies

Wild-type AB embryos or MitoMotor embryos were microinjected at the single-cell stage with 4 ng of an ATG morpholino targeted to zebrafish ALR protein (5'-GAGGGTTGCCAGATCTCTGTTAAAT) (GeneTools, Inc.). Following treatment, embryos were imaged using a LSM 510 confocal microscope (Zeiss).

Confocal Microscopy: Axon Growth Experiments

Zebrafish embryos were anesthetized in 0.01% tricaine and embedded in a sealed chamber using 1.2% low-melt agarose. Larvae were imaged for 12 hours using a 20× air objective. Stacks were scanned every 20 minutes in 0.71-μm intervals. Imaging was performed with 4 to 6 larvae per session on a LSM 510 confocal microscope (Zeiss) with an automated stage, using Multitime software. Larvae viability was maintained at 28.5°C throughout the time course using a stage heater. Maximum intensity projections of confocal stacks were generated

using Zeiss LSM software, and further processed using Image J.(12) Still images were isolated and compiled using Adobe Photoshop. Data were processed using ImageJ and Microsoft Excel.

Confocal Microscopy: Mitochondrial Movement Experiments

Zebrafish embryos were anesthetized in 0.01% tricaine and embedded using 1.2% low-melt agarose in a sealed chamber containing FCCP, 1% DMSO or 2.5 μM MitoBloCK-6. Larvae were imaged for 5 minutes using a 40× oil objective and 3× optical zoom. Stacks were scanned in rapid succession every second over a 1-μm section volume. Imaging was performed on a LSM 510 confocal microscope (Zeiss) with an automated stage, using Multitime software. Larvae viability was maintained at 28.5°C throughout the time course using a stage heater. Maximum intensity projections of confocal stacks were generated using Zeiss LSM software, and further processed using Image J.(12)

Figures

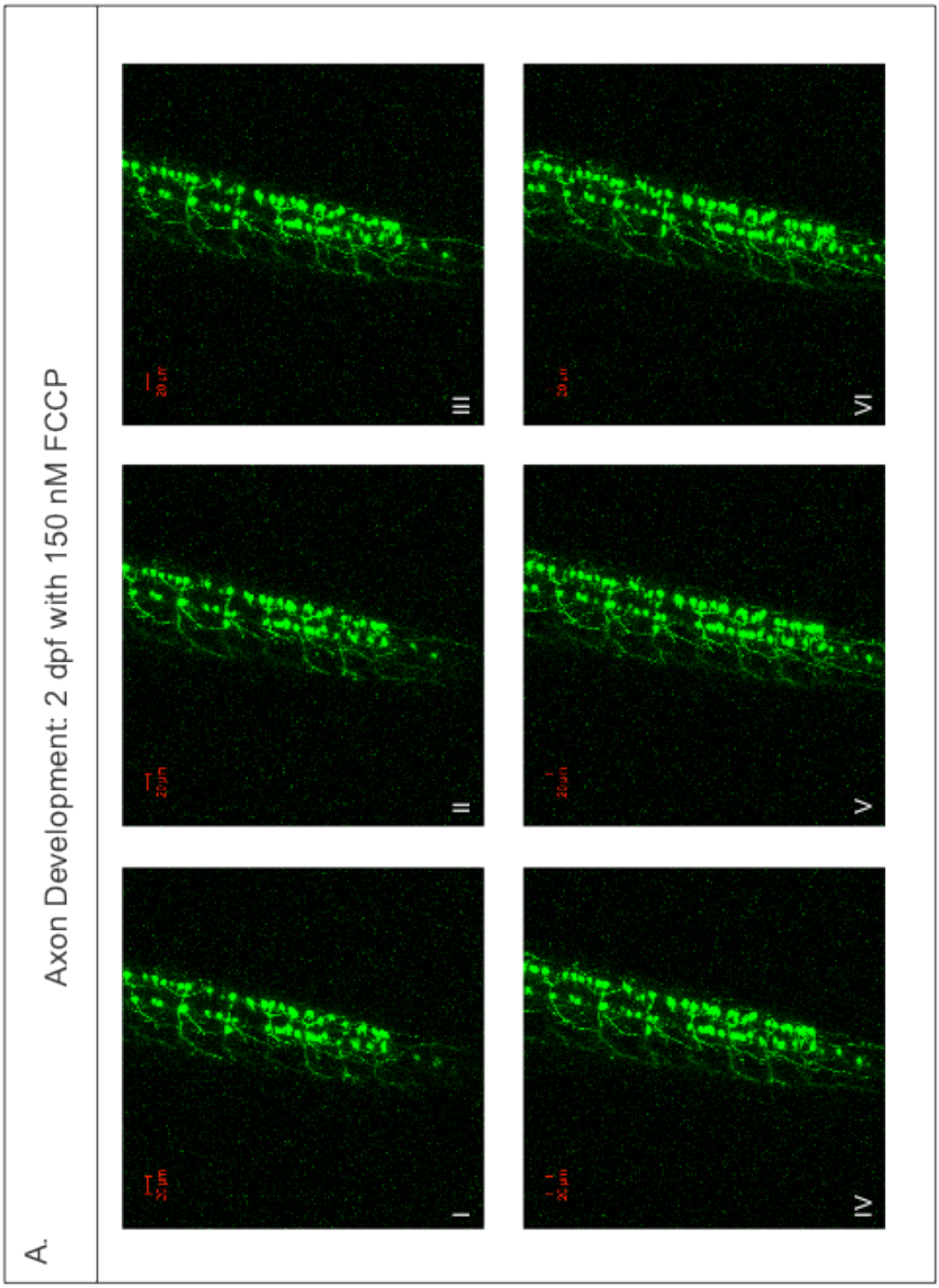

B.

Axon Development: 2 dpf with 500 nM FCCP

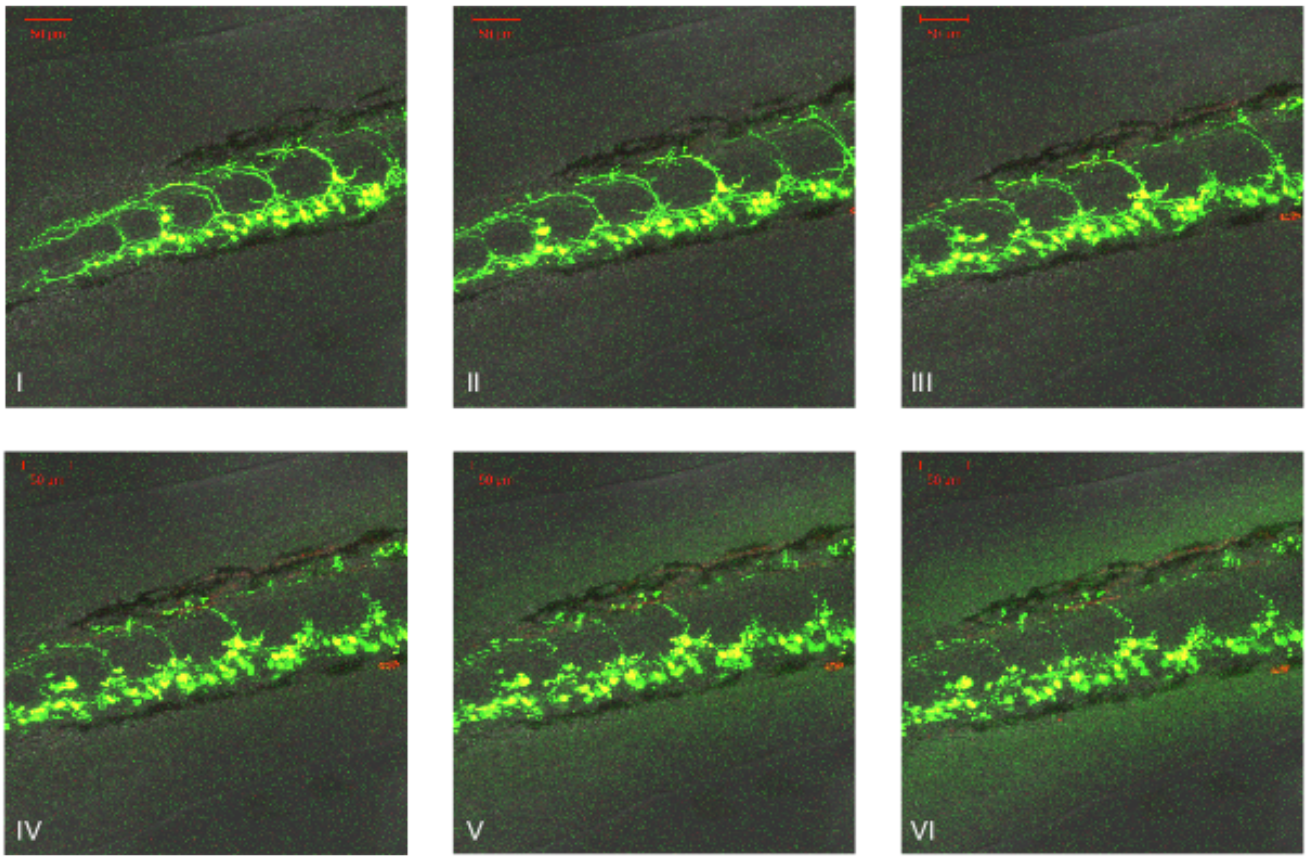

Figure 4.1: Axon development with FCCP treatment at 2dpf. A. Treatment with 150 FCCP resulted in stalled axonal development over the 12-hour time course. From panel I to panel VI, not much change is observed. This stall corresponds with a suspended animation–like state for the embryo, in which embryologic development stages stop progressing over time. **B.** Treatment with 500 nM FCCP resulted in a breakdown of the mitochondrial membrane resulting in axonal fragmentation. This defragmentation did not coincide with embryonic lethality, however, and the fish body remained intact. I. t = 0 hours, II. t = 2.3 hours III. t = 4.6 hours IV. t = 7 hours V. t = 9.3 hours VI. t = 12 hours.

A.

Axon Development: 2 dpf with 1% DMSO

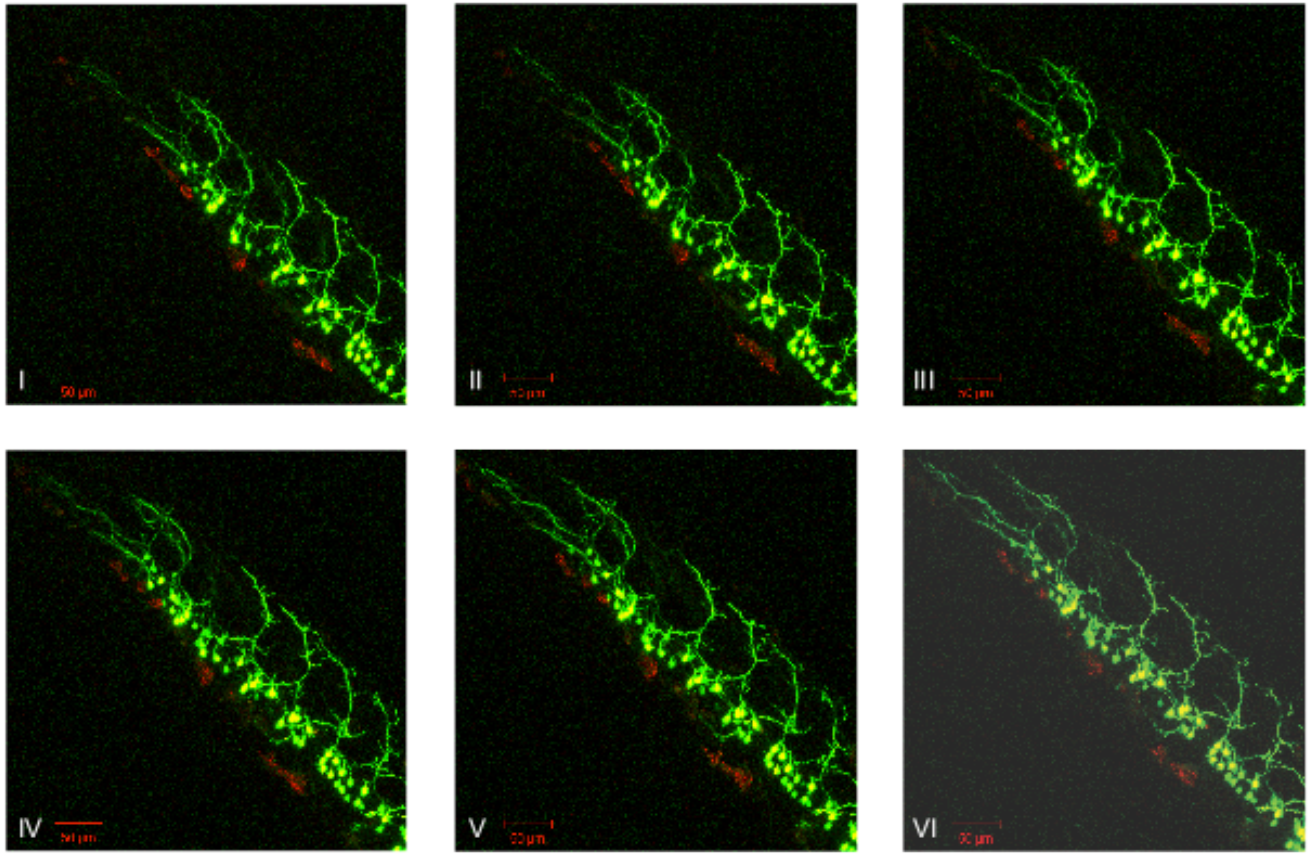

Total Growth	
Mean	29.1 µm
Standard Deviation	21.0

B.

Axon Development: 2 dpf with 2.5 µM MitoBloCK-6

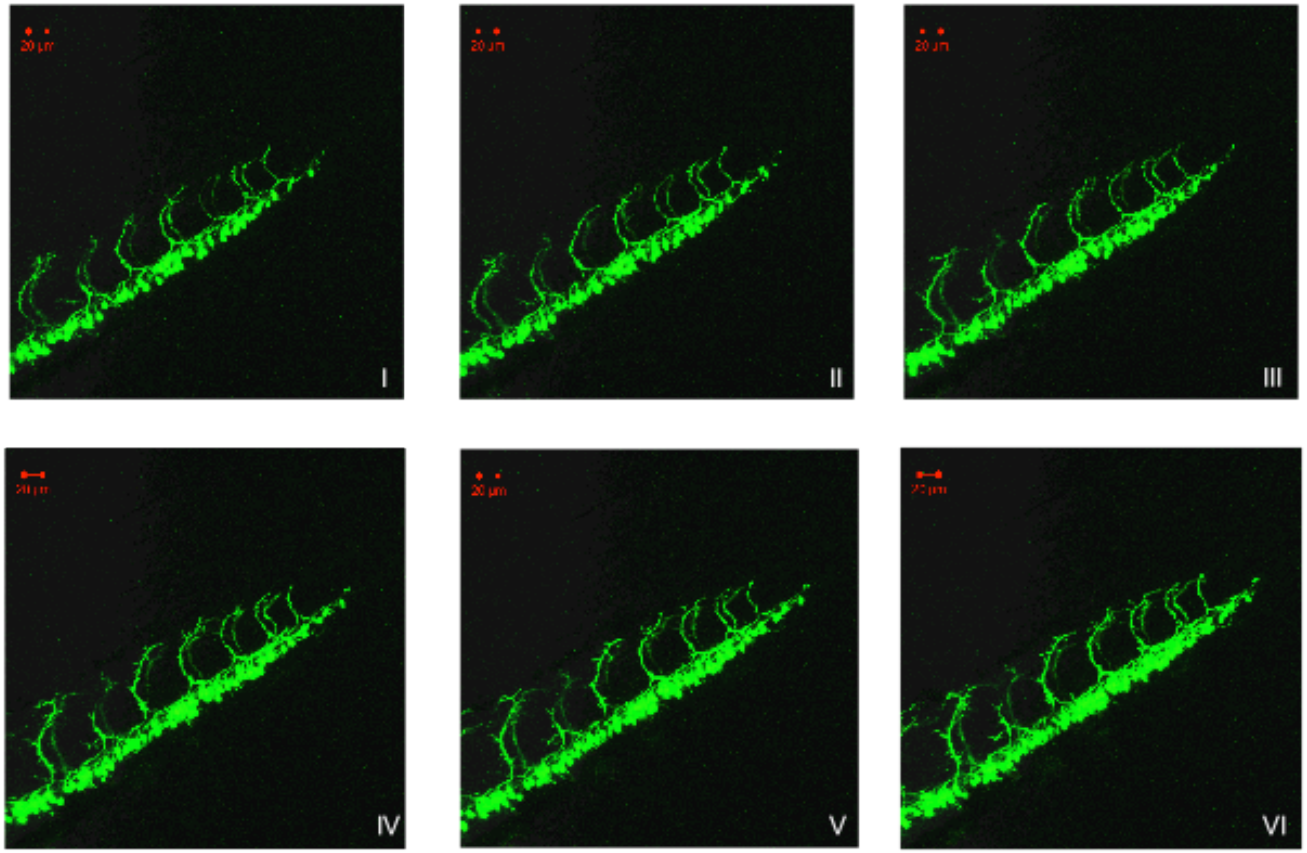

Total Growth	
Mean	17.6 µm
Standard Deviation	12.7

Figure 4.2: Axon development in the presence of 1% DMSO and MitoBloCK-6 at 2 dpf. A. Treatment with 1% DMSO resulted in a mean axon growth of 29.1 μm. Axons appear elongated and are beginning to branch by the end of the time course (panel A, I). **B.** Treatment with 2.5 μM MitoBloCK-6 resulted in a significant decrease in growth, 17.6 μm. Additionally, axons appear shorter and less branched than their DMSO counterparts by the end (panel B, I) . I. t = 0 hours, II. t = 2.3 hours III. t = 4.6 hours IV. t = 7 hours V. t = 9.3 hours VI. t = 12 hours.

A.

Axon Development: 1 dpf with 1% DMSO

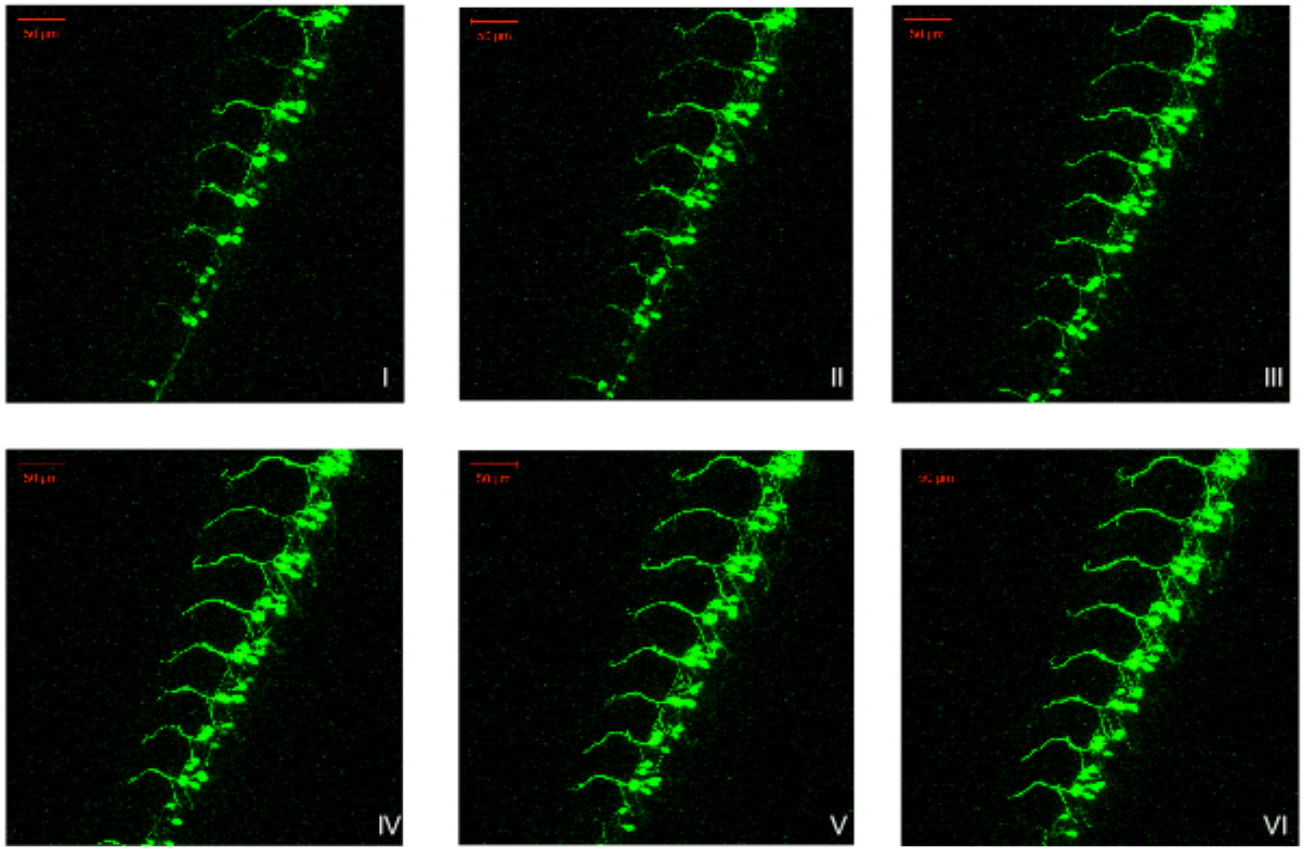

Total Growth	
Mean	41.2 µm
Standard Deviation	13.6

B.

Axon Development: 1 dpf with 2.5 µM MitoBloCK-6

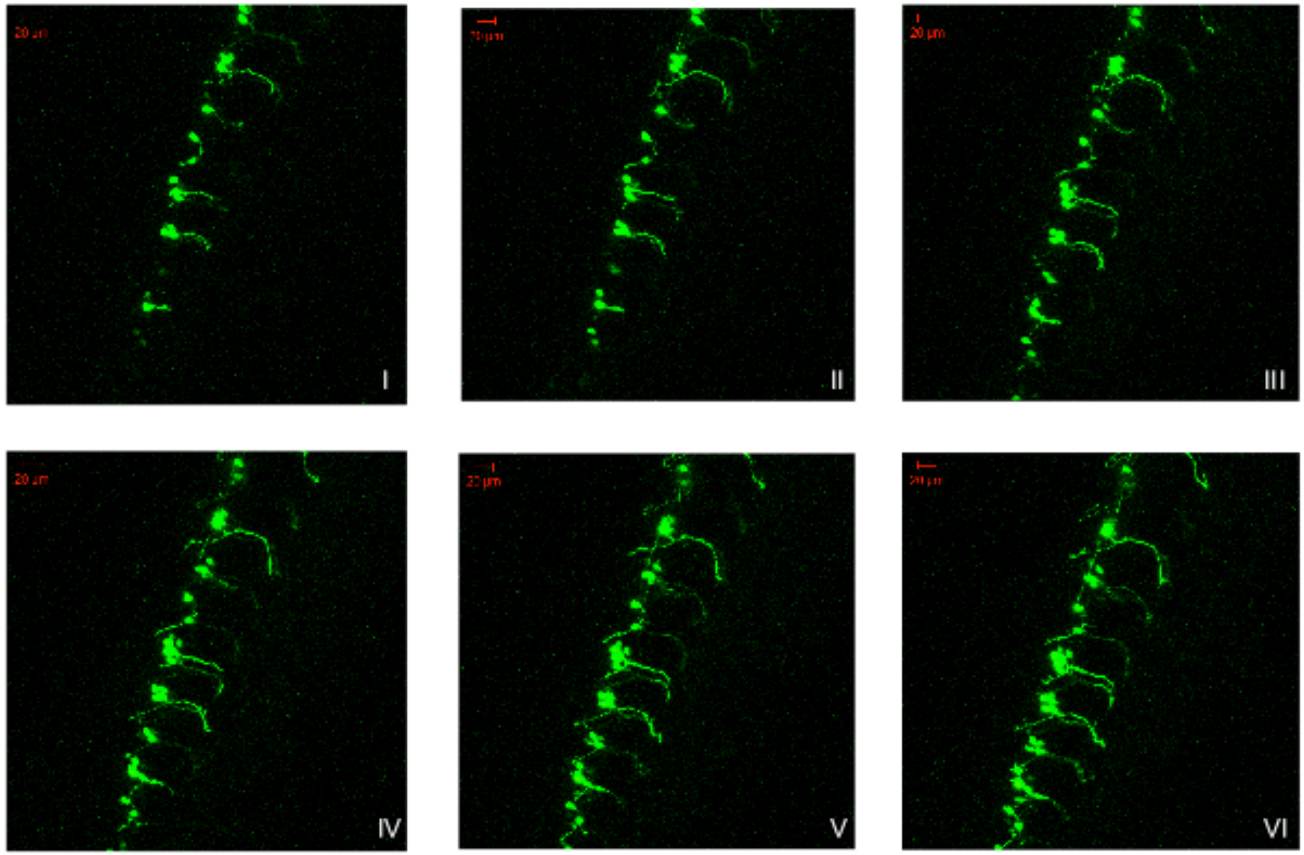

Total Growth	
Mean	34.1 µm
Standard Deviation	15.5

Figure 4.3: Axon development in the presence of 1% DMSO and MitoBloCK-6 at 1 dpf. Treatment with 1% DMSO and MitoBloCK-6 at 1 dpf had a similar phenotype trend as that of the 2-dpf series. Axons treated with DMSO (**A**) appear ordered and evenly spaced along the spine, whereas those treated with MitoBloCK-6 (**B**) appear twisted and stumplike. I. t = 0 hours, II. t = 2.3 hours III. t = 4.6 hours IV. t = 7 hours V. t = 9.3 hours VI. t = 12 hours.

A.

Axon Development: 2 dpf Untreated Control

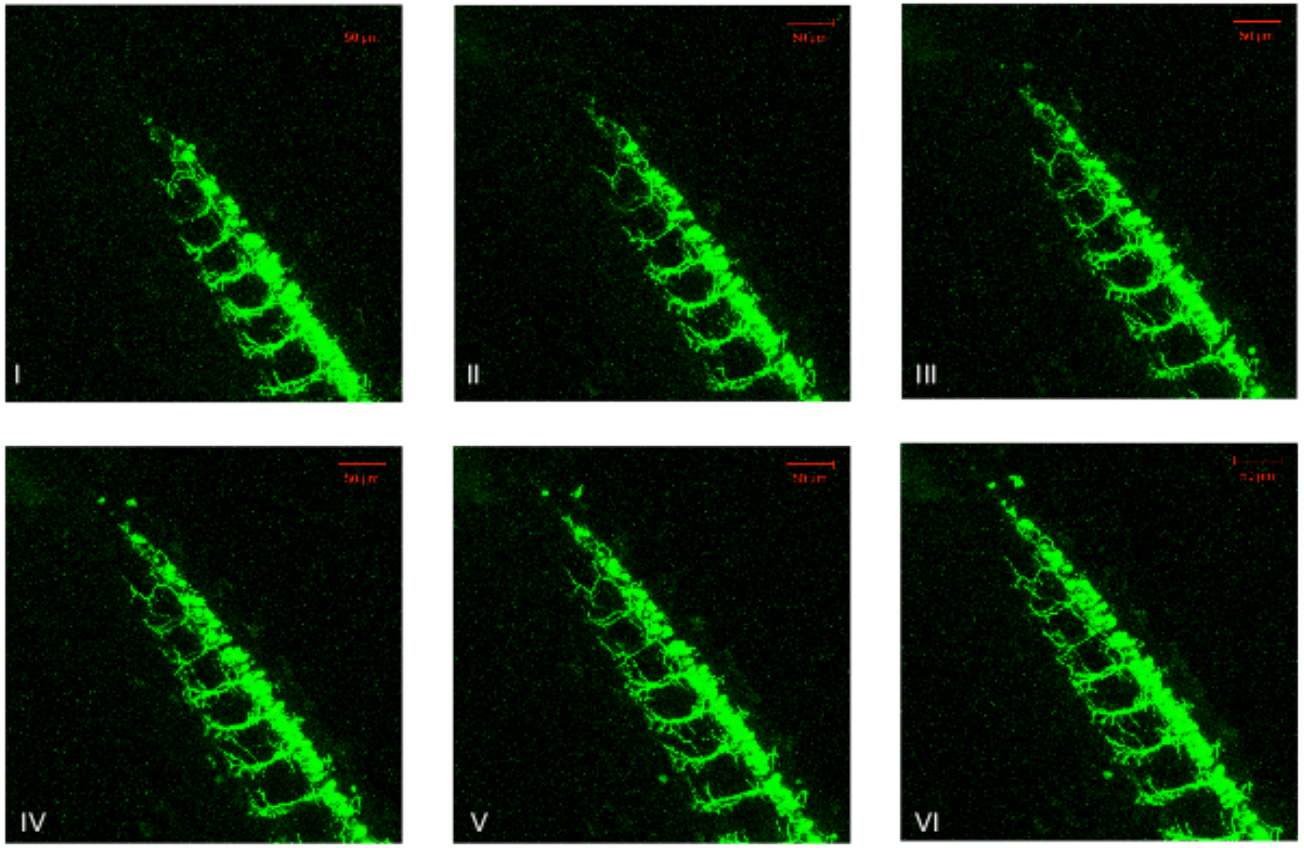

Total Growth	
Mean	25.5 µm
Standard Deviation	14.3

B.

Axon Development: 2 dpf ALR Morpholino

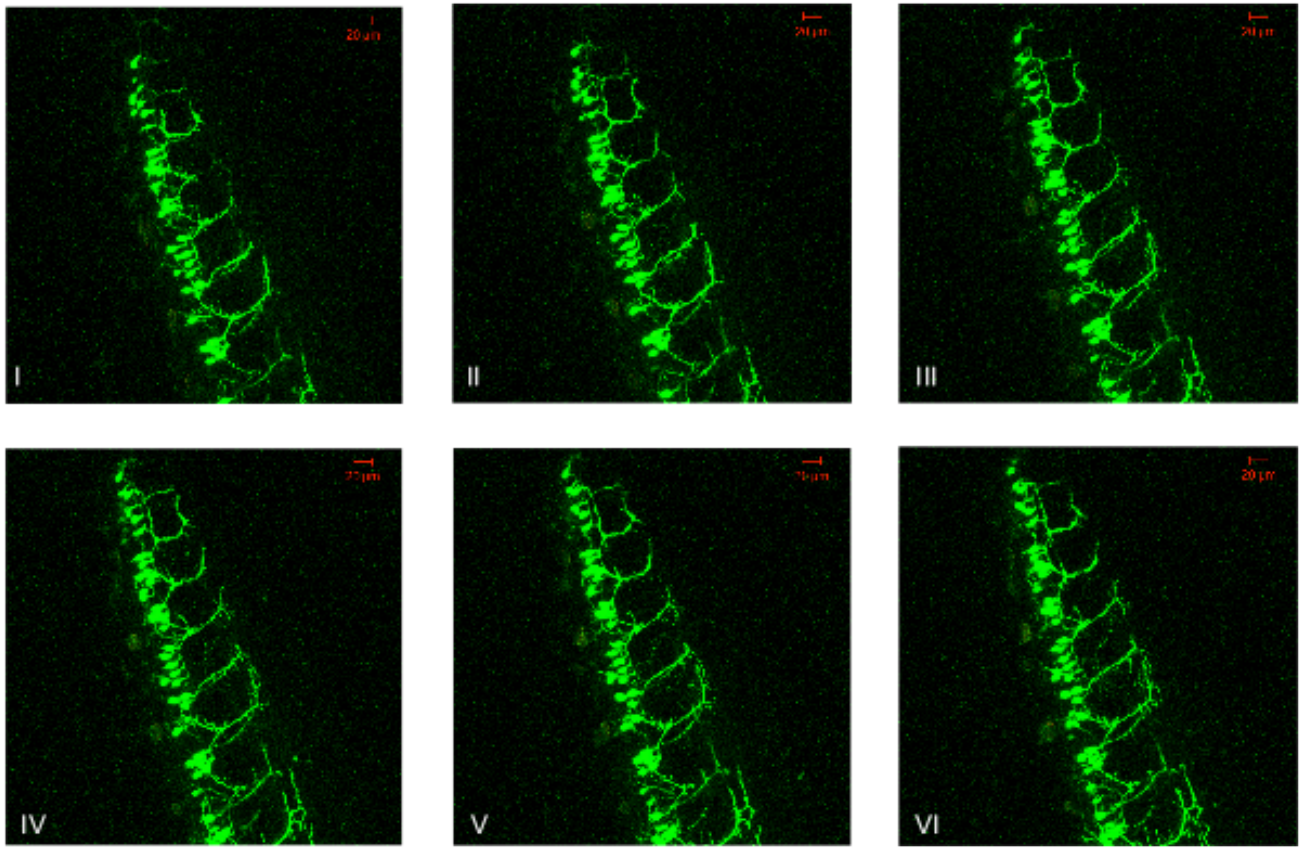

Total Growth	
Mean	25.6 µm
Standard Deviation	14.3

Figure 4.4: Axon development with ALR morpholino injection at 2 dpf. Morpholino injection (**B**) gave rise to embryos that grow at a similar rate compared with the uninjected controls (**A**). When morphology is compared, morpholino injectants appear to be developmentally behind the untreated controls, indicating that the morpholino has most likely worn off and protein levels are returning to normal levels. I. t = 0 hour, II. t = 2.3 hours III. t = 4.6 hours IV. t = 7 hours V. t = 9.3 hours VI. t = 12 hours.

I. Branching Quantification: 2 dpf 2.5 µM MitoBloCK-6

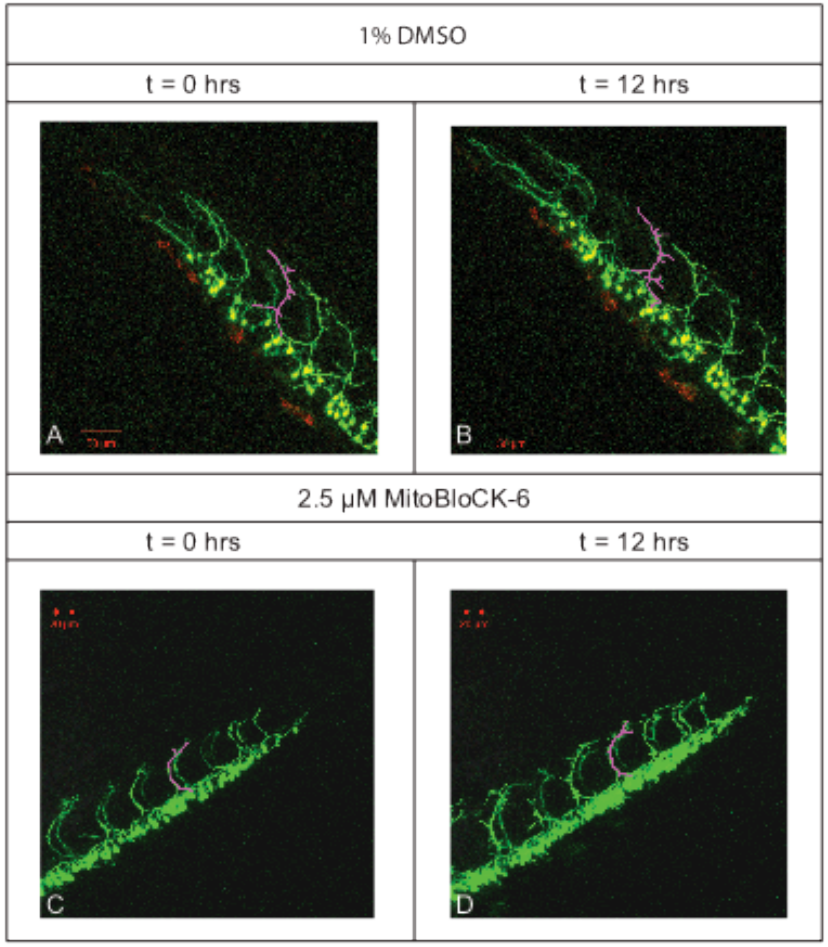

E. Branch Number Per Axon Projection			
	Axon 3	Axon 5	Axon 6
1% DMSO	4	5	7
MB-6	2	3	3

F. Branch Length Per Axon Projection (µM)			
	Axon 3	Axon 5	Axon 6
1% DMSO	13.2	21.9	22.4
MB-6	9.9	13.6	18.6

II. Branching Quantification: 1 dpf 2.5 µM MitoBloCK-6

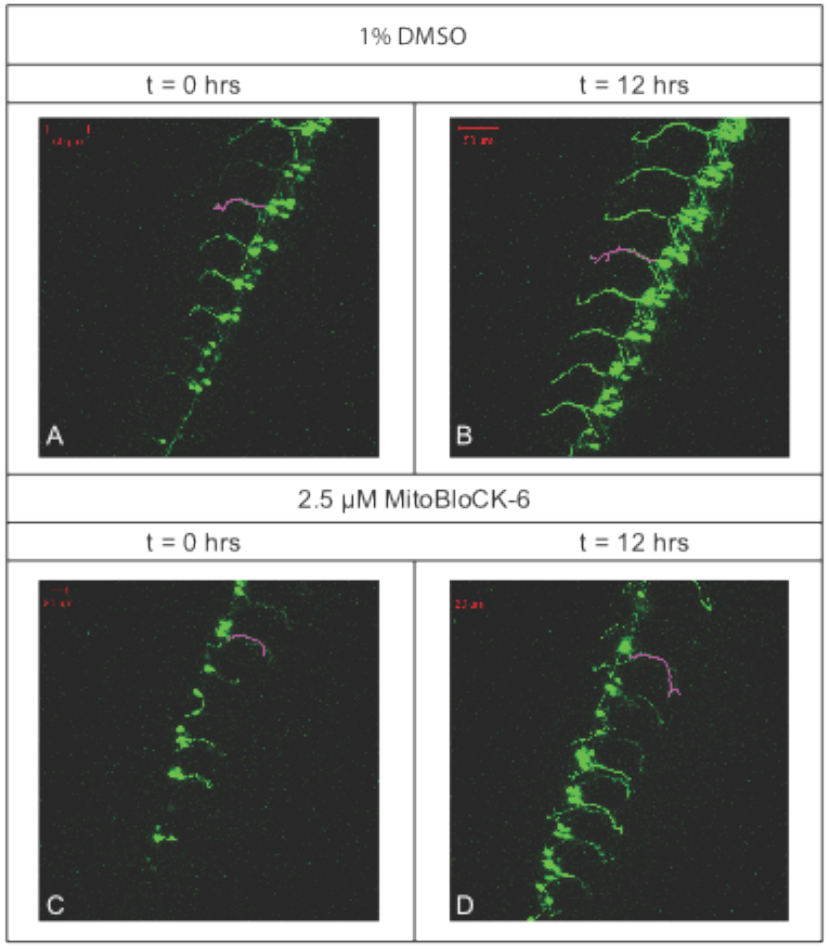

E. Branch Number Per Axon Projection			
	Axon 3	Axon 5	Axon 6
1% DMSO	<1	1	2
MB-6	<1	<1	1

F. Branch Length Per Axon Projection (µM)			
	Axon 3	Axon 5	Axon 6
1% DMSO	7.5	8.5	7.6
MB-6	8.0	9.4	13.3

III. Branching Quantification: 2 dpf ALR Morpholino

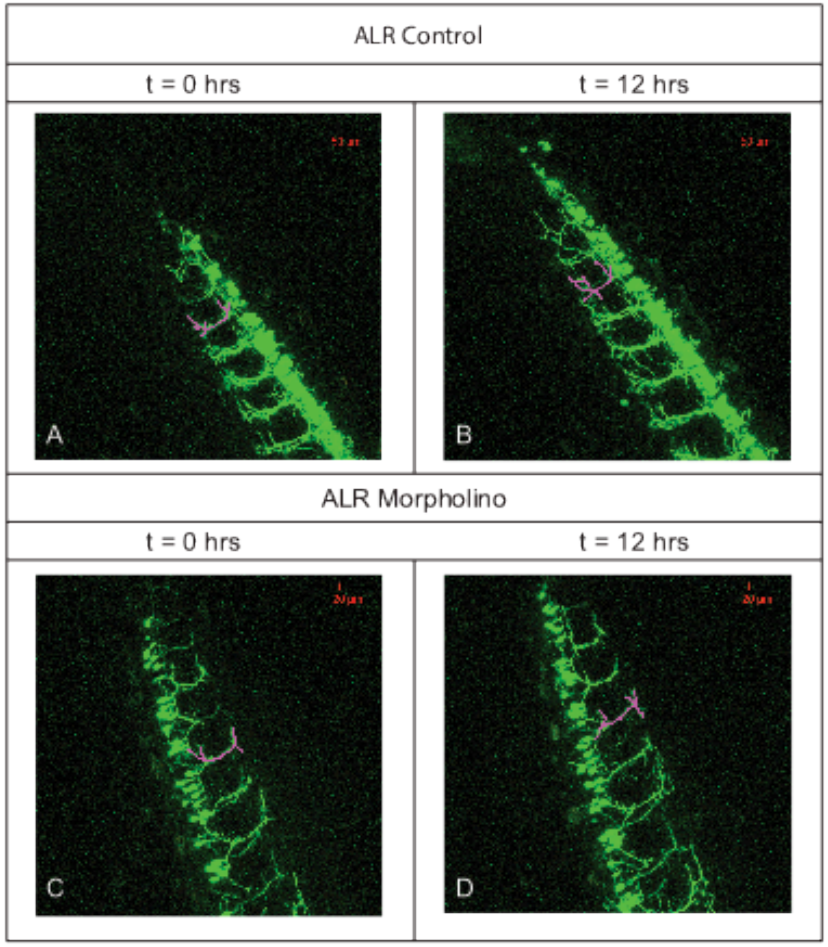

E. Branch Number Per Axon Projection			
	Axon 3	Axon 5	Axon 6
Control	5	6	7
Morpholino	4	5	6

F. Branch Length Per Axon Projection (μM)			
	Axon 3	Axon 5	Axon 6
Control	19.8	30.6	22.8
Morpholino	13.8	16.8	13.9

Figure 4.5: Branching quantification. Branching and the differences with treatment was much more pronounced at 2 dpf than at 1 dpf. **I.** Differences with MitoBloCK-6 treatment could be seen in the number of branches per axon and in branch length. **II.** At 1 dpf, DMSO treatment produced more branches than MitoBloCK-6 treatment, although a smaller difference was seen. For the branches that did form however, there was no discernible difference in length between the 2 treatments. **III.** Although the branch number was similar in the 2 groups, those injected with the morpholino has much shorter branches, providing further credibility to the hypothesis that the morpholino had worn off and the embryos are delayed.

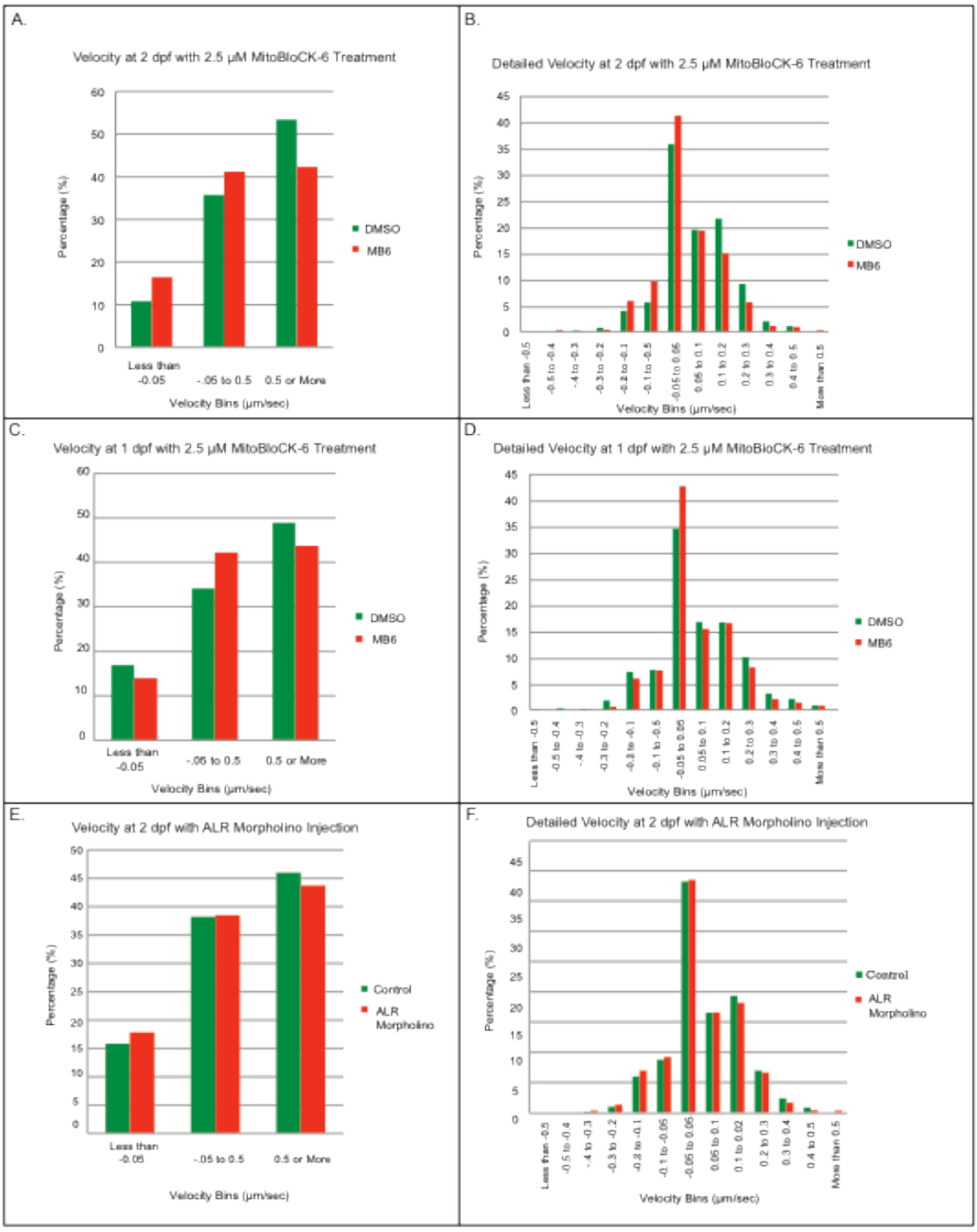
A.
Velocity at 2 dpf with 2.5 µM MitoBloCK-6 Treatment
Percentage (%)
Less than -0.05
-.05 to 0.5
0.5 or More
Velocity Bins (µm/sec)
DMSO
MB6
B.
Detailed Velocity at 2 dpf with 2.5 µM MitoBloCK-6 Treatment
Percentage (%)
Velocity Bins (µm/sec)
DMSO
MB6
C.
Velocity at 1 dpf with 2.5 µM MitoBloCK-6 Treatment
Percentage (%)
Less than -0.05
-.05 to 0.5
0.5 or More
Velocity Bins (µm/sec)
DMSO
MB6
D.
Detailed Velocity at 1 dpf with 2.5 µM MitoBloCK-6 Treatment
Percentage (%)
Velocity Bins (µm/sec)
DMSO
MB6
E.
Velocity at 2 dpf with ALR Morpholino Injection
Percentage (%)
Less than -0.05
-.05 to 0.5
0.5 or More
Velocity Bins (µm/sec)
Control
ALR Morpholino
F.
Detailed Velocity at 2 dpf with ALR Morpholino Injection
Percentage (%)
Velocity Bins (µm/sec)
Control
ALR Morpholino

Figure 4.6: Velocity comparisons. For all 3 conditions observed, inhibition of ALR resulted in more stationary growth (–0.05 to 0.5) and less anterograde movement (more than 0.05) compared with the control groups, with the strongest discernible difference happening with MitoBloCK-6 treatment at 2 dpf (**A**). Retrograde motion (less than –0.05) appeared to only be affected at 1 dpf. (**C**). Detailed velocities appear Gaussian in nature, but have a much greater percentage of stationary motion compared with all other velocities (**B, D, F**).

Mitochondrial Movement: 150 nM FCCP

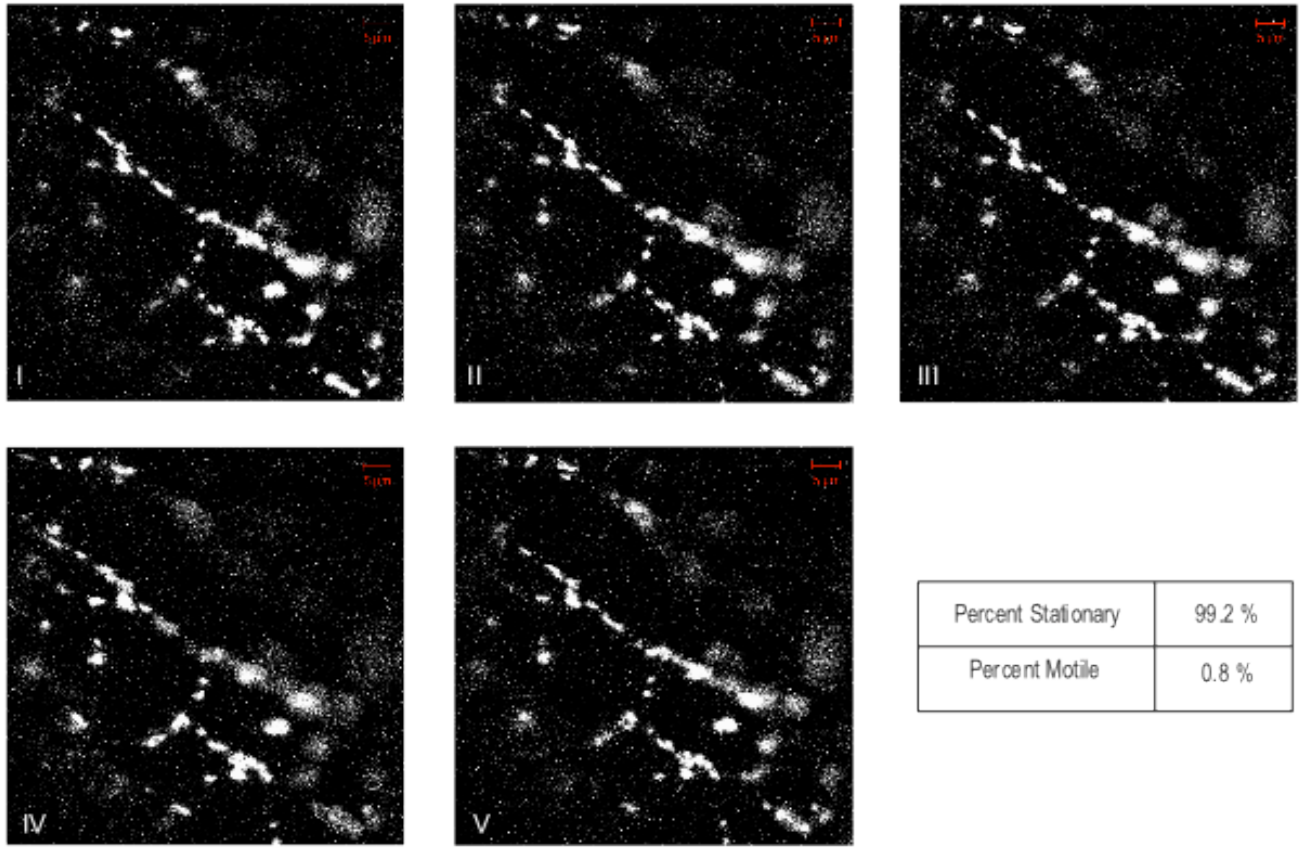

Percent Stationary	99.2 %
Percent Motile	0.8 %

Figure 4.7: Mitochondrial movement with FCCP treatment. FCCP treatment for 1 hour before imaging resulted in virtually no mitochondrial motion over the imaging time frame. Time-lapse photos were taken for 5 minutes, imaging approximately once per second. Frames are excerpted from the image sequence.

Mitochondrial Movement: 1% DMSO

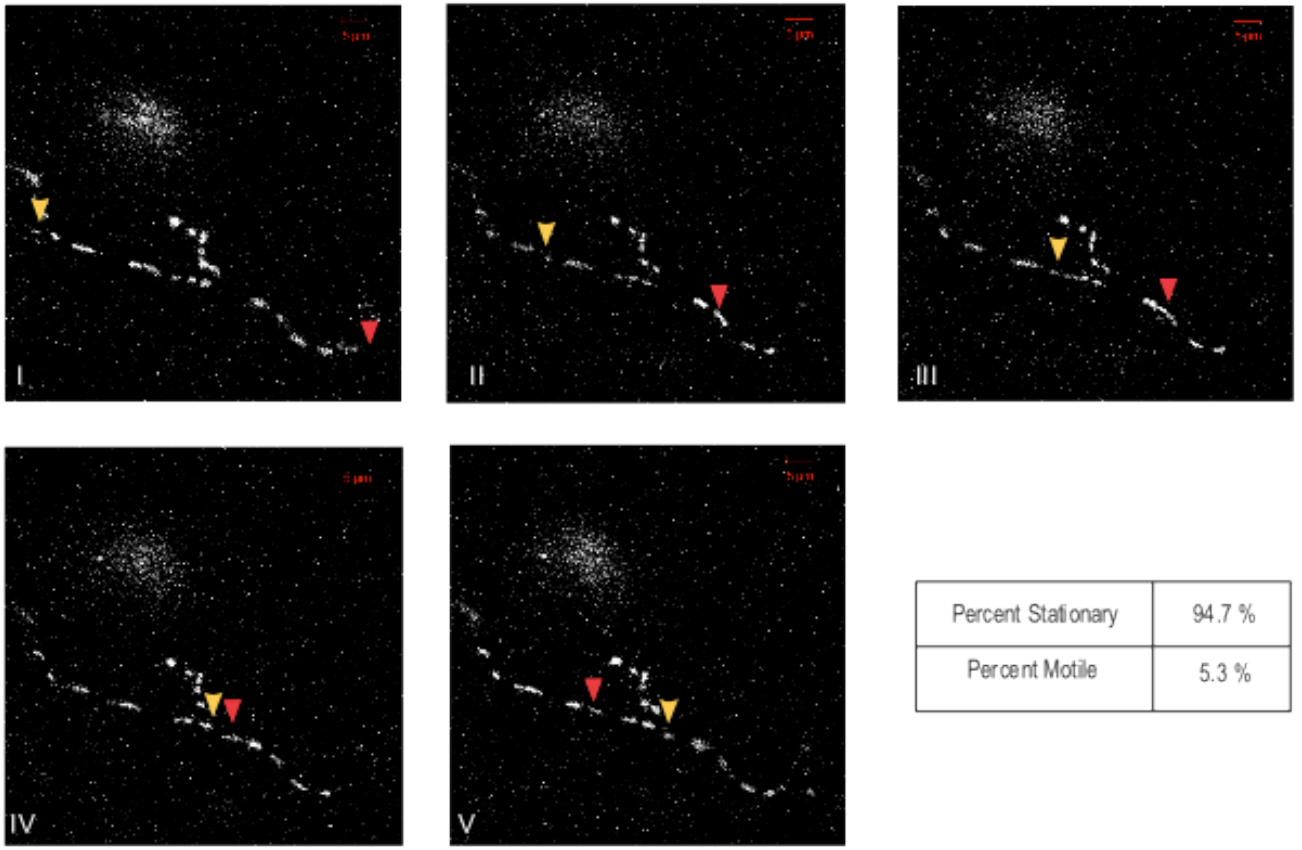

Percent Stationary	94.7 %
Percent Motile	5.3 %

Figure 4.8: Mitochondrial movement with 1% DMSO treatment. Twenty-six movies were analyzed from zebrafish treated with 1% DMSO, with a total of 827 mitochondria quantified. Treatment with DMSO did not affect mitochondrial movement. Many mitochondria can be seen traversing the screen during the time lapse; individual mitochondria are marked with different-colored arrows. Motion can also be seen in both the anterograde and retrograde direction. Frames are excerpted from larger image sequence.

Mitochondrial Movement: 2.5 µM MitoBloCK-6

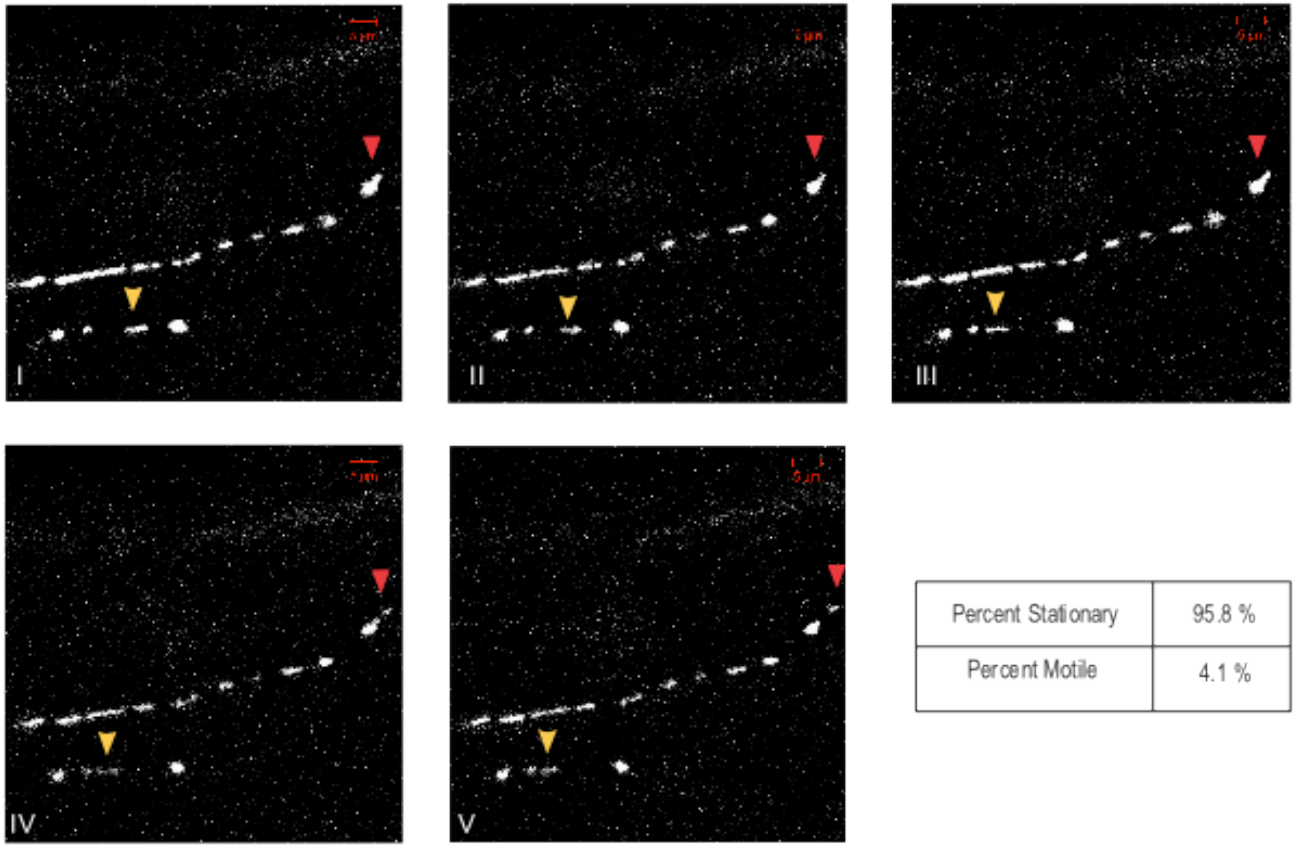

Percent Stationary	95.8 %
Percent Motile	4.1 %

Figure 4.9: Mitochondrial movement with 2.5 μM MitoBloCK-6. Thirty-six movies were analyzed from MitoBloCK-6 treatment, with a total of 1171 mitochondria being quantified. The percentage stationary vs percentage motile is similar to DMSO treatment; however, movement is constrained, and over a much shorter distance. Over the course of the time lapse, mitochondria do not cross the entire screen, as was seen with DMSO treatment. Frames are excerpted from larger image sequence.

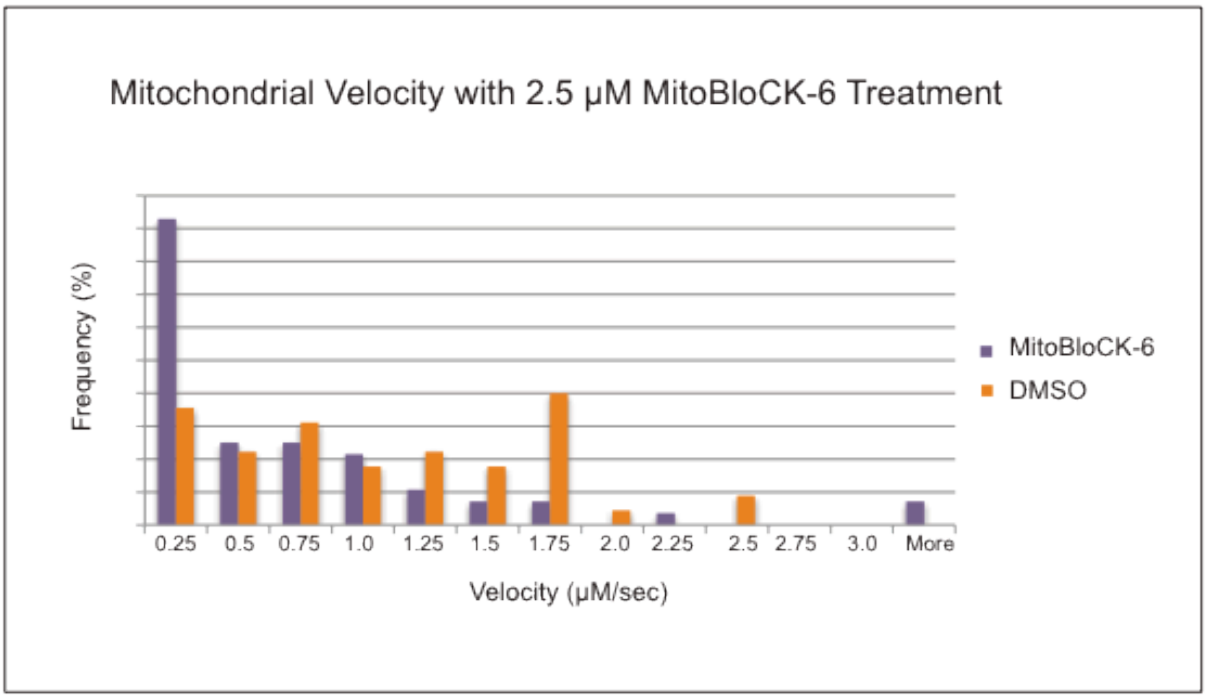
Mitochondrial Velocity with 2.5 µM MitoBloCK-6 Treatment
Frequency (%)
0.25
0.5
0.75
1.0
1.25
1.5
1.75
2.0
2.25
2.5
2.75
3.0
More
Velocity (µM/sec)
MitoBloCK-6
DMSO

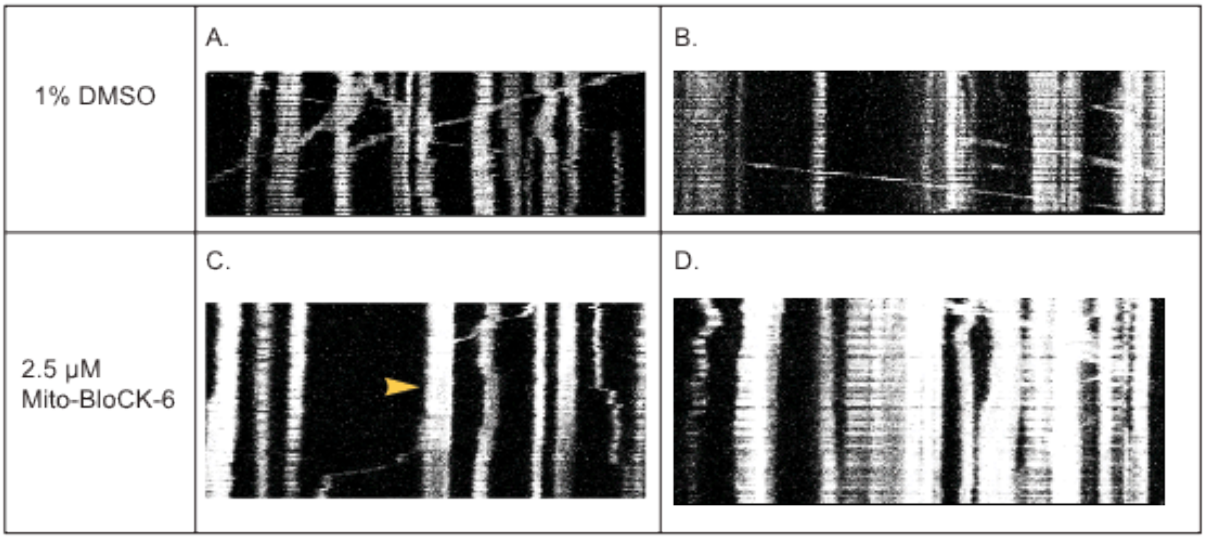
1% DMSO
A.
B.
2.5 µM
Mito-BloCK-6
C.
D.

Figure 4.10: Quantification of mitochondrial movement with 2.5 μM MitoBloCK-6 treatment. (**Graph**). Twenty-six movies were analyzed from zebrafish treated with 1% DMSO, with a total of 827 mitochondria quantified. Similarly, 36 movies were analyzed from MitoBloCK-6 treatment, with a total of 1171 mitochondria being quantified. Data were normalized for comparison. The velocity of mitochondria in axons treated with MitoBloCK-6 skewed left compared to DMSO treatment. Many more mitochondria move at much slower speeds with MitoBloCK-6 treatment than with DMSO treatment. **A–D.** Kymographs representing mitochondrial movement. More horizontal slopes indicate faster motion. Distance traveled is proportional to the length of the panel. Positive and negative slope values equate to anterograde and retrograde movement. More mitochondria can be visualized traveling longer distances at faster speeds with DMSO treatment. **A, B.** Simultaneously, the more vertical lines indicate that mitochondria are traveling shorter distances and at slower speeds in a similar length of time. **C, D.** Also, the vertical pause (marked by arrow) in panel C illustrates when a mitochondrion becomes stationary during the time frame, pausing its motion.

References

1. Mannan, A. A., Sharma, M. C., Shrivastava, P., Ralte, A. M., Gupta, V., Behari, M., and Sarkar, C. (2004) *Indian J Pediatr* **71**, 1029-1033

2. Graeber, M. B., and Muller, U. (1998) *J Neurol Sci* **153**, 251-263

3. Valente, E. M., Abou-Sleiman, P. M., Caputo, V., Muqit, M. M., Harvey, K., Gispert, S., Ali, Z., Del Turco, D., Bentivoglio, A. R., Healy, D. G., Albanese, A., Nussbaum, R., Gonzalez-Maldonado, R., Deller, T., Salvi, S., Cortelli, P., Gilks, W. P., Latchman, D. S., Harvey, R. J., Dallapiccola, B., Auburger, G., and Wood, N. W. (2004) *Science* **304**, 1158-1160

4. Narendra, D., Tanaka, A., Suen, D. F., and Youle, R. J. (2008) *J Cell Biol* **183**, 795-803

5. Chen, H., and Chan, D. C. (2009) *Hum Mol Genet* **18**, R169-176

6. Hansson Petersen, C. A., Alikhani, N., Behbahani, H., Wiehager, B., Pavlov, P. F., Alafuzoff, I., Leinonen, V., Ito, A., Winblad, B., Glaser, E., and Ankarcrona, M. (2008) *Proc Natl Acad Sci U S A* **105**, 13145-13150

7. Cho, D. H., Nakamura, T., Fang, J., Cieplak, P., Godzik, A., Gu, Z., and Lipton, S. A. (2009) *Science* **324**, 102-105

8. Shirendeb, U. P., Calkins, M. J., Manczak, M., Anekonda, V., Dufour, B., McBride, J. L., Mao, P., and Reddy, P. H. (2012) *Hum Mol Genet* **21**, 406-420

9. Song, W., Chen, J., Petrilli, A., Liot, G., Klinglmayr, E., Zhou, Y., Poquiz, P., Tjong, J., Pouladi, M. A., Hayden, M. R., Masliah, E., Ellisman, M., Rouiller, I., Schwarzenbacher, R., Bossy, B., Perkins, G., and Bossy-Wetzel, E. (2011) *Nat Med* **17**, 377-382

10. Bossy-Wetzel, E., Petrilli, A., and Knott, A. B. (2008) *Trends Neurosci* **31**, 609-616

11. Manfredi, G., and Xu, Z. (2005) *Mitochondrion* **5**, 77-87

12. Schneider, C. A., Rasband, W. S., and Eliceiri, K. W. (2012) *Nat Methods* **9**, 671-675